FEDERAL UNIVERSITY OF TECHNOLOGY,

SCHOOL OF POSTGRADUATE STUDIES

DEPARTMENT OF MECHANICAL ENGINEERING.

Ph.D THESIS

M. A. AKINTUNDE
(MEE/93/5341)

DEVELOPMENT OF A VAPOUR COMPRESSION REFRIGERATION SYSTEM BASED ON BALANCED POINTS BETWEEN OPERATIONAL UNITS

SUPERVISOR: Prof. C. O. Adegoke

Co-Supervisor: Dr. O. P. Fapetu

September, 2004

DEVELOPMENT OF A VAPOUR COMPRESSION REFRIGERATION SYSTEM BASED ON BALANCED POINTS BETWEEN OPERATIONAL UNITS

By

M. A. AKINTUNDE
(MEE/93/5341)

A THESIS IN THE DEPARTMENT OF MECHANICAL ENGINEERING SUBMITTED TO THE SCHOOL OF POSTGRADUATE STUDIES IN PARTIAL FULFILLMENT OF THE REQUIREMENTS FOR THE AWARD OF Ph.D DEGREE IN MECHANICAL ENGINEERING OF THE FEDERAL UNIVERSITY OF TECHNOLOGY, AKURE.

September, 2004

CERTIFICATION

We certify that Mr. M. A. Akintunde of the Mechanical Engineering Department, Federal University of Technology, Akure carried out this study.

24/09/04

Supervisor/signature/Date

27.09.04

Co-supervisor/signature/Date

27.09.04

HOD/signature/Date

DEDICATION

TO

YINKA

BOLU

GLORY

GRACE

ACKNOWLEDGEMENT

The author would like to thank the following people for their invaluable contributions to the success of this project and the preparation of this report:

- Prof. C. O. Adegoke and Dr. O. P. Fapetu who supervised this work, for their useful suggestions and indispensable advise throughout the period of these investigations.
- Prof. A. A. Aderoba for spearing his time in checking through the report and his useful suggestions and indispensable advise throughout the period of these investigations
- Messrs. S. O. Abadariki, F. Olojo and Femi Owolade, for their assistance in the construction of the experimental rigs and during the experimental work.
- All the staff of Mechanical Engineering Department, Federal University of Technology, Akure for their contributions in one-way or the other.
- Lastly but by no means the least, the author would like to express his sincere thanks to his wife, Oluyinka, for her patience, counsel and contributions, physically, spiritually and otherwise.

ABSTRACT

Vapour Compression Refrigerator (VCR), consists of four major components- evaporator, condenser, compressor and expansion device,- which are connected in a cycle. VCR is commonly used in a wide range of commercial and industrial refrigeration applications and represents a substantial fraction of the installed refrigeration systems. As a result special attention has been focused on this system by many researchers.

The goals of the researchers were to simulate the actual working of a vapour compression system with Carnot model as the benchmark. The task of getting the performance of Carnot model has proved difficult. Hence most researchers end-up in modeling performance of heat exchangers or a single component of the system. Though there are models for predicting the approximate performance of VCR, none of such models discussed the "balanced point" between the four major components. This study was carried out to investigate the effects of balanced point on the system performance.

In order to get the balanced point, the performance characteristics of each of the components were modelled in such a way that each of them depends on temperature only. These equations were used to develop a computer programme for refrigeration cycle. The model was then used to generate performance data, which compare very well with theoretical values.

In order to validate the model, the generated data was used to design and construct a VCR that was tested and evaluated. Two experimental rigs were constructed for the tests. Rig "**a**" was that constructed using generated data from the design model, whilst Rig "**b**" was constructed from bought out components. The investigations were carried out under the same conditions. Effects of system performance based on operational parameters such as: compressor speed, refrigerant charge, condenser and evaporator temperatures and others, have been experimentally evaluated and the results compared.

Present analysis and experimental investigations have shown that the model results are comparable to the experimental ones. The results obtained from rig **a** agreed well with those of the model, although there were some deviations. The deviations of the model results from those obtained in experiments are within the ranges of 16 % to 19 % for rig "**a**" and 28 % to 34 % for rig "**b**" respectively.

TABLE OF CONTENTS

List of Tables

List of Figures

APPENDICES **104**

NOTATIONS

A	Surface or cross sectional area (m^2)
ACR	Air-conditioning and Refrigeration
c	Heat capacity (kJ/kg.K)
C	Capacitance rate (kW/kg.K)
CBL	Chlorine–bromine loading
CFC	Chlorofluorocarbon
COP	Coefficient of Performance
ϕ	Diameter (m)
DT	Degree of Subcooling or Superheating (K)
f	Friction factor
f_h	Ratio of effective capacitance products
G	Mass flux (kg/m^2)
GHG	Green house gas
GWP	Global warming potential
Gz	Graetz Number
h	Convective heat transfer coefficient (W/m^2K), {enthalpy (J/kg)}
HCF	Hydrogen- carbon fluoride
HCFC	Hydrogen-chloro-fluoro-carbon
HFC	Hydrogen-fluoro-carbon
k	Thermal Conductivity (W/m.K)
L	Length (m)
$\dot{m}$	Mass rate of flow (kg/s)
M	Mach number
η	Efficiency (%)
Nu	Nusselt Number
Nu_a	Nusselt Number based on Arithmetic Mean
P	Pressure (N/m^2) (or Power (W))

Pt	Peclet Number
ODP	Ozone depletion potential
Q	Rate of heat transfer (W)
R	Refrigerant
Re	Reynolds number
T	Temperature (K)
T_a	Ambient temperature (K)
TEWI	Total equivalent warming impact
V	Velocity (m/s)
W	Compression Power (W)
x	dryness fraction

Greek Symbols

Δ	Change
ε	Heat exchanger effectiveness
η	Efficiency (%)
κ	Constant thermal inventory (W/K)
μ	Dynamic viscosity (Pa.s)
ν	Humid volume (kg/m^3)
ρ	Density (kg/m^3)
ψ	Optimization factor

SUBSCRIPTS

a	rig a or ambient
b	rig b
both	subcooling and superheating
Car	Carnot
cond, or c	condenser
evap,.or e	evaporator
f	fluid
fg	mixture
g	gas (or vapour)

i	inlet
kz	Khan and Zubair
m	model (or mean)
max	maximum
o	outlet
p	pressure or present work
r	refrigerant
ref	refrigeration
sj	Stoecker and Jones
sub	subcooling
sup	superheating
t	theoretical value
w	water

CHAPTER ONE

1.0 INTRODUCTION

1.1 Background

The most widely used cycle in the field of refrigeration and air – conditioning is the vapour-compression cycle. In this cycle, vapour is compressed then condensed to liquid following which the pressure is dropped so that fluid can evaporate at a low pressure. This cycle is performed by four major components, namely: – compressor, condenser, evaporator and expansion device. Each of these components has its own peculiar behaviour more so each of the components is influenced by conditions imposed by the other members of the quartet. The influence of one component on the other results in changes in the thermal properties of the working fluid. In the study of refrigeration processes, therefore, the application of thermodynamics and heat transfer is essential

The fields of refrigeration and air conditioning are interconnected but each has its own peculiar distinction. The largest application of refrigeration is for air conditioning. Refrigeration embraces industrial refrigeration including the processing and preservation of food, removing heat from substances in chemical, petroleum and petrol-chemical plants and domestic, special applications such as those in the manufacturing and construction industries.

1.2 Concepts of Models

Thermodynamics and heat transfer have developed from a general set of concepts, based on observations of the physical world, specific models and laws necessary to solve problems and to design systems. As the physical world is extremely complex, it is virtually impossible to describe it precisely. Even, if it were possible, such detailed descriptions would be much too cumbersome for engineering purposes. One of the most significant accomplishments of engineering science has been the development of models of physical phenomena, which although they may be approximations, provide both a sufficiently accurate description, and a tractable means of solution.

These models are of little value unless they can be expressed in appropriate mathematical terms (Stocker and Jones, 1982). The mathematical expression of a model provides the basic equations or laws, which allow engineering science to explain or predict natural phenomena.

Models have been developed for the design and evaluation of refrigeration components (compressor, condenser, evaporator, and expansion devices), [Glocker *et al*, 1998; Janssen *et al*, 1988; Aluares and Trepp 1987; Spaushas, 1987b, Melo *et al* 1988]. In as much as these components are connected in a closed loop in the vapour compression refrigeration cycle, there is the need to get a "compromise point" (or "balanced point") between these components before they can work together effectively. There is no available information about this balanced point except that of Stocker and Jones (1982); which is even for single unit refrigeration system. This work therefore developed a model, which can be applied for the design and optimization of vapour compression refrigeration systems. This is made possible by using mathematical models, with the aid of computer program to generate balanced points for vapour compression systems when subjected to different operational conditions. A vapour compression refrigeration system was then fabricated based on the computer-generated data, and was used to validate the model developed. This enabled the comparative analysis of the available data, generated data and the experimental results.

1.3 Objectives of the Research Project

The objectives of the research are to:

(i) develop a mathematical model for vapour compression refrigeration systems and laboratory scale vapour compression refrigeration units;

(ii) evaluate the performance of the vapour compression refrigeration system;

(iii) investigate the effect of "balanced point" on the system performance

(iv) compare the model with existing models.

1.4 Methodology

The project

The project consists of the development of a mathematical model to be used in the design of vapour compression refrigeration systems. The development of the mathematical model involves the following features:

(i) Modelling of condensing unit

(ii) Modelling of capillary tube.

(iii) Modelling of a complete system

(iv) Fabrication of various components and testing

CHAPTER TWO

2.0 LITERATURE REVIEW

2.1 General Views

Vapour compression refrigerators are commonly used for commercial and industrial refrigeration applications. They represent a substantial fraction of all installed refrigeration systems. The system consists essentially of: - an evaporator, a compressor, a condenser and an expansion device. All the components are connected in a closed loop.

The development of refrigeration model, which simulates the actual working of a vapour compression system, has been the goal of many researchers (Klein, 1994; Gordon *et al* 1996; Stoecker and Jones, 1982; Kuehn and Liang, 1991). The simplest model is the Carnot model, which represents an ideal refrigeration cycle without any irreversible losses (Jung *et al*, 1999). The Carnot model was considered in many designs to be a design goal for actual systems. It should be noted that the finite – time thermodynamic model accounts for irreversibility existing due to the finite temperature difference in the heat exchangers as well as the losses due to non – isentropic compression and expansion in the compressor and expansion device of the system respectively. The thermodynamic model can therefore be modified by including the heat leaks to- and from- the system. The model using the actual refrigeration properties can be reduced to an ideal refrigeration cycle model by eliminating irreversible losses in the heat exchangers and compressor of the system.

Many researchers have focused their attentions on the elimination of the irreversible losses in the heat exchangers and compressors. Klein (1994), published model and data on design consideration for refrigeration cycles. His arguments were based on the work of Stoecker and Jones (1982), which does not include any information about pressure drop in the capillary tube or control devices. Gordon *et al* (1996) presented a model based on the experimental study of the fundamental properties of the reciprocating chillers and their relations to the thermodynamic modelling and chiller design. Their model seems to be popular except for the fact that friction and fouling effects were suppressed in the modelling. Janssen *et al* (1988), reviewed five published models and made comparison among these models. They then presented another model for small refrigerating systems based on theoretical and experimental investigations. Their results, both theoretical and experimental, agreed well. But the model concentrated on heat exchangers alone. The model was based on the conservation equations of mass, momentum and energy. It described the transient response of the fluid inside the heat exchangers. They also assumed a one-dimensional flow, without pressure loss, gravity effects or axial conduction (i.e. high Peclet number). They neglected the kinetic energy of the fluid and viscous dissipation. Their work was improved upon by Chi *et al* (1999), in whose model an expression was derived for the friction factor. In their study a total of 12 fin-and-tube heat exchangers having slit geometry were tested. Based on their work and some previous investigations, a general correlation was proposed to describe the airside performance of the slit fin configuration. The mean deviations of the proposed heat transfer and friction correlation were 5.5 and 3.8% respectively as compared with the work of Mahayana and Xu (1983). Jameel *et al* (1999) reported a model for design and performance evaluation of reciprocating refrigeration system. From the experimental investigations of their model, the characteristic performance curves of vapour compression refrigeration systems were defined as a plot between the inverse Coefficient of Performance ($\frac{1}{COP}$) and inverse of system capacity ($\frac{1}{Q_{evap}}$). The curves were found to be linear and this linear relation between $\frac{1}{COP}$ and $\frac{1}{Q_{evap}}$ is explained in the light of various losses in the system. These losses include: irreversibility due to finite rate of heat transfer in the heat exchanger, non-isentropic compression and expansion in the compressor and expansion valve of the system. The model was used to study the performance of a variable speed refrigeration system in which the evaporator capacity is varied by changing the mass flow rate of the refrigerant while keeping the inlet chilled water temperature constant.

Most of the available models are majorly on either heat exchangers or a single component of the system. There is none of such models that discus the balancing points between the four major components (condenser, evaporator, compressor and the expansion devices) except Stoecker and Jones (1982). This study is carried out to investigate the effect of balanced points on the system design performance.

2.2 Heat Exchangers:

There are three main types of heat exchangers. These are: parallel flow; counter (or cross) flow and mixed flow heat exchangers. What is of paramount importance in refrigeration and air conditioning practice is the type of fin(s) used in the design of heat exchangers. The enhanced fin patterns commonly used for refrigeration and air conditioning applications include: wavy, louver, convex - louver, and slit fins.

One of the popular enhanced fin geometries is the wavy fin. It has long been used in fin-tube heat exchangers because of the superior heat transfer characteristics. There are two basic variants of the basic wavy fin geometry. They may have a smooth wave configuration or they may have a herringbone wave configuration. The herringbone wave has flat sides.

Goldstein and Sparrow (1976) used a mass transfer technique to measure local and average mass transfer coefficients on a fin-tube model having the herringbone wave configuration. Their test simulated a one-row geometry having 606 fins/m on an 8.53 mm diameter tubes. The reports showed that at Reynolds number (based on fin spacing) of 1000, the average mass transfer coefficients were 45 % higher than a flat fin design of the same basic geometry. They concluded that the enhancement results from Goetler vortices that form as the flow passes over the surfaces. The presence of the Goetler vortices was confirmed by the visualization study by Ali and Ramadhyani (1992) in a corrugated channel. A corrugated channel is known to enhance the heat transfer by stream-wise vortices formed from the concave wave surface as well as by space-wise eddies shed from the peaks of corrugated facets (Kim *et al* 1999). Particularly at low Reynolds number, space wise vortices are important to heat transfer enhancement. In a narrow inter fin spacing, space wise vortices may not form as was shown by Ali and Ramadhyani (1992). They claimed that, in a narrow channel vorticity generated at the channel walls is convected and diffused sufficiently rapidly to preclude the formation of a concentrated roll-up vortex. This explains the j-factor over prediction for cores 11 and 12 at low Reynolds number. A correlation was then developed using both sets of data.

Beecher and Fagan (1987) published heat transfer data for twenty three-row plate fin-and-tube geometries. Their cores had staggered tube layout. The tests were conducted using a model consisting of a pair of brass plates that were machined to form the fin-channel geometry. The tubes were simulated by cylindrical cross sectional spacers inserted between the plates. The fins were electrically heated and thermocouples were embedded in the plates to determine the plate surface temperature. The Nusselt number (Nu) data were presented as ($Nu = h_a \frac{D_h}{k}$) versus the Gz (=Graetz number) the Nu_a was based on the arithmetic mean temperature difference (AMTD) rather than on the log mean temperature difference (LMTD). Beecher and Fagan (1987) did not provide pressure drop data. Webb (1990) developed multiple regression correlations based on the Beecher and Fagan data. His correlating equations contain Nu_a and Gz.

Wang *et al* (1995) published experimental data on eighteen wavy fin configurations. They utilized both staggered and in-line tubes with one to four rows. In their work pressure drop data were also presented. They built sample cores and used the same to perform experiments in a forced draft wind tunnel. Heat was supplied to the heat exchanger coil by circulating hot water. They presented the heat transfer data in the form of "j-factor" versus Re_D. Additional pressure drop data on the herringbone wave fin geometry were available from Beecher (1968). His cores had three different fin pattern depths for a fixed fin pattern length of x_f (= 4.58 mm).

One of the available correlations for the herringbone wavy fin configurations is that of Webb (1990). His correlations were based on the Beecher and Fagan (1987) data, which is limited to three-row cores. Webb's correlation is given in the form of Nu_a and Gz, which is not as popular as "j-factor" and Re_D.

Mirth and Ramadhyani (1994) tested five cores with different types of wavy fins. Three cores have smooth wavy-fin on 13.2 mm diameter tubes and a tube pitch (P_t) of 31.8 mm. The other two cores did not have a continuous wavy fins instead, the fins had a relatively large pitch between each pair of waves, with P_t of 38.1 mm. They make use of Beecher (1968) method to develop a correlation from their own data.

Kim *et al* (1997) published data, which deals with heat exchanger having plate fins of herringbone wave configuration. In their work, correlations were developed to predict the airside heat transfer coefficient and friction factor as a function of flow conditions and geometric variables of the heat exchanger. Correlations were also provided for both staggered and in-line arrays of circular tube. A multiple regression technique was used to correlate 41 wavy fin geometries based on Beecher and Fagan (1987), Wang *et al* (1995) and Beecher (1968) works. For the staggered layout, 92% of the heat transfer data were correlated within ±10% and 91% of the friction data are correlated within ±15%.

The airside performance of fin-and-tube heat exchangers having slit geometry is experimentally investigated by Wang *et al* (1999). In their Work a total of 12 fin-and-tube heat exchangers having slit geometry were tested. The edges of the test samples were fixed with sheet metal which was insulated by a 5-mm thick rubber. The effective width (fin area) of the test samples is equal to the width of the test section, and the connection hair-pins are also wrapped with 5 mm thick rubber to minimize the heat loss to ambient air. During the experiment, initial friction loss for airflow without mounting samples was recorded and then subtracted from the total pressure drops to account for the actual pressure drop of the test samples. In their work, the effects of fin pitch and the number of tube row were examined. Their results were compared with test result of louver fin, and plain fin taken from some previous investigations. Their test result indicated that, the heat transfer performance increase with decrease of fin pitch for N = 1 (N = Number of longitudinal tube rows.). However, for N $\geq$ 4, the effect of fin pitch on the heat transfer performance is reversed. In addition to the effect of fin pitch the heat transfer performance decreases with increase of the number of tube row and the friction factor are relatively independent of the number of tube rows. Based on their result and those from previous investigations, a general correlation was proposed to describe the airside performance of the slit fin configuration the mean deviation of the proposed heat transfer and friction are 5.5 and 3.8 % respectively.

Systematic studies of continuous fin-and-tube heat exchangers under dehumidifying conditions were reported by Wang *et al* (1997). The tested fin-and-tube heat exchangers were tension wrapped having a "L" type fin collar. The test conditions were approximate to those encountered with typical fan-coils and evaporators of air-conditioning applications. The test rig consists of a closed – loop wind tunnel in which air is circulated by a variable speed centrifugal fan. The air duct is made of galvanized sheet and has an 850 mm x 550 mm cross-section. The dry-bulb and wet-bulb temperatures of the inlet air are controlled by an air – ventilator that can provide a cooling capacity up to 21.12 kW (or 6 TR). The air flow-rate measurement station is an outlet chamber set up with multiple nozzles based on ASHRAE standard (1998). A differential pressure transducer was used to measure the pressure difference across the nozzles while the air temperature at the inlet and exit zones across the sample heat exchangers were measured by two psychometric boxes. The working medium on the tube side is cold water. A thermostatically controlled reservoir provided the cold water at selected temperatures. The temperature differences on the water side are measured by two pre-calibrated RTDs. The water volumetric flow rate was measured by a magnetic flow meter with a ± 0.001 L/s precision. All the temperature measuring probes were resistance temperature devices (P_t 100), with a calibrated accuracy of ± 0.05 ^{0}C.

The heat exchangers used consist of nine fin-and-tube having plane fins. The effects of fin spacing, the number of tube row and inlet conditions were investigated. Data were presented in terms of j-factors and friction factors (f). It was concluded that the inconsistencies in the open literature may be associated with the wet fin efficiency. A correlation was then proposed for the plate fin configurations. These correlations can describe 92 % of j and 91 % of the f data within ± 10 % as compared with the experimental data.

Both condenser and evaporator were treated together as heat exchanger, except some very few authors that treated them separately under some special conditions.

Jia *et al* (1999) presented distributed model to describe both steady and dynamic behaviours of dry - expansion evaporators. The experimental work was carried out on a full-scale refrigeration system with R-134a as the working fluid and without frost formation at the evaporator. Comparison between the modelling and experimental measurements showed that the drift fluxes flow model gives satisfactory predictions. The simulation results indicated that an even air temperature distribution of the evaporator might be obtained by controlling liquid dry-out point at the two ends of evaporator coil. The study also indicated that, the counter flow configuration provides a higher heat exchanger efficiency with a slower transient response compared with the concurrent-flow (or parallel flow) configuration.

The heat transfer and pressure drop performance of three tubes with many small inner-fins, called micro-fin tubes, having 9.5 mm outside diameter and 8.9 mm maximum inside diameter were reported by Schlager *et al* (1990) using R-22 as the working fluid. The test apparatus had a straight horizontal test section with a length of 3.67 m and was heated or cooled by water circulated in a surrounding annulus. Nominal evaporation conditions were 0 ^{0}C to 5 ^{0}C (0.5 to 0.6 MPa) with inlet and outlet qualities of 10 % and 90% respectively. Condensation conditions were 39 ^{0}C to 42 ^{0}C (1.5 to 1.6 MPa) with inlet and outlet qualities of 90 % and 10 % respectively. Mass flux was varied from 150 to 500 kgm^{-2} s^{-1}. The micro-fin tubes were generally found to have an enhancement of heat transfer ranging from 50 to 100 % when compared to an equivalent smooth heat exchangers. The maximum increase in pressure drop was only 40 %. A model for estimation of pressure drop was then proposed for R22 only.

2.3 Expansion Devices

The last of the basic elements in the vapour compression cycle, after compressor condenser and evaporator, is the expansion device. This serves the following purposes: to reduce the pressure of liquid refrigerant and to regulate the flow of refrigerant to the evaporator. The most common examples of expansion devices are capillary tube and super heat controlled expansion valves. Other examples include, float valve and constant pressure expansion valve.

Liquid refrigerant enters the expansion device and as it flows through, the pressure drops because of friction and acceleration of the refrigerant, as a result some refrigerants flash into vapour. The compressor and the expansion device must search for a common suction pressure, which allows them to pass equal mass rates of flow. The balancing point for the two must be located on standard chart or determined by calculation. Capillary tube will be employed in this model and design.

The main function of capillary tube expansion device is to maintain the minimum possible pressure in the condenser at which all the refrigerant can condense without choke flow (Stoecker and Jones, 1982).

The capillary tube, although physically simple, is behaviorally complex. Some items of complex mathematical analysis include the friction factor for the two phase flow, the thermal contact with the suction line, the metastable flow, the oil circulation with the refrigerant to mention a few. Many researchers have investigated the flow through a capillary tube and a review on the subject can be found in the works of Melo *et al*, (988); Schultz, (1985); Stoecker and Jones, (1982); and Jung *et al* (1999).

Melo *et al*, (1988) reported a simplified capillary tube model, which takes into account some of the factors that influence the flow rate of refrigerant along the tube. They argued that if all the factors have to be considered an enormous CPU time would be required. They therefore, decided to develop a first stage model based on some assumptions.

Jung *et al* (1999) reported a model of pressure drop though a capillary tube in an attempt to predict the size of capillary tubes used in residential air conditioners and also to provide simple correlating equations for practicing engineers. In their work, Stoecker's basic model was modified with consideration of various effects due to subcooling, area contraction, and different equations for viscosity and friction factor, and finally mixture effect.

The model was validated with experimental data for CFC-12, HFC-134a, HCFC-22 and its alternatives viz; HFC-134a, R-407c. Performance data were generated for HCF-22 and its alternatives viz; HFC-134a, R-407c and R-410a under the following conditions: condensing temperature; 40 ^{0}C, 45 ^{0}C, 50 ^{0}C, 55 ^{0}C, subcooling; 0 ^{0}C, 2.5 ^{0}C, 5^{0} C, capillary tube diameter of; 1.2 to 2.4 mm, mass flow rate; 5-50 g/s. These data proved that the capillary tube length varies uniformly with the changes in condensing temperature and subcooling. A regression analysis was performed to determine the dependence of mass flow rate on the length and diameter of capillary tube' condensing, temperature and subcooling. As obtained for two pure and two mixed refrigerants examined in their work the simple practical equations developed, coupled with McAdam's equation for the two-phase viscosity and Stoecker's equation of the friction factor, yielded a mean deviation of 2.4% for 1488 data.

2.4 Refrigerants

Over the years so many different substances have been used as refrigerants. A considerable number of practical experiences exist regarding the properties which are important to the production of reliable, safe and cost effective installations under varying conditions of applications. These properties are classified into two broad groups:

- Thermodynamic and transport properties, basic to the engineering design of the plant, its operational performance and energy economy.
- Chemical and physiological properties, deciding the choice of construction materials and measures to ensure safety.

Although, there are other practical considerations to be accommodated such as ease of leak detection, relation to oil and cost price etc.

The relevant thermal properties (thermodynamic and transport) may be specified in a large number of individual data. Examples of such listing can be found in textbooks and journals (Stoecker and Jones, 1982; McLinden and Didion, 1988). The essential criteria can be summarized in three crucial points:

- Vapour pressure level
- critical temperature
- Molecular mass.

While the influence of chemical and physiological properties centers around:

- Compatibility with machine building materials
- Effects on the external environment
- Poisonousness, suffocation and warning properties (e.g. smell)
- Inflammability and explosion hazard.

The latter two points define the safety measures which will be required. There is no available detail on how the emissions of CFC are distributed on the various types of plant world wide except for USA, which was believed to be responsible for about one-third of the total emission. But it has been established that about 30 % of potentially ozone depletion chemicals, are used as refrigerants (Statt, 1988; Kutter, 1988).

The much-cited Rowland and Molina publication of 1974 which predicted a rapid breakdown of the ozone in the upper atmosphere by the release of fully saturated Chloro-Fluoro-Carbon (CFC) compounds, started an intensive and often emotional discussion world wide. Environmental organization in many countries were pressurized to restrict the use of such substances. As a result, extensive investigations and modelling of chemical reactions which are responsible for the ozone balance between its continuous creation and destruction have been carried out (Segelstard, 1998; McMullan, 2002; Foerg, 2002 and Calm, 2002). These efforts agreed that most of the previous results, greatly exaggerate the risk and predict a much more modest rate of possible breakdown. These brought about the Montreal Protocol of September 1987, which fixes a requirement of a 20 % reduction for the important CFC refrigeration except R-22 as from 1- July, 1993, 50% from 1998 while some countries are planning for an even more rapid reduction (Lorentzen, 1988a and b).

These lead to the search for alternatives to R-11 and R-12. Many of the apparent alternatives have to be eliminated, for reasons of their incompatibility with thermodynamic, transport, chemical and physiological properties. R-134a, R-22, R-124, R-142b and R-152a are close alternatives to R-12, while R-123 and R-141b are close alternatives to R-11. The most important problem is the immiscibility of these alternatives with naphthenic and paraffinic oils now in use. Extensive work is being done to identify new oil for R-134a (Kutter, 1988; Foerg, 2002). Also studies have shown that the refrigerant critical temperature, vapour and heat capacity are the key thermodynamic criteria in determining the performance of the theoretical vapour compression cycle. For a fixed set of condenser and evaporator temperatures, as the critical temperature is increased the volumetric heating or refrigerating capacity (defined as the capacity per unit volume of refrigerant vapour entering the compressor) decreases (McLinden and Didion, 1988). This invariably affect the COP. This points out the fundamental trade off between high capacity and high efficiency one must face in choosing refrigerant alternatives. In order to have a similar capacity, efficiency and operating pressure, a replacement refrigerant will need to have a similar boiling point temperature. In this search for the fully halogenated CFC refrigerants, thousands of compounds have been investigated (Lorentzen, 1988b). It has been demonstrated both by theoretical and empirical reasoning that this same class of compound – the chlorofluorocarbons – remains the clear choice by virtue of their stability, excellent thermodynamic, health and safety characteristics and familiarity to both manufacturers and users (Calm, 2002). However, some of the presently used CFCs are no longer acceptable because of environmental considerations. Out of the most promising replacements which are receiving much attention are R-22, R-134, R-134a, R-152 and R-152a. Only R-134, R-134a, R-152, and R-152a are hydrogen – containing and non-flammable, but their toxicity testing is incomplete but promising (Shankland *et al*, 1988; Foerg, 2002).

2.5 Emission and Environmental Impact

The primary global environmental impacts from air-conditioning and refrigeration (ACR) systems arise from emissions of refrigerants and of gases associated with energy use. These gases are usually released at the power plants that provide the electricity, steam or hot water used in manufacturing, transportation, installation, operation, services and ultimately to dispose of the equipment and ancillary devices. Of the total, the most significant impacts stem from the release of refrigerants and of combustion emissions to provide operating power. Specifically, discharge or leakage of stable refrigerants containing chlorine, bromine and other halogens, though generally negligible, affects the stratospheric ozone equilibrium. Likewise, both the common refrigerants and the combustion products, notably carbon dioxide (CO_2) and to a lesser extent nitrous oxide (N_2O_x), act as green house gases (GHGs). The release of refrigerants have multiple effects, variously including ozone depletion following breakdown, direct action as GHGs, and efficiency reduction leading to increased energy use. The performance reductions occur with departures from the optimal charge or-for refrigerant blends- charge and composition. Hence, the critical issues in addressing stratospheric ozone depletion and climatic changes for ACR systems come down to selection of refrigerants that minimize impacts, reducing their release and increasing net efficiencies to lower energy-related GHG emissions.

The severe consequences of ozone depletion are being averted through international adherence to the Montreal Protocol. The levels of chlorine and bromine reaching the stratosphere, referred to as chlorine-bromine loading (CBL) have peaked or are now peaking, and the ozone layer has begun or soon will start to recover (Calm, 2002). The outlook for global warming and the severity of its consequences are far more threatening. Even if releases stopped for all other GHGs, carbon dioxide emissions from energy use still would increase in concert with foreseen economic improvement in developing countries and with population growth (Ko *et al*, 1993). Whereas the net carbon dioxide impact overshadows the combined effects of all other GHGs, reduction in energy demands and efficiency improvement are crucial. As a minimum, no changes that decrease efficiency can be deemed acceptable.

The functional measures for the Montreal and Kyoto Protocols (beyond those addressing scientific assessments and international assistance) differ. The Montreal Protocol restricts the production of the individual chemicals of concern, leading to their ultimate phase-out for most uses. The Kyoto Protocol imposes national limits on emissions of important GHGs, but does so by a collective approach encompassing six specific gases or groups of gases. The most critical gas among them is CO_2. Although they have a much lower impact, namely 1.4% of the total for USA at present (McMullan, 2002). HFCs and PFCs (Perfluorocarbon) as groups constitute two of the six GHGs in the Kyoto Protocol. Some analysis project that their impact will reach 4 – 10 % of the global total by the year 2100 and double that if not controlled (Ko *et al*, 1993).

The measure to reduce refrigerant releases are therefore not limited to CFCs, HFCS, HCFCs and PFCs. Many of them also are applicable to ammonia, carbon dioxide, hydrocarbons, and other nonfluorocarbon refrigerants (Adegoke, 2002). Their release could increase flammability or toxicity hazards, risk pressure injuries, degrade system reliability, or exacerbate other environmental problems. For instance, hydrocarbon emissions may contribute to local smog formation; such releases will be concentrated in urban areas in which smog problems are most acute. Released ammonia that is washed into the surface water by rain is highly toxic to aquatic life, and most importantly, loss of refrigerant from vapour-compression machines, or air leaks into sub-atmospheric equipment reduces operating efficiency and thereby increases energy use and GHG emissions.

It has been pointed out that, the direct effects of refrigerant emissions amounts to only 3 – 5 % of the annual total for chillers using R-22, which is one of the refrigerants with highest Global Warming Potential (GWP) (Calm, 2002). Therefore from comparative warming and or total equivalent warming impact (TEWI) perspective, the phasing out of the HCFCs and HFCs provides only a small gain in the refrigerants related warming component.

Calm and Didion (1998) presented a detailed analysis that showed that there were no known ideal refrigerants. According to this report such fluids would offer zero ozone depletion, zero global warming, high efficiency, very low toxicity, no flammability and high chemical and thermal stability. The reference also provides a rationale based on thermodynamics and chemical composition to suggest that the elusive ideal refrigerant probably does not exist.

The first generation refrigerants (1830s to 1930) were retired for safety reasons, (Sand *et al*, 1997). They were selected based on equivalent GHG emissions versus less than a 0.001% increase in peak ozone impact.

It is highly probable that R-123 (an HCFC) and possibly other short-lived CFC replacements would have survived restrictions for stratospheric ozone protection had the global warming response occurred first. With keener awareness of the more-limited options remaining, the framers of the Montreal Protocol might then have been more cautious in rejecting chemicals with indiscernible ozone impacts and offsetting environmental benefits.

Likewise, phaseout of HFCs from the refrigeration industrial use for very small benefits in direct (refrigerant-related) warming impacts at the expense of greater CO_2 and N_2O emissions will increase rather than decrease net warming.

The key distinction that makes most ACR applications and especially chillers unique from other HCFC, HFC and PFC uses is that the refrigerant is used in closed systems with very low life-cycle release rates. Most of the refrigerant can be and is being recovered upon ultimate equipment retirement. A second difference, at least for R-123 and HFCs, is that abandoning these proven options would increase the GHG emissions from associated energy use.

Therefore, the importance of a refrigerant's ODP or GWP diminishes with very low loses. For refrigerants with low ODP and low GWP, the most damaging environmental effects from refrigerant losses is suboptimal operation resulting in increased energy use and, thereby availability and thermal suitability. Some, such as ammonia and hydrocarbons, survived or were later revived for limited applications in which their risks were manageable, such as industrial or small-charge systems. Most second generation refrigerants (1930s to 1990s) have been or are being retired to protect the stratospheric ozone layer. They were selected for safety, durability and performance. The criteria for third generation refrigerants ("Alternative refrigerants") include both safety and environmental issues. Whereas the first generation lasted approximately 100 years and the second generation lasted approximately 60 years, care is needed in dismissing options with minor defects if manageable. According to Calm, (2002) the third generation will be more vulnerable as the global population increases, industrial and economic development expands and environmental understanding increases. These considerations demand greater attention to atmospheric lifetime to ensure that the error made with CFCs and halons, namely releasing large quantities of long-lived compounds before discovering their impacts, were not repeated. Likewise, more attention is required for containment and recycling instead of phasing out.

According to Calm *et al*, (1999), there is no common denomination to equate the demerits of ozone depletion and global warming. It is clear however that a 13-19% increase in global warming to switch from R-123 to R-134a, at the best performance levels, is more significant than a 0.002% or lower peak impact on ozone depletion. This comparison is more dramatic for newer data, namely increases of 14 – 20 % carbon increased emission of CO_2 and other GHGs to power the system. Suboptimal efficiency thus exacerbates climate change even with zero-GWP refrigerants. Any refrigerant substitution that lowers overall efficiency is likely to have more adverse impacts than benefits based on net global warming impacts (e.g., life-cycle GHG emission or TEWI).

2.6 Model.

The common procedure in most of the compressor and/or refrigerator manufacturing companies in establishing dynamic behaviour of a vapour compression refrigerator is to perform experimental test to ascertain the refrigerator's performance as a function of time. This normally requires a long period of time. One way to speed up such procedure is to employ computational techniques to numerically simulate the refrigerator performance.

Since the dynamic modelling of the refrigerator requires each element of the refrigeration system to be considered in depth, the model allows not only the simulation of the experimental tests but also helps to develop a deep understanding of the fundamental processes occurring.

Most of the models, published in the open literature are directed towards heat pump simulation and only very few of them are experimentally validated (Melo *et al*, 1988). The model, now considered in this study, is limited to the reciprocating compressor, condenser, accumulator, capillary tube and evaporator system. This model combines many of the features presented in earlier models while modifying and introducing several features.

CHAPTER THREE

3.0 BASIC THEORY AND MODEL DEVELOPMENT

This section describes basic theory required in the model development and the development of the model itself.

3.1 Theory and Modelling

3.1.1 System Modelling:

The development of refrigeration system models, which simulates the actual working of vapour compressing cycle system components –viz, compressor, condenser, evaporator and the expansion device has been the goal of many researchers (Klein, 1994; Gordon *et al*, 1996; Stoecker and Jones, 1982, Kuehn and Liang, 1991). The simplest model is the Carnot model which, represents an ideal refrigeration cycle without any irreversible losses. The Carnot cycle is one whose efficiency cannot be exceeded when operating between two given temperatures. It consists of reversible processes which make its efficiency higher than could be achieved in an actual cycle. This cycle is very important for two reasons:

(i) it serves as a standard of comparison;

(ii) it provides a convenient guide to the temperature that should be maintained to achieve maximum effectiveness;

The Carnot cycle is considered to be a design goal for actual systems. For the reasons of reversibility processes in Carnot cycle- the thermodynamic model must account for irreversibilities existing due to the finite - temperature difference, in the heat exchangers [evaporator-isothermal addition; condenser - isothermal rejection of heat] as well as the losses due to non-isentropic compression and expansion in the compressor and expansion device of the system respectively. This can be accomplished by using actual refrigeration state properties.

Equations of state were developed which were temperature and pressure dependent for each of the components. In as much as these components cannot work in isolation, computer programs were written to compute "balanced points" for the components, which of cause, is the design point. In order to get those balanced points, the performance characteristics of each of the components were modeled in such a way that each of them depends on temperature only. The intersection of corresponding curves indicates the condition at which the performance characteristics of the components are satisfied; it is at this point that the system composed of these components will operate effectively.

Khan and Zubair, (1999) presented performance data for the components of a vapour-compression refrigeration system. The data for the refrigeration capacity (Q_e) and the power requirement (P) were presented as shown in equations (3.1) and (3.2) respectively.

$$Q_e = c_1 + c_2T_1 + c_3T_1^2 + c_4T_2 + c_5T_2^2 + c_6T_1T_2 + c_7T_1^2T_2 + c_8T_1T_2^2 + c_9T_1^2T_2^2 \quad (3.1)$$

$$P = d_1 + d_2T_1 + d_3T_1^2 + d_4T_2 + d_5T_2^2 + d_6T_1T_2 + d_7T_1^2T_2 + d_8T_1T_2^2 + d_9T_1^2T_2^2 \quad (3.2)$$

The constants applicable to equations (3.1) and (3.2) were determined by equation – fitting procedure into the catalogue data of a specified compressor to develop a set of nine simultaneous equations to find the values of c and d (Stoecker and Jones, 1982). The numerical values are given in Table 3.1.

Table 3.1 Numerical values for constants in equations (3.1) and (3.2).

Subscript Number	c	d
1	137.402	.00618
2	4.60437	-0.893228
3	0.061652	-0.01426
4	−1.118157	-0.870024
5	− 0.001525	-0.0063397
6	−0.0109119	0.633887
7	−0.00040148	0.00023875
8	−0.00026682	-0.00014746
9	0.000003873	0.0000023876

The heat absorbed by the evaporator and the heat added by the compressor must be rejected at the condenser. Therefore, the rate of heat rejection required at the condenser (Q_c) cannot be less than the sum of the refrigeration capacity and the compressor power for a given combination of evaporating and condensing temperatures. This is given by equation (3.3).

$$Q_c = Q_e + P \qquad (3.3)$$

Condenser performance for an air-cooled condenser using refrigerant 22 is given by equation (3.4), (Khan and Zubair, 1999; Stoecker and Jones, 1982)

$$Q_c = 9.39\ (T_2 - T_a) \tag{3.4}$$

3.1.2 Condensing Unit

Equation (3.1) is the model for vapour compression system capacity while equation (3.2) gives the required power and equation (3.3) is the model for condenser performance. Fig. 3.1 shows the nomenclature for condensing unit modelling. All these equations are based on condensing-, and evaporating- temperatures only, while equation (3.4) is based on the condensing and ambient temperatures. The first thing to do in this analysis is to combine the components, in order to get balanced point, (a balanced point is a point of agreement between two components). A balanced point between the condenser and the compressor forms a "condensing unit". It is more comfortable to combine condenser and compressor to form the condensing unit because both of them work on the high-pressure side. The condensing unit was later combined with evaporator and finally with the capillary tube (the expansion device) to form or model the complete system.

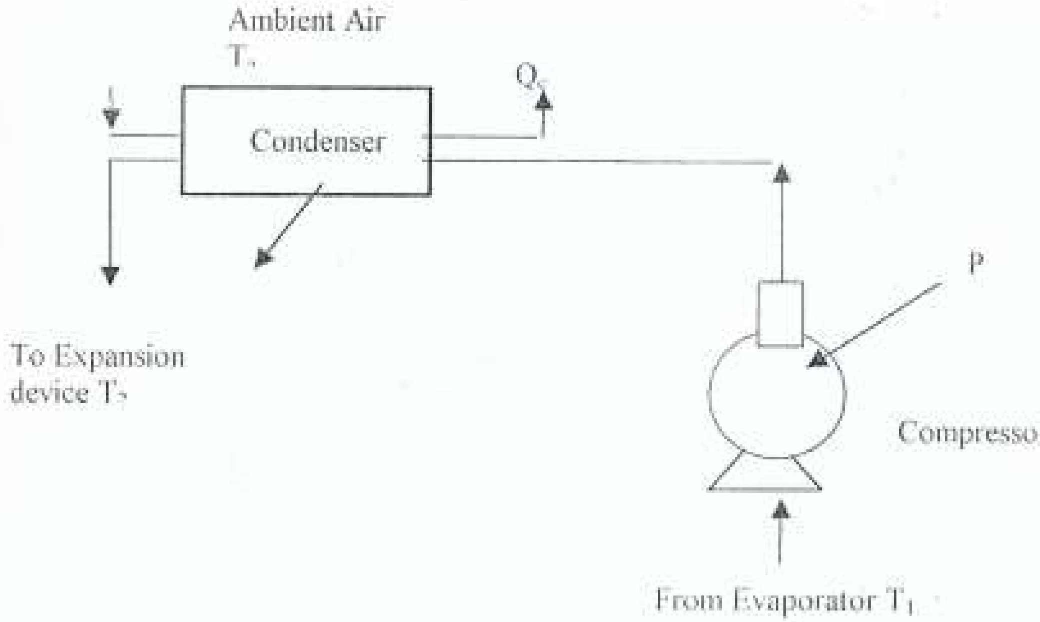

Fig. 3.1 A Schematic Diagram of a Condensing Unit.

The balanced point between compressor and condenser (or the condensing unit) is therefore a set of data (P, Q_e, Q_c, T_2, T_1) at a given "T_a" that simultaneously satisfy equations (3.1) to (3.4). This constitutes a number of iterations and is as show in Fig (3.2), with the variation of T_a and T_1. The program is as shown in Appendix I, while balancing points for various condensing temperatures are shown in Fig. 3.3.

3.1.3 Complete System

The next step is to combine evaporator with condensing unit (Fig. 3.4). In this respect, a model representing the performance of an evaporator is required.

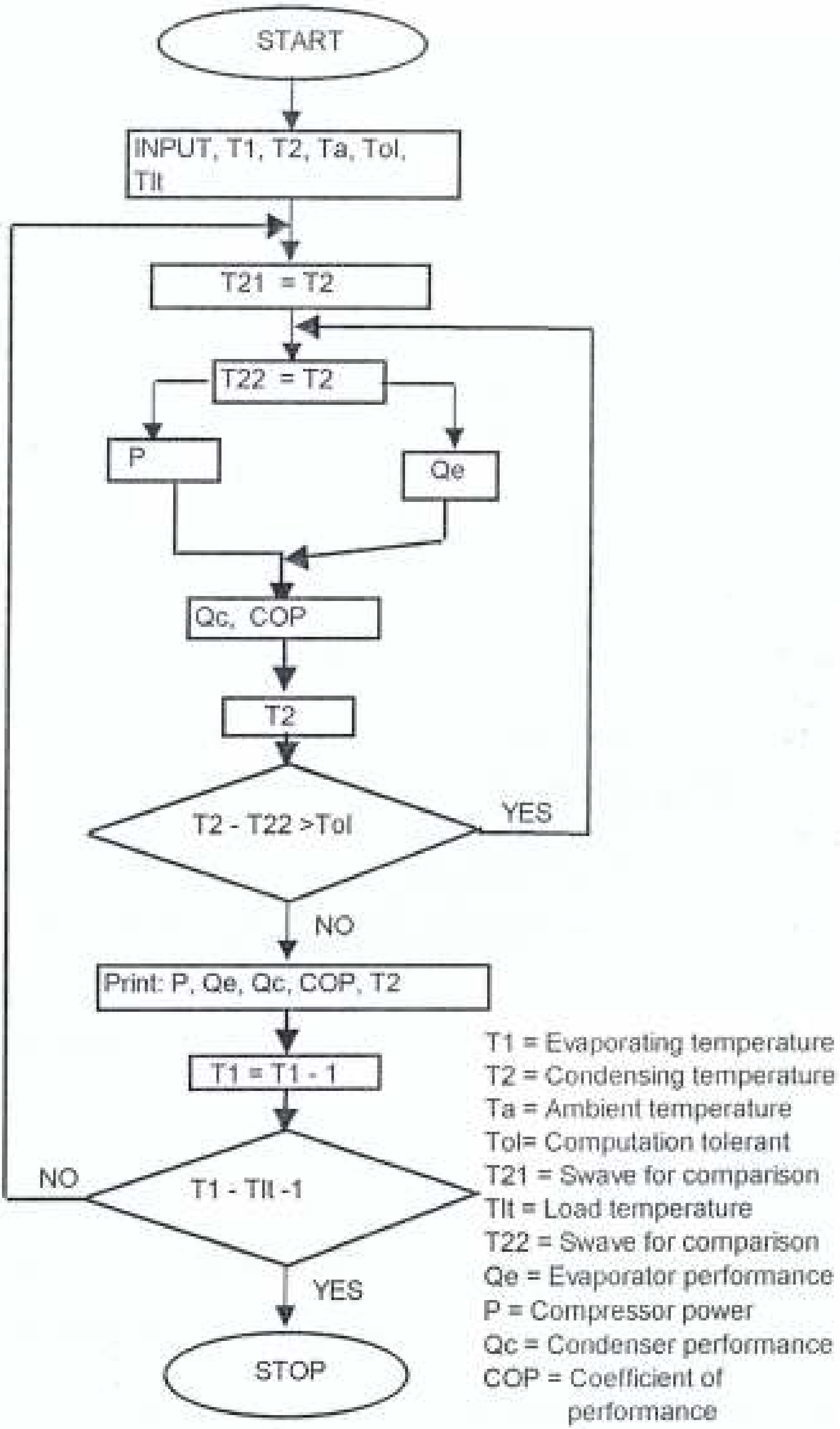

Fig. 3.2 Flow Chart for Condensing Unit

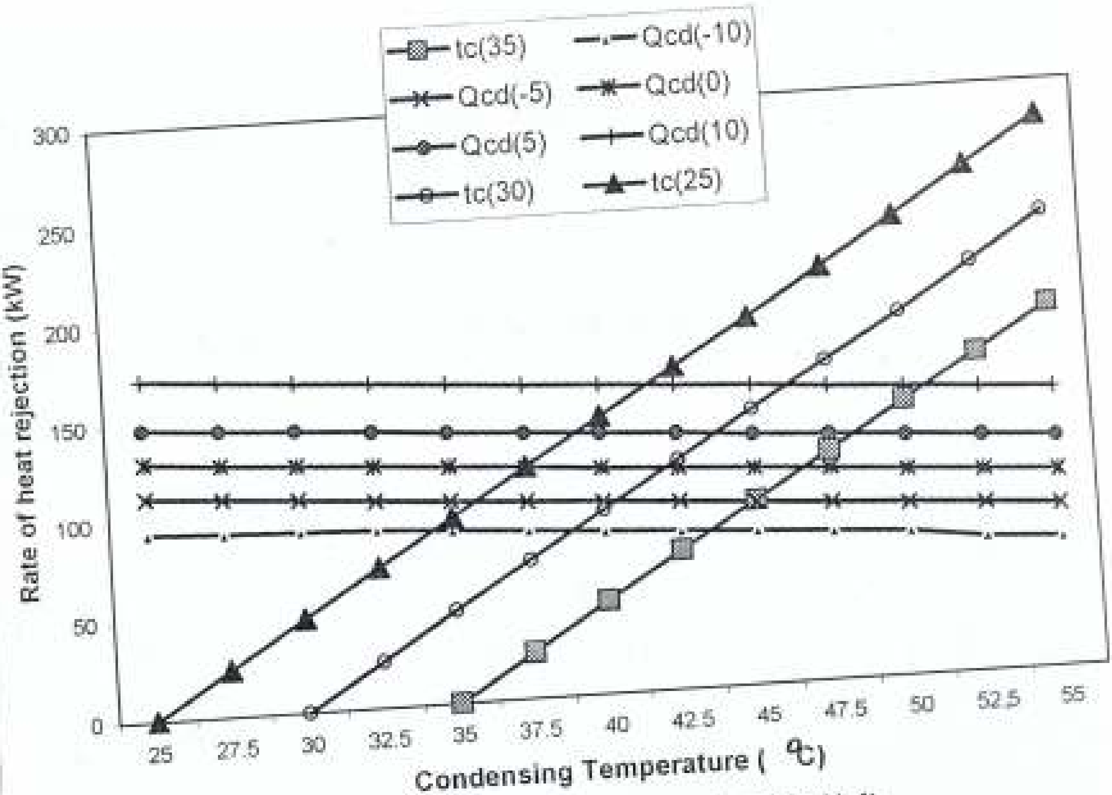

Fig. 3.3 Balancing Points for Condensing Unit

There are lots of models to this effect two of which are:

Stoecker and Jones (1982) $$\left\{\begin{array}{l} Q_e = G(T_w - T_1) \\ G = 1 + 0.046(T_w - T_1) \\ Q_e = 6\left[1 + 0.046(T_w - T_1)\right](T_w - T_1) \end{array}\right\} \quad (3.5)$$

Khan and Zubair (1999) $$Q_e = 8.20(T_w - T_1) \quad (3.6)$$

The result of Stoecker and Jones and Khan and Zubair are more accurate compared with theoretical system (ASHRAE, 2002). The Stocker and Jones' model was about 22.6 %, while that of Khan and Zubair was about 25.30% below the theoretical values. Data were generated using Stoecker and Jones model and equation of the form shown in equation (3.7) was fixed.

$$Q_e = a + bT_1 + cT_1^2 + dT_w + eT_w^2 + fT_1T_w^2 + gT_1^2T_w + hT_1^2T_w^2 \quad (3.7)$$

The constants "a to h" were determined by substituting values for Q_e and T_1 at constant T_w.

Some of these constants were found to be too small and the effects were neglected. The equation was reduced to a simple quadratic equation (3.8).

$$Q_e = aT_1 + bT_1^2 + c \quad (3.8)$$

Where:
$$\left\{\begin{array}{l} a = 0.276 \\ b = 6.0 - 0.552T_w \\ c = 0.276T_w^2 - 6T_w \end{array}\right\}$$

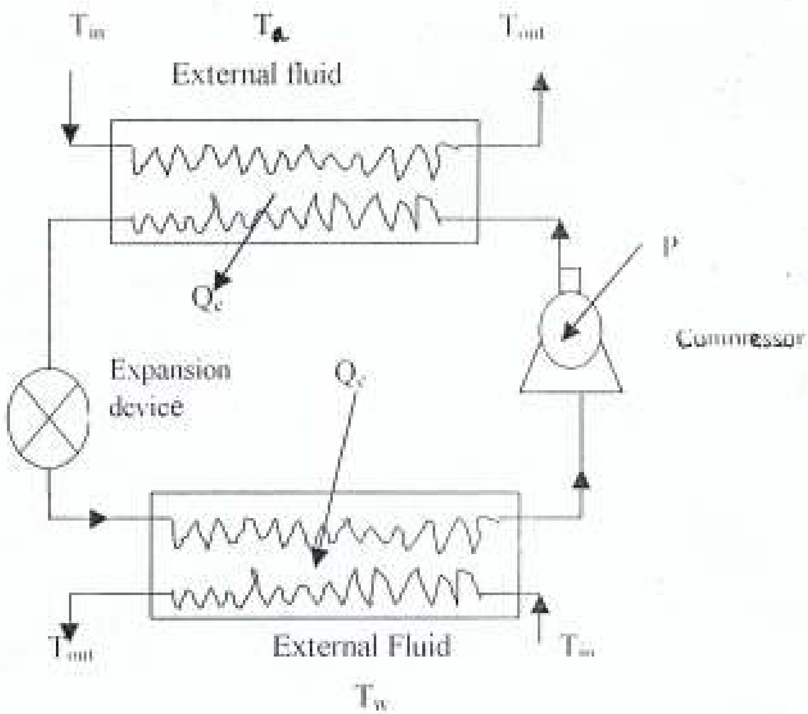

Fig. 3.4.A Schematic Diagram of a Complete Refrigeration System.

The performance was found to be 20.78 % below the theoretical values. This result is as indicated in Fig. 3.5.

A balancing point between the condensing unit and equation (3.8) forms a complete vapour compression system. The flow chart for this system is shown in Fig.3.6. The program is given in Appendix II, while the balancing points are shown in Fig. 3.7.

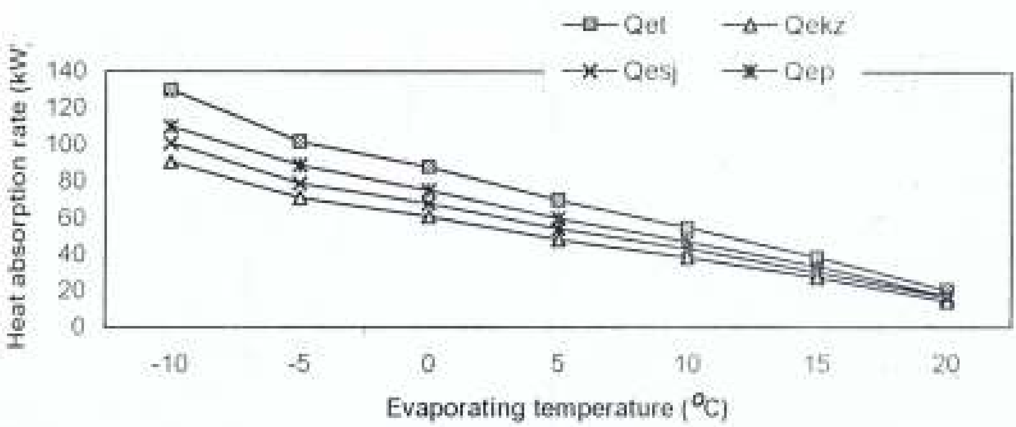

Fig.3. 5 Comparison of Evaporator performance

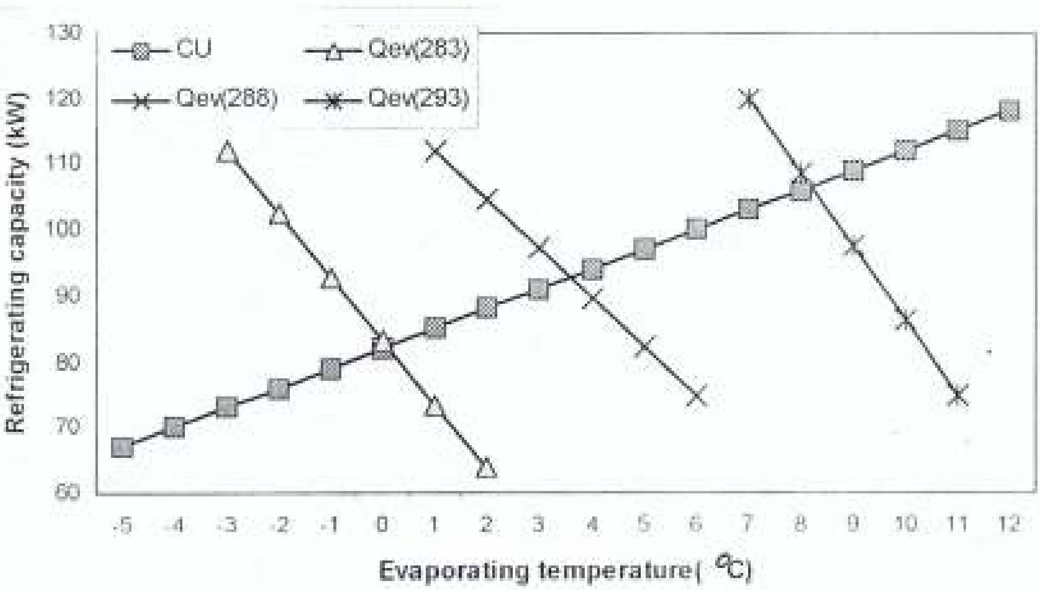

Fig. 3.7 Balancing Points for Complete Unit (CU)

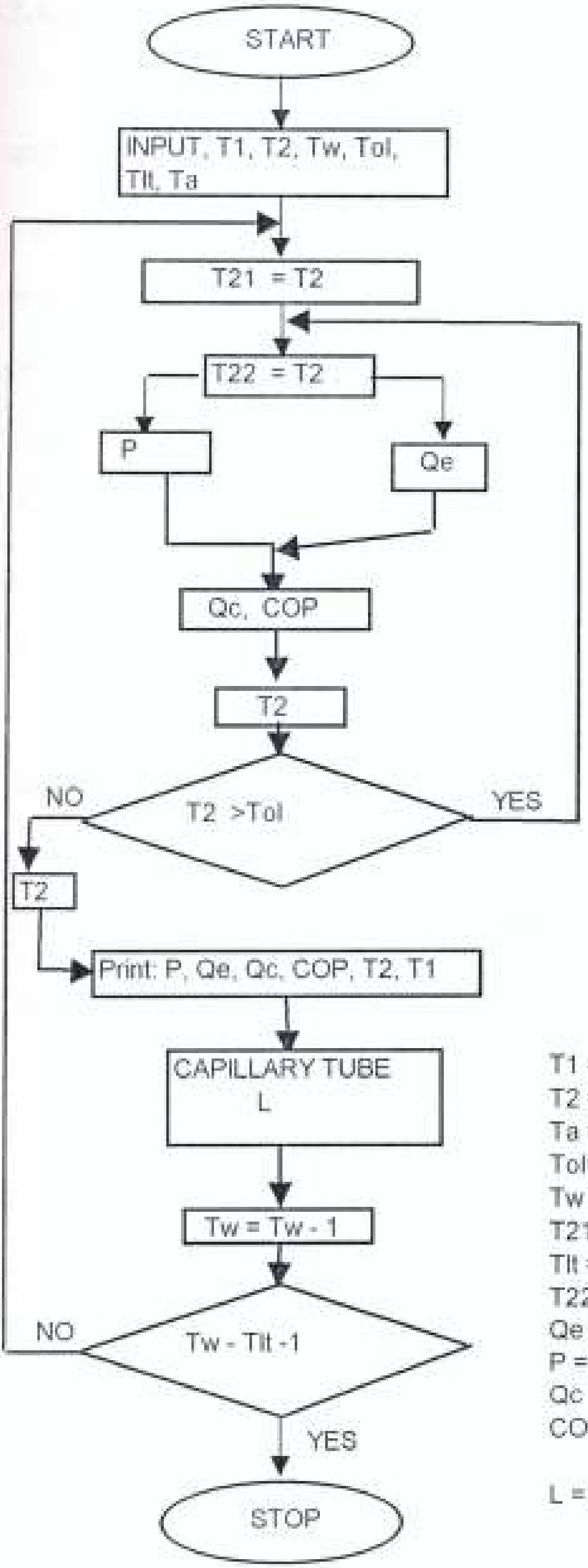

T1 = Evaporating temperature
T2 = Condensing temperature
Ta = Ambient temperature
Tol= Computation tolerant
Tw = Water temperature
T21 = Swave for comparison
Tlt = Load temperature
T22 = Swave for comparison
Qe = Evaporator performanc
P = Compressor power
Qc = Condenser performanc
COP = Coefficient of performance
L = Capillary tube length

Fig. 3.6 Flow Chart for Complete System

3.1.4 Capillary Tube Model

3.1.4.1 Preamble

The next approach is to find a means of reducing high pressure and the temperature from the condensing unit to the working pressure and temperature of the evaporator since they work on different pressure and temperature levels. This can be done through several means, for example, capillary tube, expansion valve, EEV (Electronic Expansion Valve) etc. In this work capillary tube was used for the following reasons:

i It is simple

ii It is not expensive

iii It requires low starting torque for the compressor.

Capillary tube has one disadvantage of reducing cycle efficiency when load condition changes abruptly, because the capillary tube does not have any functional element to actively adjust to this sudden load change. This situation was catered for by taking readings at steady state; also several readings were taking and the average recorded.

From the literature, the model developed by Stoecker and Jones (1982) and Jung *et at* (1999) are among the best capillary tube models used in refrigeration systems. Actually, Jung *et al*'s model was a modification of Stoecker and Jones' model. These two models were reviewed with other available models (Fukuta *et al*, 2002; Sahin and Kodal, 2002; Chen *et al*, 2002; Kim *et al*, 2002) to develop the model presented in this work.

These two basic models [Stoecker and Jones and Jung *et al*] ignored the influence of kinetic energy. However, if this effect is neglected in the other sections of the system it may not actually be neglected in the capillary model for the following reasons:

(i) As a result of smaller cross-sectional area there is a considerable increase in refrigerant velocity through the capillary.

(ii) The quality at the entrance is not the same as that at exit. Hence there is a strong possibility of two-phase flow.

(iii) Flow in capillary (especially when the two phase flow sets in) is purely turbulent (Hopkins, 1996)

(iv) If the kinetic energy portion is neglected a shorter capillary length will be required for sonic flow resulting in high evaporator temperature and hence a reduction in the system capacity (Spauschas, 1987b).

Furthermore, both models still neglected the influence of pressure drop and fouling factor. These three factors neglected by the available models are hereby taken into consideration.

In a capillary tube however, there are two major dimensions that have to be considered in the design. These are the length and the internal diameter of the capillary tube. In most of the available models one of these dimensions is kept constant (mostly the internal diameter) while the other is determined either theoretically or experimentally. The diameter is usually kept constant because pipes or tubings are produced according to certain standard codes. Determination of the capillary length therefore depends on the following factors:

(i) Thermodynamic properties of the refrigerant

(ii) The condensing and evaporating temperatures.

(iii) The condensing and evaporating pressures and

(iv) The mass flow rate

The limitation in the determination of the length of capillary tube is the point at which the flow in the capillary becomes sonic (i.e. choked flow or when the Mach number becomes unity), (Stoecker and Jones, 1982 and Jung et al, 1999). From ASHRAE handbook (2002), it could be understood that for a given internal diameter the required length should be at most that to obtain sonic flow.

3.1.4.2 The Modelling of the Capillary Tube

The following assumptions were made:

(i) The mass flow rate ($\dot{m}$) is constant.

(ii) Adiabatic condition prevailed in the capillary tube, (Kim, *et al*, 2002; Wijaya, 1992; Chang and Ro, 1996; ASHRAE handbook (2002)).

Fig. 3.8 shows a representation of the capillary tube used for this analysis.

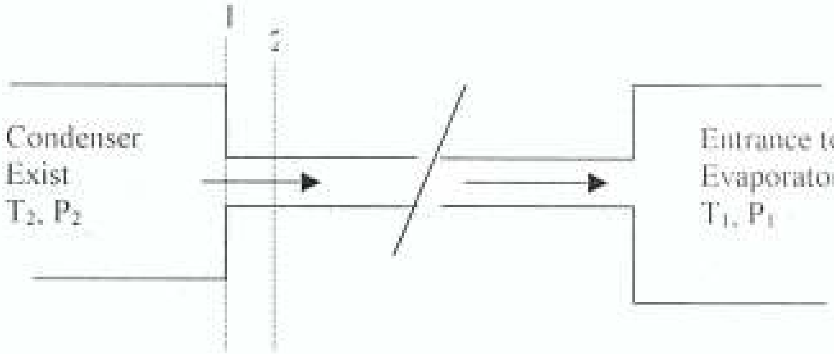

Fig. 3.8 Capillary tube

At steady state, the mass flow rate ($\dot{m}$) is assumed to be constant therefore the mass flow equation can be written as follows:

$$\dot{m} = \frac{V_1 A}{v_1} = \frac{V_2 A}{v_2} \tag{3.9a}$$

or

$$\frac{\dot{m}}{A} = G = \frac{V_1}{v_1} = \frac{V_2}{v_2} \tag{3.9b}$$

$$V = Gv \tag{3.10}$$

A = cross sectional area (m^2)

Where: v is the humid volume (m^3/kg) (= v_f at the entrance to the capillary tube)

G is the mass flux (kg/(m^2s)

Since an adiabatic condition is assumed in the capillary tube, then an energy equation can be written as follows, (Jung et al, 1999)

$$500h_1 + \frac{V_1^2}{4} = 500h_2 + \frac{V_2^2}{4} \tag{3.11}$$

While the momentum equation can be written as:

$$\dot{m}(V_2 - V_1) = \left\{(P_1 - P_2) - f\frac{\Delta L V^2}{2Dv}\right\}A \qquad (3.12a)$$

or

$$\frac{\dot{m}}{A}(V_2 - V_1) = \left\{(P_1 - P_2) - f\frac{\Delta L V^2}{2Dv}\right\} \qquad (3.12b)$$

or

$$G(V_2 - V_1) = \left\{(P_1 - P_2) - f\frac{\Delta L G^2}{2D}v_m\right\} \qquad (3.12c)$$

(v_m is the average humid volume, as defined in equation (3.15))

$$L = \sum_{i}^{n} \Delta L \qquad (3.12d)$$

Equation (3.12) (modified from Stoecker and Jones, 1982) is therefore a balancing of forces due to pressure difference and friction (right hand side) and acceleration (left hand side). From this equation (3.12), the design length "L" of the capillary is to be calculated. This length strongly depends on pressure variation, friction factor, flow velocity and humid volume.

Though, the enthalpy remains constant as a result of continuous flow of refrigerant (adiabatic situation) but there will be a progressive decrease in pressure. This results in refrigerant becoming two phase and hence the quality increases with capillary length. The humid volume and the enthalpy of the two-phase fluid region were determined by equations (3.13) and (3.14) respectively.

$$v = (1 - x)v_f + xv_g \qquad (3.13)$$

$$h = (1 - x)h_f + xh_g \tag{3.14}$$

Since the velocity (V), friction factor (f) and specific volume (v) in equation (3.12) changes as the refrigerant flows from point (1) to point (2) (see Fig. 3.8) the mean values of these parameters are used in the computation. This is as given in equations (3.15), (3.16) and (3.17) respectively.

$$v_m = \frac{v_1 + v_2}{2} \tag{3.15}$$

$$f_m = \frac{f_1 + f_2}{2} \tag{3.16}$$

$$V_m = \frac{V_1 + V_2}{2} \tag{3.17}$$

The factor left in the determination of "ΔL" from equation (3.12c) is the friction factor (f). Hopkin (1996) observed that the refrigerant flow through a capillary tube is turbulent. He then obtained a relationship between the friction factor and Reynolds number using Moody chart in conjunction with Stoecker and Jones report. Hopkin's equation of friction factor is as shown in equation (3.18).

$$f = \frac{0.217}{\mathrm{Re}^{0.1}} \tag{3.18}$$

where:

$$\mathrm{Re} = \frac{V_m D}{\mu . v} \tag{3.19}$$

where: $v = \frac{1}{\rho}$ (specific volume)

Since the flow of refrigerant is in two phase, the following equation can be used to determine dynamic viscosity coefficient (μ), (Stoecker and Jones, 1982).

$$\mu = (1-x)\mu_f + x\mu_g \tag{3.20}$$

To determine quality (x) equations (3.10), (3.13), (3.14) and (3.20) are combined with equation (3.11), these result in equation (3.21).

$$1000h_{f2} + 1000h_{fg2}x_2 + G^2\frac{(v_{f2} + v_{fg2}x_2)^2}{2} = 1000h_2 + \frac{V_1^2}{2} \tag{3.21}$$

Equation (3.21) is solved for x_2 [x_1, is assumed to be zero-saturated or subcool liquid leaving the condenser] the quality at the state point (2). For the purpose of the computer modelling the program will be terminated at the point where the Mach number becomes unity. Hence, for the dynamic states, the Mach number (M_ϕ) as expressed by Jung *et al* (1999) (equation 3.22) is:

$$M_\phi = \left\{G^2\left[x\frac{dv_g}{dp} + (1-x)\frac{dv_f}{dp} + v_{fg}\left(\frac{dx}{dp}\right)_h\right]\phi\right\}^{\frac{1}{2}} \tag{3.22}$$

where:

$$\phi = \left[1 + G^2\frac{v_{fg}(v_f + xv_{fg})}{h_{fg}}\right] \tag{3.23}$$

Equation (3.22) was modified for steady state- condition; this is given in equation (3.24).

$$M_\phi = \left\{G^2\left[x\frac{v_{g1} - v_{g2}}{P_1 - P_2} + (1-x)\frac{v_{f1} - v_{f2}}{P_1 - P_2} + v_{fg}\left(\frac{x_1 - x_2}{P_1 - P_2}\right)_h\right]\phi\right\}^{\frac{1}{2}} \tag{3.24}$$

The model also should account for pressure drop and this is calculated from equation (25) (Jung *et al*, 1999).

$$\Delta P_c = \frac{G^2}{2\rho_{\cdot f}}\left[\left(\frac{1}{C_c}-1\right)^2+\left(1-\frac{1}{\sigma_o^2}\right)\right]\left[1+\frac{\rho_{\cdot f}}{\rho_{\cdot g}}\right] \tag{3.25}$$

Since P, v, h, and μ are temperature dependent equations (3.26) to (3.32) were derived for R22. (Adopted from Stoecker and Jones, 1982).

$$P = 1000\exp(15.06-(2418/T_2)) \tag{3.26}$$

$$v_f = (0.777+0.002062T_2+0.00001608T_2^2)/1000 \tag{3.27}$$

$$v_g = (-4.26+94050T_2/P)/1000 \tag{3.28}$$

$$h_f = 200+1.172T_2+0.001854T_2^2 \tag{3.29}$$

$$h_g = 405.5+0.3636T_2-0.002273T_2^2 \tag{3.30}$$

$$\mu_f = 0.0002367-1.715X10^{-6}T_2+8.869X10^{-9}T_2^2 \tag{3.31}$$

$$\mu_g = 11.945X10^{-6}+50.06X10^{-9}T_2+0.256X10^{-9}T_2^2 \tag{3.32}$$

The flow chart for capillary tube model is shown in Fig. 3.9. The program for the modelling is shown in Appendix III. Appendix IV shows the programs for the calculations of the lengths of the heat exchangers.

3.2 The Program

The computer program, (FRE - 2003), was written using MATLAB 5.3. The program consists of intractable files, functions and subroutines. It is compactable to windows and requires 1.07 GB of computer memory. Some of the output results are shown in Appendix V.

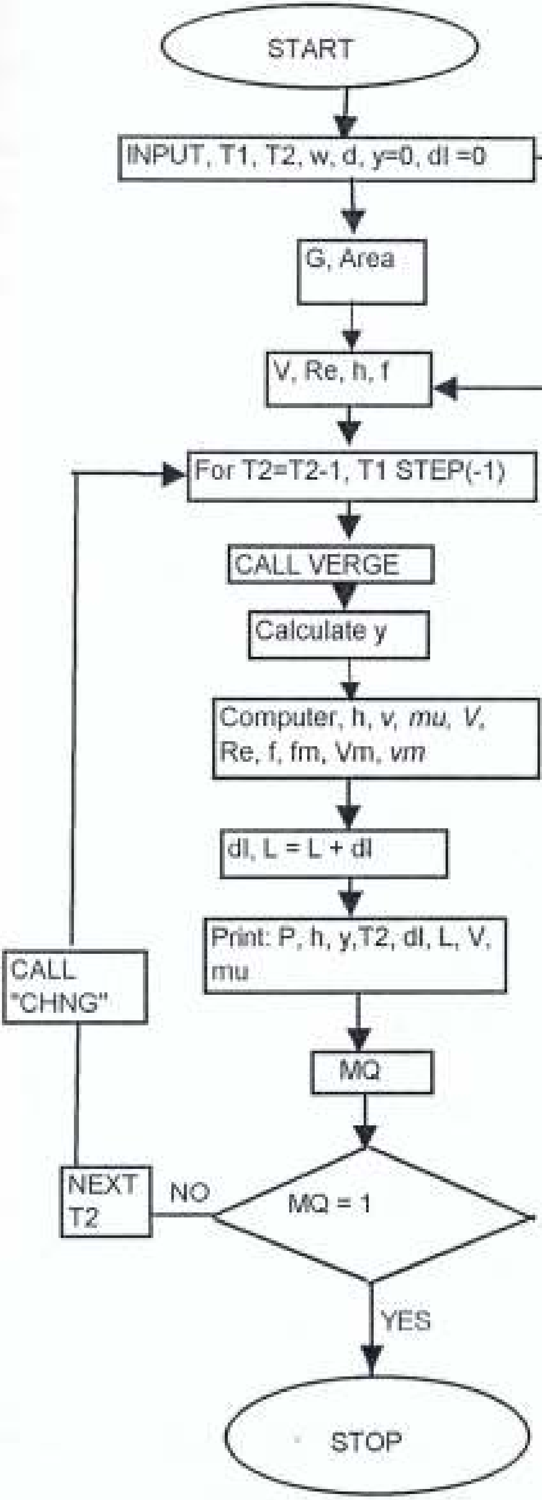

VERGE= Refrigerant properties subroutine
T1 = Evaporating temperature
T2 = Condensing temperature
y = Dryness fraction
h = Enthalphy
v = humid volume
mu = Viscosity factor
V = Velocity
Re = Reynolds number
f = Friction factor
fm = Mean friction factor
Vm = Mean velocity
vm = mean vsccosity factor
L = Length
dl = Change in length
MQ =Mach number

Fig. 3.9 Flow Chart for Capillary Tube Model

3.3 Theoretical Model Verification

3.3.1 Capillary Tube Testing

In the capillary tube analysis, the most important factor is the friction factor (Jung *et al*, 1999). Many researchers have carried out capillary tube modelling and used empirical or semi empirical values of the friction factors to represent experimental data, some of these expressions are presented in Table 3.2.

Table 3.2: Friction factor equations (Source: Jung *et al*, 1999).

S/N	Author	Equation
1	Stoecker	$f = \frac{0.33}{\mathrm{Re}^{0.25}}$
2	Blausius	$f = \frac{0.3}{\mathrm{Re}^{0.25}}$
3	Goldstein	$f = 0.02$
4	Erth	$f = \frac{3.1}{\mathrm{Re}^{0.5}} Exp\left(\frac{1.0 - x^{0.25}}{2.4}\right)$
5	Sami	$f = \frac{3.1}{[\mathrm{Re}(1-x)]^{0.5}} Exp\left(\frac{1.0 - x^{0.25}}{2.4}\right)$
6	Pate *et al*	$f = \frac{3.49}{\mathrm{Re}^{0.47}}$
7	Hopkins	$f = \frac{0.217}{\mathrm{Re}^{0.2}}$
8	Jung *et al*	$f = \frac{0.25}{\mathrm{Re}^{0.27}}$
9	Present work	$f = \frac{0.25}{[\mathrm{Re}(1-x)]^{0.28}}$

In addition, Table 3.3 lists the widely used and cited two-phase viscosity. With the equations in Tables 3.2 and 3.3, 18 combinations and calculations are made for these combinations under the same conditions of, 40 ^{0}C condensing temperature, 0.01 kg/s mass flow rate, 1.62 mm capillary inside diameter and (-5 ^{0}C) evaporating temperature keeping the ambient temperature constant at 35 ^{0}C. The generated tube lengths were compared with that of ASHRAE (which is 2.03 m) to check which combination is the best, the result is as presented in Table 3.4.

Table 3.3: Two-phase dynamic viscosities (Jung *et al*, 1999).

S/N	Author	Equation
1	McAdams	$\mu = (1-x)\mu_f + x\mu_g$
2	Duckler	$\mu = \left[v_f(1-x)\mu_f + v_g x\mu_g\right]/v$

Table 3.4: Capillary lengths using various equations for friction and viscosity.

S/N	Friction Factors of	Viscosity equations of:			
		McAdams		Duckler	
		Length (m)	% Deviation	Length (m)	% Deviation*
1	Stoecker	2.139	5.37	2.552	25.71
2	Blausius	2.351	15.81	2.807	38.28
3	Goldstein	2.391	17.78	2.391	17.78
4	Erth	2.674	36.06	3.917	92.95
5	Sami	2.762	36.10	4.010	97.54
6	Pate et al	2.157	6.26	3.049	50.20
7	Hopkins	1.894	-6.70	2.180	7.39
8	Jung et al	2.612	28.67	3.118	53.60
9	Present work	2.068	1.87	2.122	4.53

* Deviation from ASHRAE length of 2.03 m.

It can be seen that Duckler's equation for two-phase viscosity yielded longer length than that of McAdams' equation. From the comparison made in Table 3.4, it can be seen that the present model yielded a length, which is closer to that of ASHRAE with only 1.87 % deviation.

3.3.2 System Testing.

This section deals with the comparison of the results obtained from the model with a theoretical system (ASHRAE, 2002) under some predetermined conditions.

3.3.2.1 Evaluation of characteristic curves

The characteristic curve of vapour compression refrigeration systems was defined as a plot between the inverse coefficient of performance (1/COP) and inverse cooling capacity ($1/Q_e$) of the system (Khan and Zubair, 1999). Using the actual data of a simple vapour compression system performance curve of the system is obtained. Fig. 3.10 shows the characteristic curves of the model compared with that of an ideal system (a theoretical system; ASRHAE, 2002) for varying condensing Temperature (T_2) and evaporating temperature of -5 ^{0}C, with the ambient temperature kept constant at 35 ^{0}C. The nature of the curves agree very well with the ones obtained in the literature. The Figure suggested that, the higher the rate of heat absorption (Q_e), the higher the coefficient of performance (COP). This agrees with the Carnot model, (which is the actual set standard), as indicated in Fig. 3.10, working within the same temperature limits. The curves indicated an average deviation of 4 % above the theoretical values.

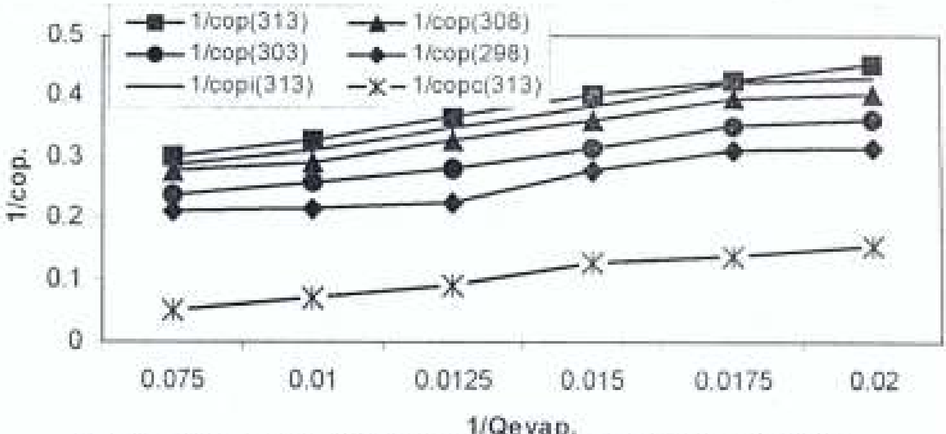

Fig. 3.10 Characteristic performance curves compared with actual system

3.3.2.2 Evaluation of efficiency

In this comparison a refrigerating efficiency was defined by equation (3.33), and was used to compare the efficiency of the model and the actual system.

$$\eta_{ref} = \frac{COP_{ref}}{COP_{Carnot}} \tag{3.33}$$

the result is as shown in Fig. 3.11, which indicates that the smaller the refrigeration capacity the higher the efficiency. Also, as the capacity reduced the theoretical and the model results agree more closely. This indicated that a smaller refrigeration system would be more effective than a bigger one and justifies the argument of Jabardo, *et al* (2002) for automobile air conditioning.

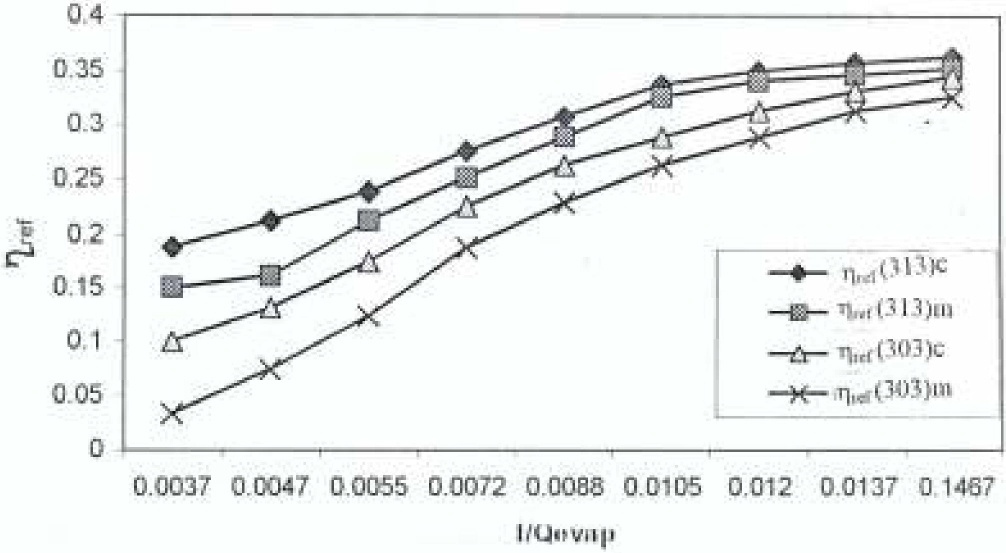

Fig. 3.11 Variation of refrigerating effeciency with cooling capacity

3.3.2.3 Effect of subcooling and superheating

The superheating of refrigerant (after exiting from evaporator before entering compressor) may occur owing to the

(a) Heat gain in the line joining the evaporator and compressor

(b) The actual length of evaporator.

It was noted that the specific volume of refrigerant vapour is increased as a result of superheating thus reducing the mass flow rate through the compressor. While subcooling the refrigerant beyond the saturated state after exiting the condenser and before entering the expansion valve normally occurs owing to heat losses in the line joining the condenser and the expansion valve. This is shown in Fig. 3.12. Since, the specific refrigeration capacity increases by subcooling, it is expected that subcooling increases the system performance.

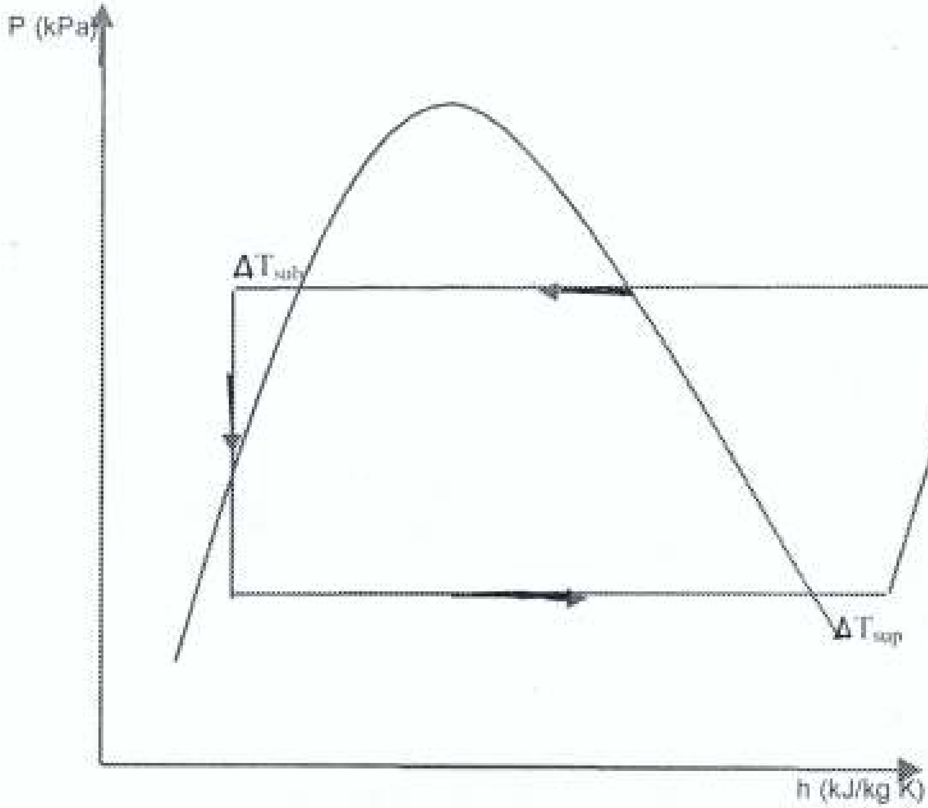

Fig. 3.12 P – H Curve for Degree of Subcooling and Superheating

The effect of superheating, subcooling and both subcooling and superheating are shown in Fig.3.13. From Fig. 3.13, it is seen that superheating degrades the performance of the system, while subcooling improves the system COP. When equal degrees of subcooling and superheating were considered, the performance degrades. This shows that the effect of superheating has more influence on the system overall performances. The relative effects of subcooling and superheating are shown in Fig. 3.14. This suggests that superheating should be prevented as much as possible, while subcooling should be encouraged. This calls for the optimization of the system; to allocate heat transfer areas appropriately between the two heat exchangers in order to minimize superheating.

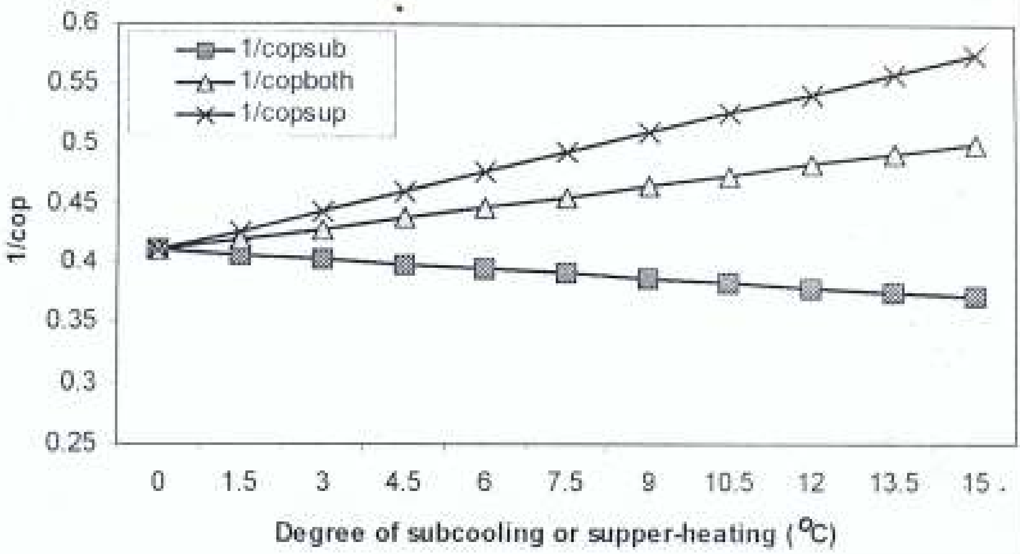

Fig. 3.13 Effects of subcooling and supper-heating

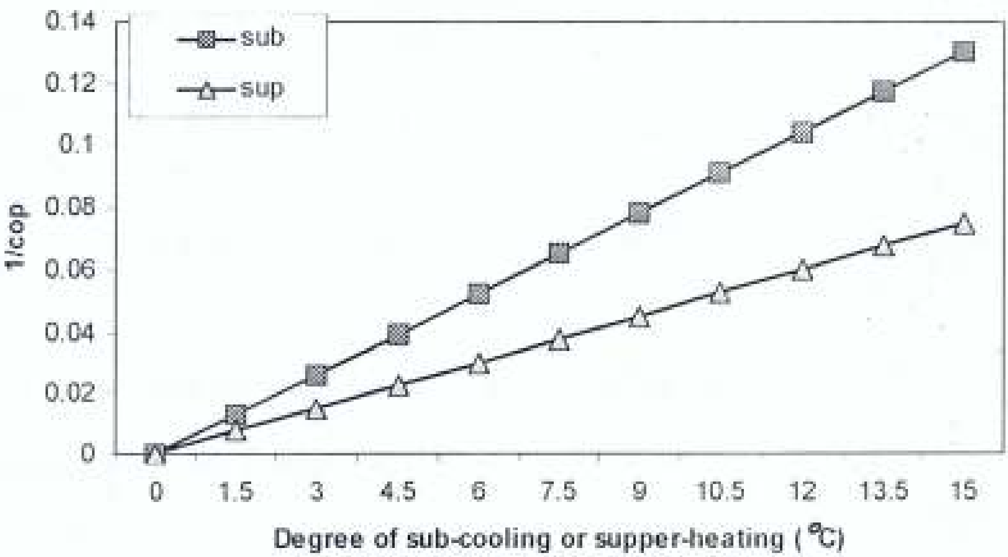

Fig. 3.14 Effects of sub-cooling and Supper-heating on 1/COP

3.3.2.4 Optimization

Optimization of the system now hinges on the heat exchangers (both evaporator and condenser, in this case). This is influenced by proper selection of the external fluid capacitance rates and heat exchanger sizes. The capacitance rate (C) for external fluid is given by equation (3.34).

$$C = \dot{m}c_p \tag{3.34}$$

where:

C = Capacitance rate (kW/K)

$\dot{m}$ = mass rate of flow (kg/s)

c_p = heat capacity at constant pressure (kJ/kg K)

Heat exchanger's effectiveness (ε) is a function of the effective heat transfer area; this is given by equation (3.35).

$$\varepsilon = \frac{Q}{Q_{max}} \tag{3.35}$$

where:

Q= is the rate of heat transfer in an exchanger (W).

$Q_{max.}$ = is the maximum possible rate of heat transfer in this exchanger (W).

The determining factor (ψ = optimization factor) for the optimization is the product of ε and C given in equation (3.36).

$$\Psi = \varepsilon . C \tag{3.36}$$

The function "ψ" of all the heat exchangers is an expensive parameter. Increasing the size of the heat exchanger increases the overall performance of the system, and increases the system cost. Hence a compromise is sought between the initial cost and system operating cost.

In this case, we have two heat exchangers (condenser and evaporator). A heat exchanger inventory parameter k is defined by equation (3.37), which is considered as the design constraint (Jung *et al* 1999 and Jabardo *et al* 2002).

$$k = (\varepsilon . C)_{cond} + (\varepsilon . C)_{evap} \tag{3.37}$$

Where, k is the constant thermal inventory (kW/K).

Now the problem of heat exchanger optimization is to allocate the total heat exchange area between the two heat exchangers so that maximum performance of the system is obtained. This problem is solved by using a model, which simulates closely the working of an actual vapour-compression system. To investigate the relative size of heat exchangers, a factor "f_h", which is the ratio of condenser effectiveness-capacitance product to the sum of the effectiveness-capacitance rate products for condenser and evaporator. Equation (3.38), as defined by Klein, (1998) was used to study the variation in COP.

$$f_h = \frac{(\varepsilon C)_{cond}}{(\varepsilon C)_{cond} + (\varepsilon C)_{evap}} \tag{3.38}$$

It has been established that the Carnot model and ideal vapour compression cycle show constant COP values for all values of "f_h" (Klein, 1998; Jung *et al*, 1999), because the irreversible losses due to the finite rate of heat transfers are not present in these models.

Fig. 3.15 shows a set of sample curves, drawn between 1/COP and f_h for R22 using the output from the model, when Q_e = 10 kW, T_1 = -5 ^{0}C and T_2 = 40 ^{0}C. It can be seen from these curves that as the heat exchangers thermal inventory factor (k) is increased beyond 120 kW, the COP reaches almost a constant value, which is the same as the COP of an ideal system for the same input conditions. It has been pointed out that Carnot model and ideal cycle model show constant COP values for all values of f_h because the irreversible losses due to the finite rate of heat transfers are not present in their model (Khan and Zubair, 1999).

Fig. 3.16 shows the variation of f_h with $1/Q_e$. This Figure shows that, the values of f_h are higher for lower evaporator capacity, indicating that a greater portion of the total heat exchanger area is to be allocated to the condenser and vice-versa for higher evaporator capacity. Since the curves are very close together irrespective of the values of condensing temperature (T_2), then the actual system is operating very close to optimum for all values of condensing temperatures.

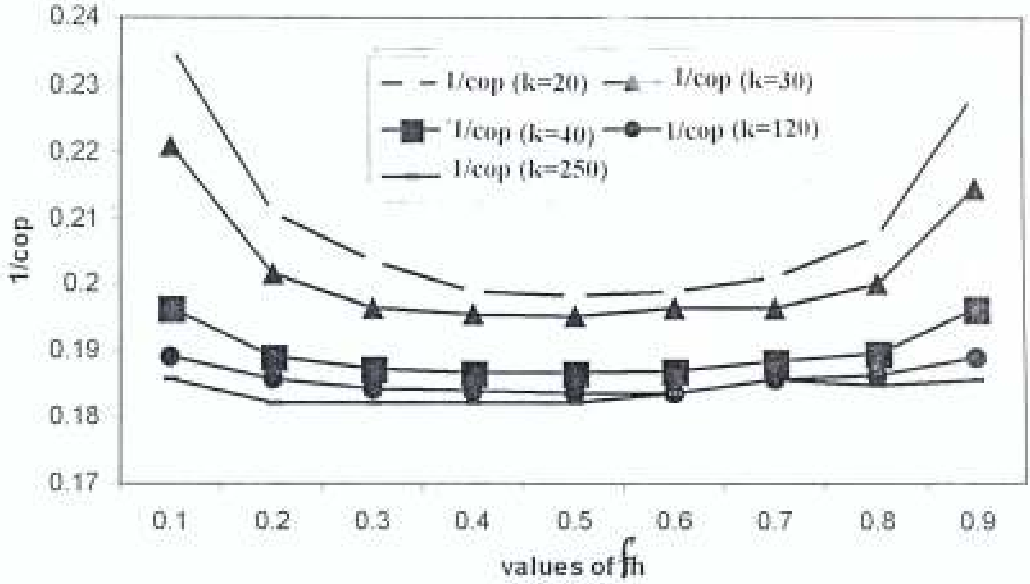

Fig. 3.15 Variation of 1/cop with fh for various values of k

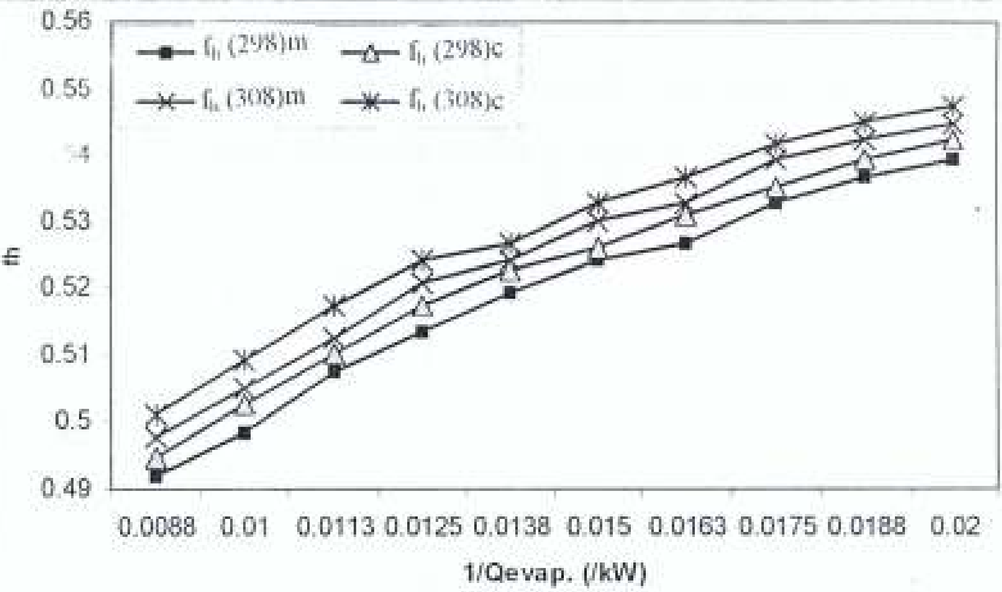

Fig. 3.16 Variation of fh with 1/Qevap. at various ambient temperatures

CHAPTER FOUR

4.0 EXPERIMENTAL STUDIES, RESULDS AND DISCUSSIONS

The objective of this work is to develop a property-dependent thermodynamic model of vapour compression refrigeration systems, which can simulate the performance of actual systems as closely as possible. In this regard, analysis of an actual system is studied in detail and a thermodynamic model developed and compared with a theoretical system. Effects on system performance of such operational parameters as compressor speed, circulating water temperature, evaporating and condensing temperatures, degree of subcooling and superheating have been theoretically evaluated and simulated by means of the developed model. Model results deviated from the theoretical results within a ± 0.6 % range.

The test data have been used to assess the quality of the computer simulated results. The summary of the experimental and simulated system performance results and their comparison is presented along with an additional feature related to the effect of refrigerant charge, which is of major concern to air-conditioning and refrigeration systems manufacturers (Jabardo *et al*, 2002).

This section is based on the experimental validation of the developed model. In this regard, experimental rig was designed and constructed based on the data generated from the developed design model, and some of the operational performances predicted by the model were compared with the experimental results.

The diagram of the experimental rig is as shown in Fig. 4.1. The components of rig "a" and the main parameters are listed as follows:

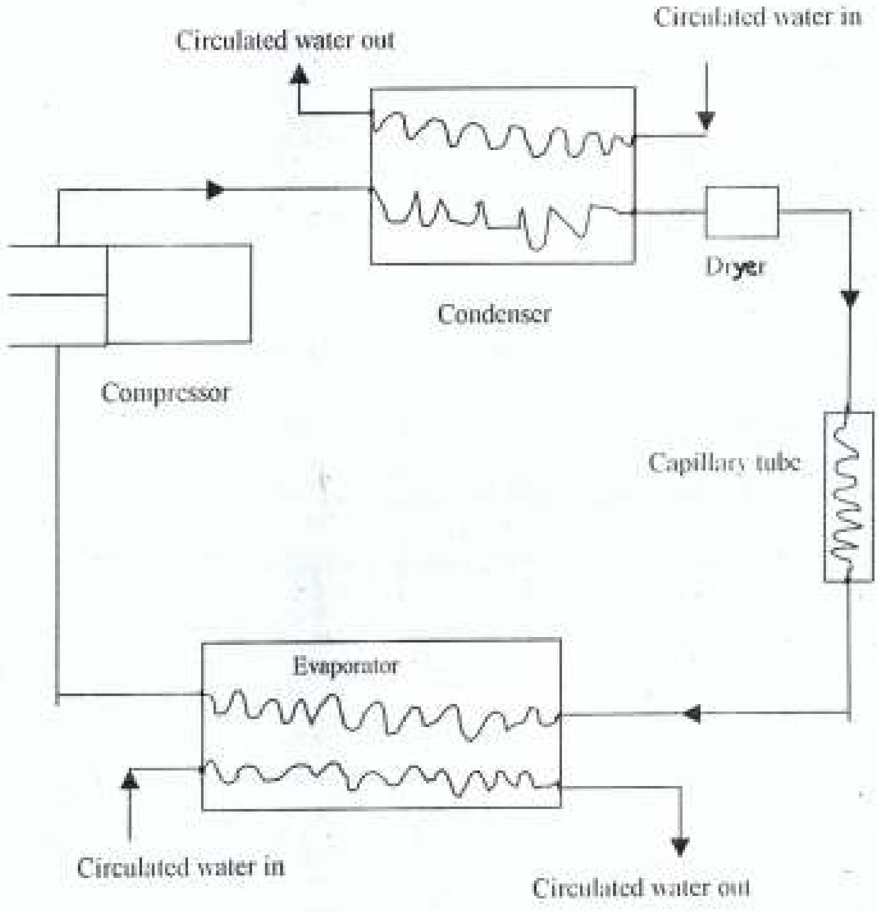

Fig. 4.1 The schematic diagram of the experimental rig.

1) **Compressor**: reciprocating type. Power 0.09325 kW, Refrigerant R-12, with swept volume of 32.7 cm^3.

2) **Evaporator**: Bare coil, immersed in water being cooled, pipe inner diameter 5.588 mm, outer diameter 6.3500 mm, tube length 30.71 m, which yields equivalent of 0.09325 (kW) on calculation.

3) **Condenser**: Bare coil, pipe inner diameter 5.588 mm, outer diameter 6.3500 mm, and tube length 14.362 m, which yields equivalent of 0.09325 (kW) on calculation.

4) **Circulating Water**: In order to change the load of the evaporator, water was circulated at various flow rates.

The objectives of this experimental rig are to:

i test and check system and components performance;

ii compare data for validation of the computer model;

iii carry out performance evaluation of the refrigeration system;

while the experimental runs were intended to validate system operation under steady state conditions.

The second experimental rig (rig "b") was built from bought out components of vapour compression refrigeration system. This system is an assembly of 0.09325 kW compressor and equivalent condenser (0.09325 kW), evaporator (0.09325 kW) and capillary tube. Rigs "a" and "b" are as shown in Plate 1

The performance of these systems (computer model, rig "a" and rig "b") were evaluated based on the following parameters: Cooling load

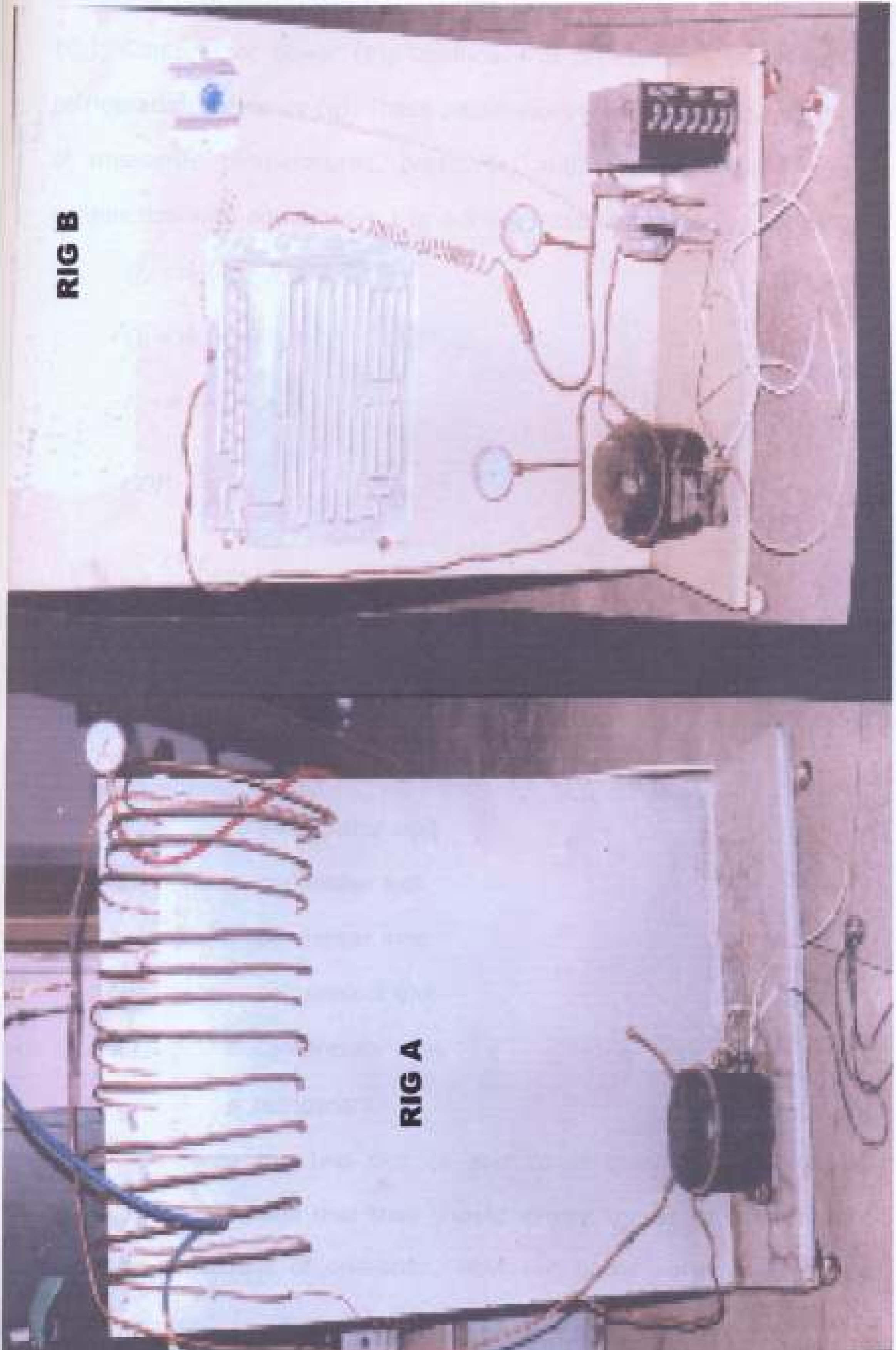

PLATE 1 RIG A AND RIG B

or rate of heat absorption (Q_e); condensing load or rate of heat rejection (Q_c); Compressor power (P); Coefficient of performance (COP) and the refrigeration efficiency (η). These parameters were evaluated with the aid of measured temperatures, pressures, and the steam table data in conjunction with equations 4.1 to 4.5 suggested by Jabardo *et al* (2002).

$$Q_e = \dot{m}_r (h_{ee} - h_{ei}) \tag{4.1}$$

$$Q_c = \dot{m}_r (h_{ce} - h_{ci}) \tag{4.2}$$

$$P = \dot{m}_r (h_{cpe} - h_{cpi}) \tag{4.3}$$

$$COP = \frac{Q_e}{P} \tag{4.4}$$

$$\eta = \frac{COP_{system}}{COP_{Carnot}} \tag{4.5}$$

where the subscripts are:

ee	-	evaporator exit
ei	-	evaporator inlet
ce	-	condenser exit
ci	-	condenser inlet
cpe	-	compressor exit
cpi	-	compressor inlet
r	-	refrigerant.

Since the two rigs (a and b) in question are of equal capacity, it is assumed that they should exhibit the same performance under the conditions of operation. However, some variations may be envisaged as a result of difference in refrigerant charge and compressor speed, these were effectively examined in the next two sections.

Since capillary tube was modelled in this work, it is required that the system capacity should lie between 90 W and 90 kW as reported in ASHRAE handbook (2002). The compressor capacity required could not accommodate R22, which was used in the theoretical part of the model development, because of its peculiar thermodynamic properties (high humid volume). Hence, R12 (low humid volume) was used for the experimental investigations. The substitution was made possible by the usage of conversion factors for R12, R12, R134a and R407c published by: Kutter (1988); Wolf *et al* (1995); Wolf and Pate (2001) and Kuehl and Goldschmidt (1991). The studies assume that the effect of refrigerant is negligible. Further research may be needed in future to ascertain this.

4.1 Effect of Charging

Since refrigerant cannot be charged into the model developed, it is necessary to examine how the amount of the refrigerant charge affects the performance of the experimental rigs. Generally, refrigerant charge should lie within the range 750 g to 900 g inclusive as reported by Lee *et al* (2000).

In order to evaluate the effect of the refrigerant charged, tests were performed with an initial refrigerant charge of 1.1 kg. In subsequent tests the refrigerant charged was reduced by removing 50 g at a time, down to a minimum of 600 g, when a significant amount of bubbles started to appear in the liquid line sight glass.

For this experiment the following parameters were used: Evaporating temperature (T_1) = -5 ^{0}C, Condensing temperature (T_2) 40 ^{0}C Ambient temperature (T_a) 35 ^{0}C and a constant compressor speed of 1750 rpm.

The experimental results are shown in Fig. 4.2. As indicated in Fig. 4.2 (and Figs. 4.2a and 4.2b), the refrigerating capacity (Q_e) and the coefficient of performance (COP), are not strongly affected over a wide range of refrigerant charges. It can be seen that between 950 g and 700 g both Q_e and COP are relatively constant for both experimental rigs. The expected range of refrigeration charge falls within 950 g and 700 g. Hence there is no fear of the influence of the refrigerant charge on the result. Care must, however, be taken as well since refrigerant charge lower than 700 g tend to reduce system COP. This effect is of course due to the increase in the amount of vapour in the liquid being fed to the expansion device. On the other hand, refrigerant charge higher than 950 g tends to promote flooding of the condenser. At constant ambient temperature, the condensing pressure increases and so does the liquid subcooling at the condenser exit. This results in a slight gain in the refrigeration effect. The effect of subcooling and superheating will be discussed latter. Fig. 4.3 shows that within the expected refrigerant charge, the mass flow rate is relatively constant. This effect also will not influence the expected result negatively.

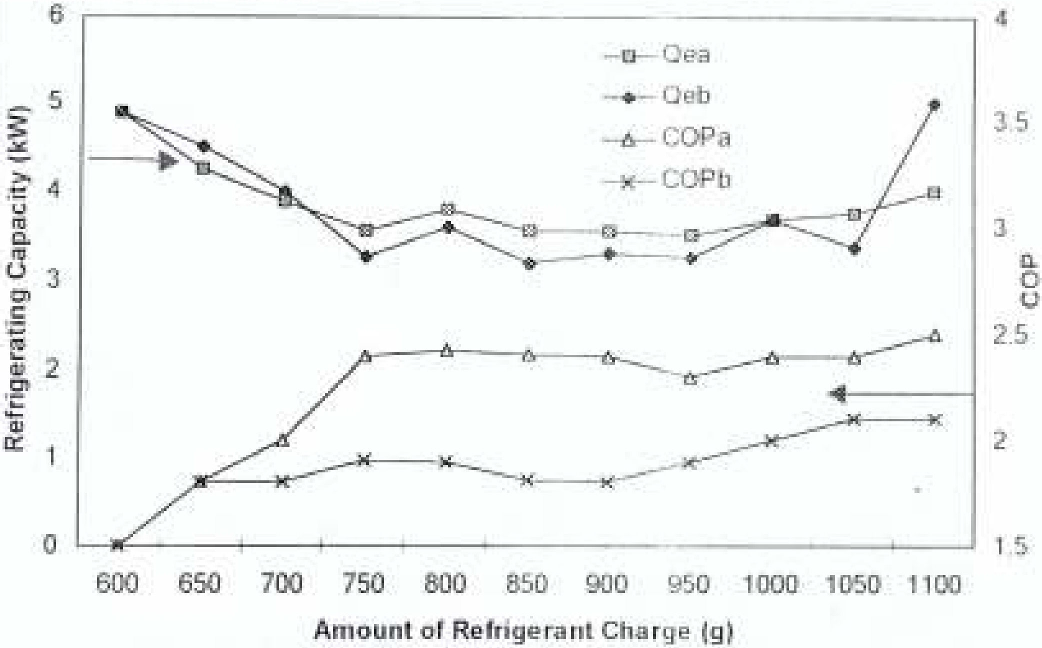

Fig. 4.2 Effects of Refrigerant Charge on COP and Refrigerating Capacity

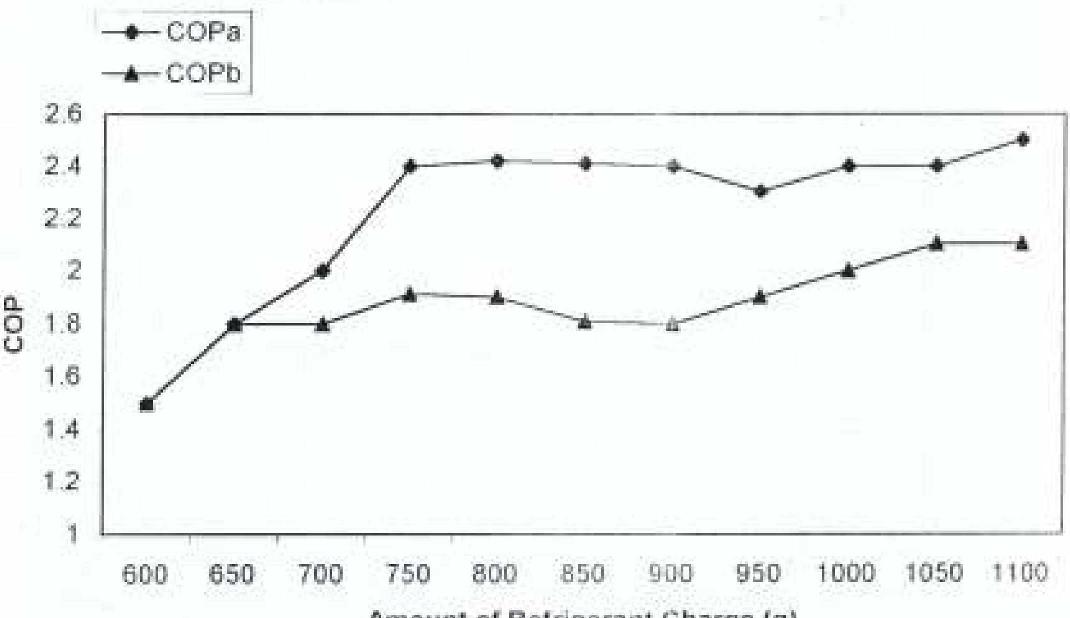

Fig. 4.2 a Effects of Refrigerant Charge on COP

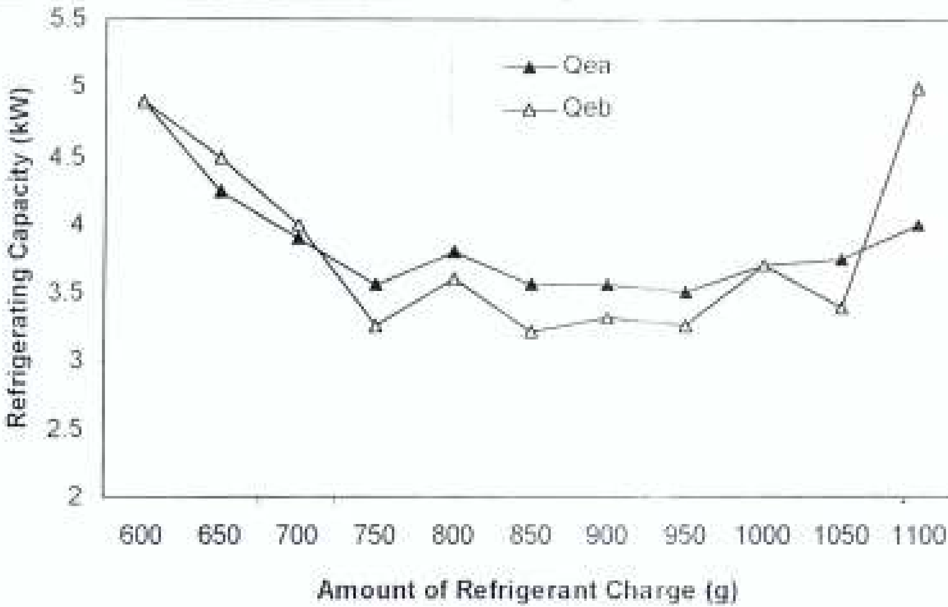

Fig. 4.2 b Effects of Refrigerant Charge on Capacity

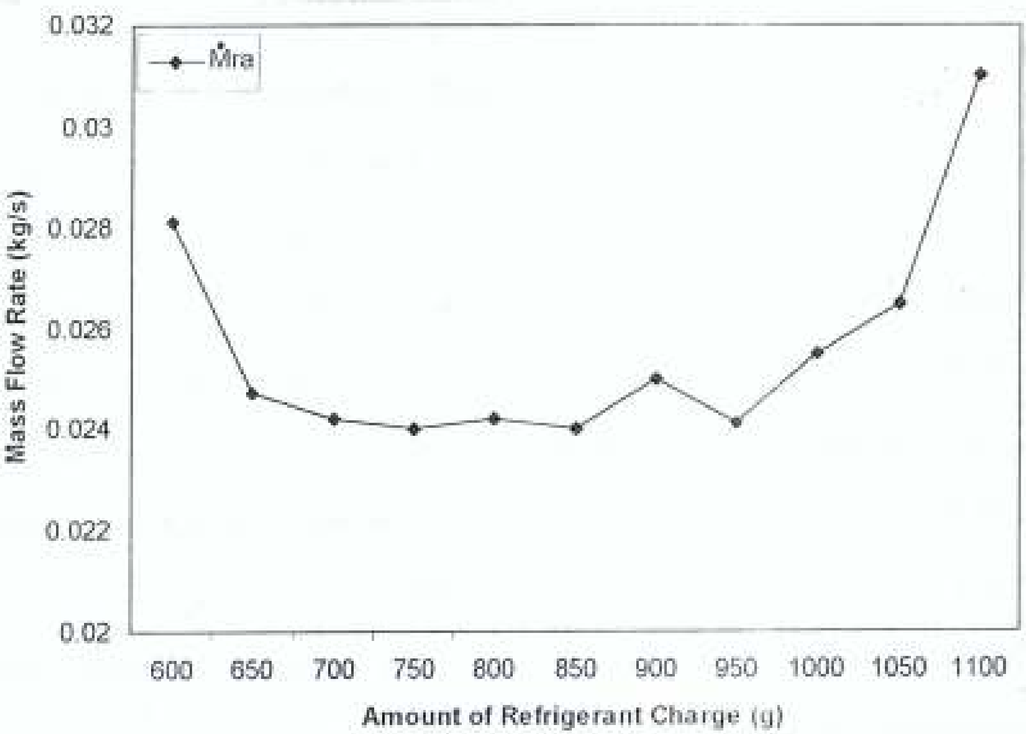

Fig. 4.3 Effect of Refrigerant Charge on Mass Flow Rate

4.2 Effect of Compressor Speed

In this experiment, four compressors from the same maker, of different speed but same capacity were used. The speeds of these compressors were: 1500; 1750; 2000; and 2250 rpm The aim is to investigate the effect of compressor speed on, refrigeration effect (Q_e), Coefficient of performance (COP) and the mass flow rate ($\dot{m}_r$). The condensing and evaporating temperatures were kept constant at 40 ^{0}C and 5 ^{0}C respectively.

The result of this investigation is as presented in Fig. 4.4. According to Fig. 4.4 the refrigerating capacities Q_{em}, Q_{ea} and Q_{eb} remain constant over the whole range of speeds, so also the corresponding mass flow rate. As reported by Jabardo *et al* (2002), for systems with variable capacity compressors, the running speed should be of no major concern regarding the refrigerating capacity. In other words, the refrigeration capacity should not vary with running speed. This result justifies Jabardo et al's report. This is not so for the COPs which diminishes with increase in compressor speed as a result of the compression work increment. This is also related to the rise in the discharge temperature associated with the increment in the compression irreversibility with speed. It must be noted also that the mass flow rate remain almost constant (Fig. 4.4), and that it is independent of rotational speed, this in indicated in Fig. 4.3. This situation justifies the performance of the variable capacity compressor and its ability to accommodate different conditions of operations.

Figs. 4.4a, 4.4b and 4.4c show that the results from the simulated model compared very well with the experimental results. As indicated by the above mentioned Figures, it can be seen that system rig "a" performed better than rig "b", which justifies the initial argument that a "balanced point" must be sought between the components of the system. The deviation between the simulated data and the experimental data is mostly within 3 %. This deviation is likely to be as a result of heat loss, which is very difficult to be controlled.

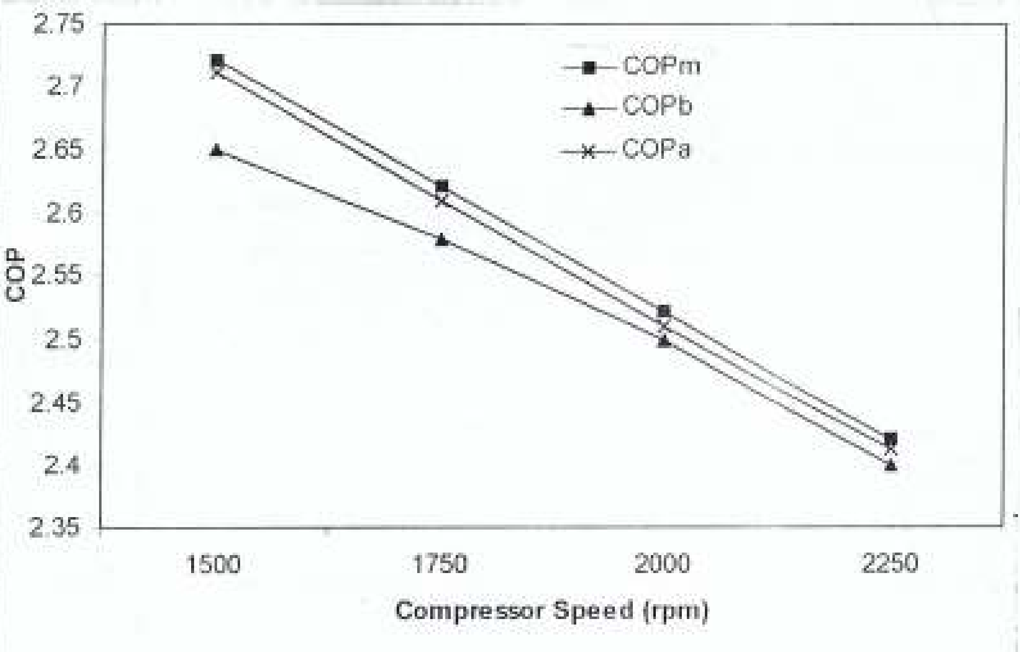

Fig. 4.4a Effect of compressor speed on COP

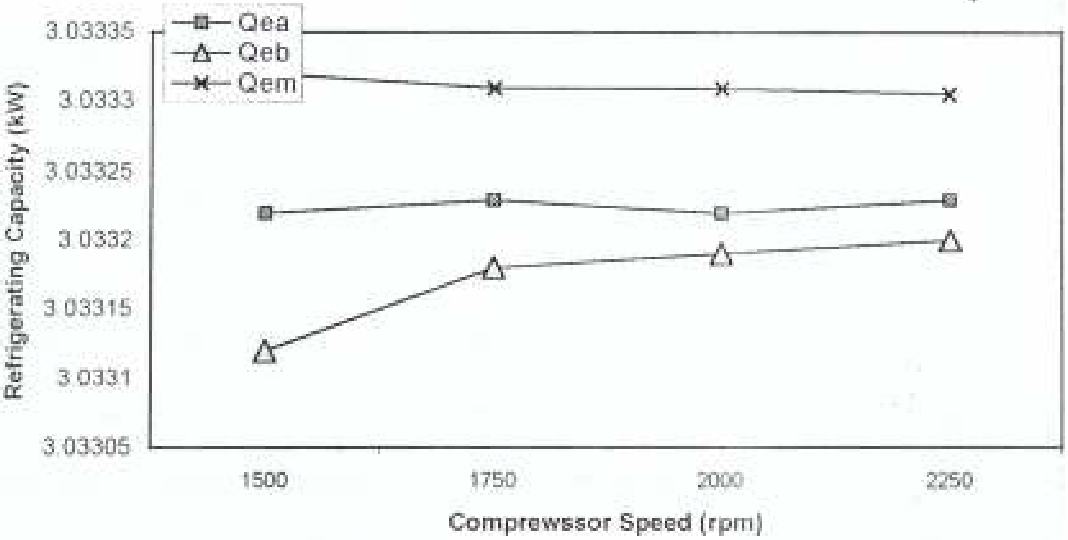

Fig. 4.4b Effect of Compressor Speed on Refrigerating Capacity

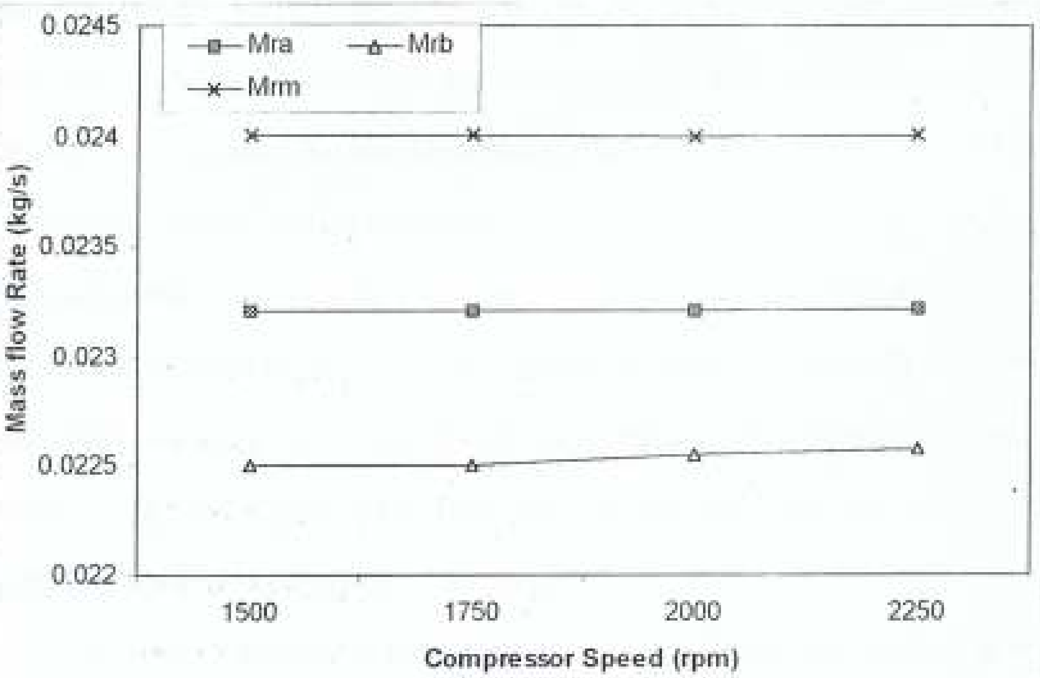

Fig. 4.4c Effect of Compressor Speed on Mass Flow Rate

4.3 Effect of Circulating Water Temperature

In this test, the effect of changing the temperature of water circulating around the evaporator was examined on the performance of the refrigerating system. In this experiment $T_2 = 40\ ^0C$; $T_1 = 5\ ^0C$ and $T_a = 35\ ^0C$ while the temperature of the circulated water was varied between $20\ ^0C$ and $35\ ^0C$. The same experiment was repeated for the condenser. The obtained results were recorded.

With a constant evaporating temperature, the refrigerating capacity is directly related to the circulating water temperature. The behaviour is clearly indicated in Fig. 4.5. It can be observed that as the circulating water temperature (T_w) increases the compressor must accommodate higher loads in order to keep constant the suction pressure. This is accomplished by increasing the refrigerant flow rate through the control device, this implication is shown in Fig. 4.6. When T_w increases, there will automatically be an increase in the degree of superheating. As a result, the rate at which the compression power (W) increases is more than that of refrigerating capacity (Qe) (Fig. 4.5) hence the COP reduces with increasing circulating water temperatures, T_w, (Figs. 3.13, 3.14, and 4.5). This justifies the fact that the COP reduces with increase in the degree of superheat.

It is interesting to note that the model predicted almost a linear relationship for both Qe and COP with T_w (Fig. 4.4) while the experimental data justifies the same. The variation is due to heat loss, which at present it is almost impossible to prevent since there is no

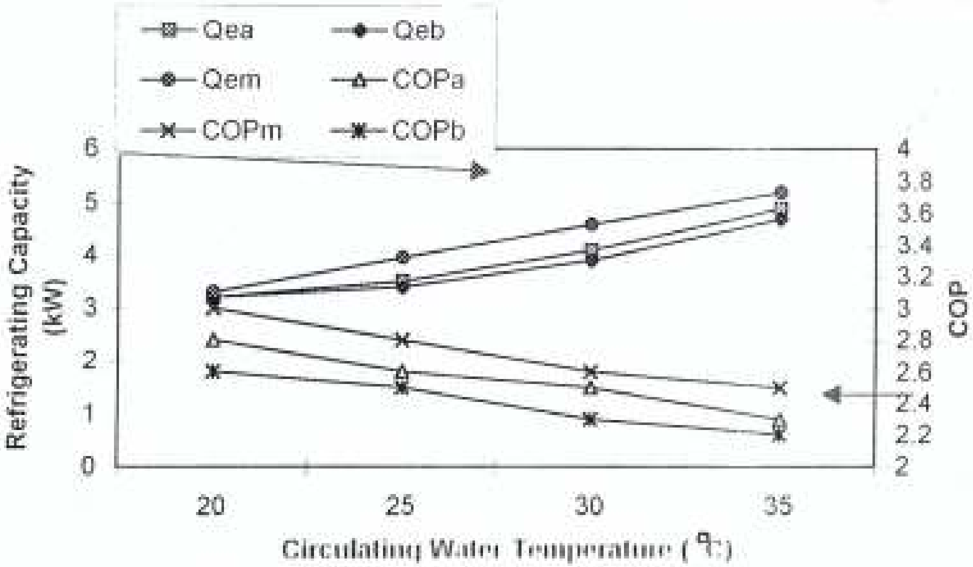

Fig. 4.5 Effect of Evaporator Circulating Water on COP and Refrigerating Capacity

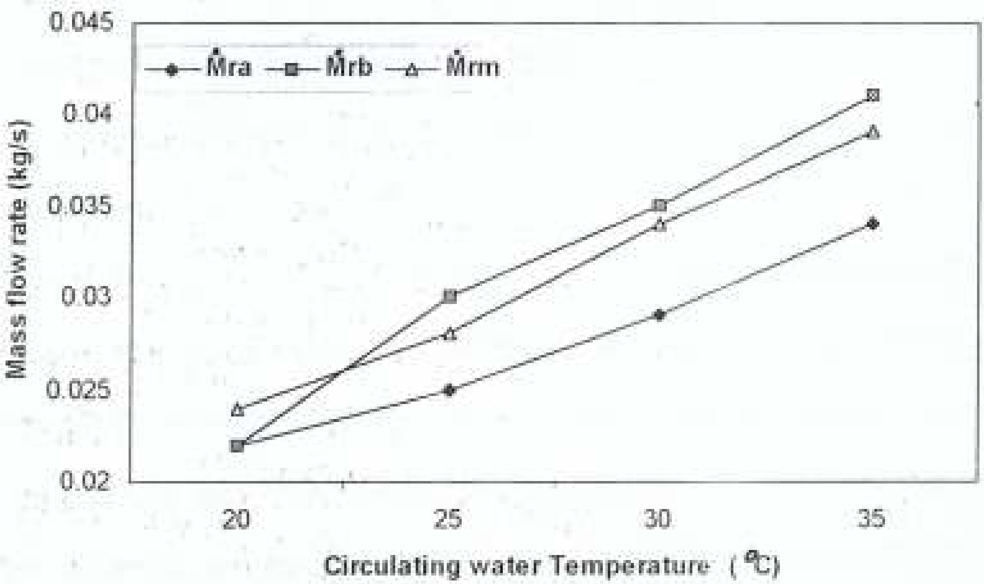

Fig. 4.6 Effect of evaporator circulating water temterature on mass flow rate

perfect insulation of heat. On the other hand, the mass flow rate deviated from linear characteristics most especially at lower circulating water temperatures, T_w. This might be related to the inability of the compressor control system to adequately accommodate low thermal loads.

Considering the results shown in Figs. 4.5 and 4.6, deviations between the simulated results and the experimental results are a maximum of 16 %, for mass flow rate and 18% for COP values. In conclusion, the simulated results predicted system performance with reasonable accuracy for T_w within a typical range from 20 ^{0}C to 35 ^{0}C.

4.4 Effect of Condenser Inlet Water Temperature

The experiment in section 4.3 was repeated for varying inlet water temperatures circulating around the condenser, the effect was recorded and compared with the theoretical results.

In this result, the evaporating pressure (P_e) was relatively constant while the condensing pressure (P_c) increases with the circulating water temperature (Fig. 4.7a). As shown in Fig. 4.7, the refrigerating capacity (Q_e) is not significantly affected by the condensing inlet water temperature, except for rig "b", which shows great anomalies, which may be due to the fact that the major components are not working on the same balanced points. This shows that the variation in the atmospheric temperature has a significant negative effect on the system; if the balancing point is not sought. But if the components are working on a common balancing point, the effect of variation in the atmospheric conditions will not have significant effect. This is possible due to a slight reduction in the refrigerating effect that compensates for the increment in refrigerant mass flow rate (Fig. 4.8). As a result of increase in P_c, the compression work also increases and so also the mass flow rate and this led to a reduction in the COP.

From thermodynamics points of view, since an increment in T_a widens the difference between the condensing and evaporating temperatures (T_2 and T_1 respectively) hence there should be a reduction in the cycle COP. This is justified by both the model and the experimental rigs.

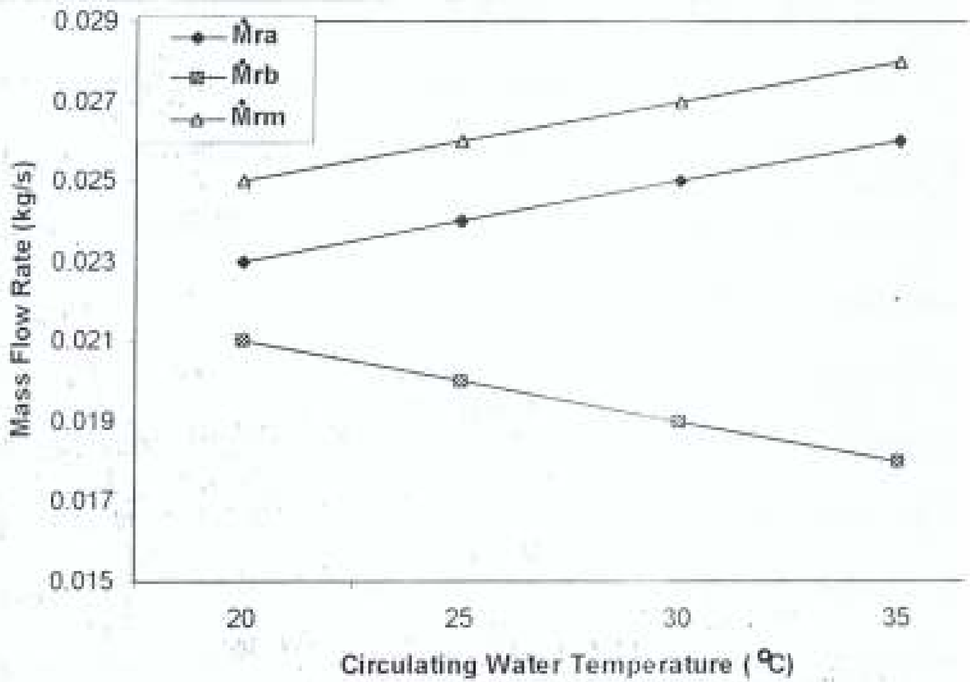

Fig. 4.8 Effect of Condenser Circulating Water Temperature on Mass Flow Rate

4.5 Influence of Charge loss on Performance

Undercharging may occur after commissioning due to leakages or even from repeated maintenance practices such as oil changes. Likewise, small amounts are lost when systems are opened for service even after evacuation. Awareness of the possibility of leakage and performance penalty from charge loss may suggest deliberate overcharging to compensate for potential leaks.

The effects of overcharging and undercharging which may result from refrigerant leakage were therefore investigated. In this experiments, experimental rigs were charged to 1.4 times their usual optimal capacity of 850 g of refrigerant. The charge cannot exceed this because overcharging results in carryover of refrigerant from the evaporator and risk compressor damage (Calm, 2002).

Fig. 4.9 shows the sensitivity of Coefficient of Performance (COP) to variations in charge values. Performance sensitivity to charge is primarily as a result of heat transfer effects and specifically evaporator starvatio3n.

Fig. 4.9 shows that the three systems agreed well during undercharging. Nevertheless, rig "b" shows the greatest discrepancy. It is expected that at the optimal COP the three systems will indicate a relative performance of unity (1.0). At this point, however only the model gives the expected value while **rig "a"** gives a value of 0.994 (about 6 %) difference.

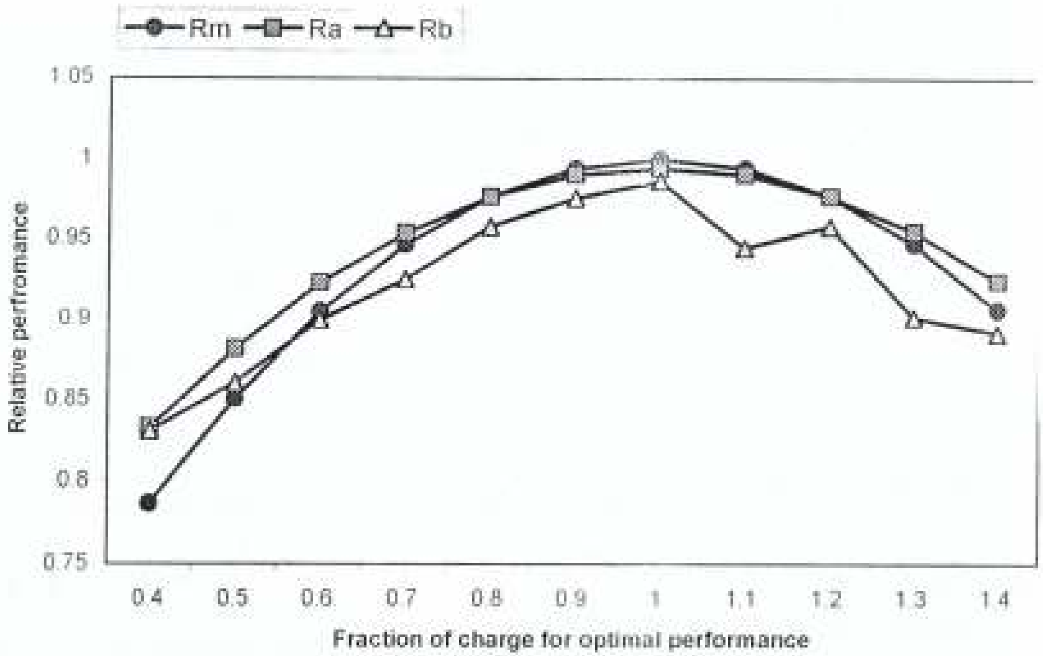

Fig. 4.9 Influence of charge loss on Performance

This may be attributed to heat losses since the rig could not be isolated from the immediate environment and also to the level of accuracy of the measuring instruments used. In the case of **rig "b"** a value of 0.986 (about 1.4 % difference relative to the simulation model and 0.81 % relative to **rig "a".** These figures show that the relative performance of **rig "a"** is about 2.3 times that of **rig "b"**. Since the experiments were performed under the same conditions and the same instruments were used in the measurements, this discrepancy may be attributed to the effect of reaching a balanced point for the system components. This effect is also strongly pronounced on the over-charging side of the curve, it could be seen that, the performance of **rig "b"** deviated widely from the normal as predicted by the simulation model.

Fig. 4.9 further shows that between the charge fractions of 0.8 and 1.2, **rig "a"** and the simulation model approached each other closely. Even at both under- and over-charging conditions both the simulation model and **rig "a"** followed the same pattern. This shows that the simulation model can be used for the optimal design of refrigeration systems.

The refrigerant was then withdrawn into an empty "can" placed on a balance via a valve. The mass of the can was increased by 85 g and the valve closed. The system was then left to run for about 15 to 20 minutes before the evaporator and condenser temperatures were taken. This process was repeated until a charge of about 0.4 times the optimal charge remains in the rigs. The charge could not be withdrawn below this level because the evaporator was already starved and if further reduced, the compressor could be damaged (Lee *et al*, 2000).

4.6 Effect of Subcooling and Superheating

This investigation was divided into three sections:

(a) Effect of Subcooling

(b) Effect of Superheating

(c) Combined Effects of Subcooling and Superheating.

The methodology and results of experimental investigation of the effects of subcooling and superheating on COP, Q_e, Q_c and η are discussed below:

4.6.1 Effect of Subcooling

Subcooling of the liquid refrigerant in the condenser is a normal occurrence and serves the desirable function of ensuring that 100 % liquid will enter the expansion device.

In this experimental investigation, the refrigerant pressure at the exit of condenser was adjusted to, and kept at, the saturation pressure (961 kPa) corresponding to the condensing temperature of 40 °C. The flow rate of the circulating water was increased in order to vary the degree of subcooling. The circulating water temperature used was varied between 20 °C to 35 °C to facilitate different degrees of subcooling. The rigs were left to run for 30 minutes so that a steady condensing temperature could be measured. The following parameters were then measured: Condenser temperature, inlet and outlet temperatures of circulating water and the rate of flow of the circulating water. Steam table published by Stoecker and Jones (1982) was used to determine the flow rate and equations 4.1 to 4.5 were used to determine Q_e, Q_c, COP, and the efficiency. The evaporator temperature and pressure were kept constant at –5 °C and 261 kPa respectively.

As predicted by the model, a linear relationship exists between the degree of subcooling and the refrigeration capacity. This is obvious from the p-h diagram (Fig. 4.10), which shows an increase of refrigerating effect from point 5 to 6 for subcooling from point 3 to 4. As shown in Fig. 4.11, rig "a" also exhibits the same linear relationship except when the degree of subcooling is low. This justifies the reports of Chen *et al*, (1990) and Wijaya, (1992), that evaporator capacity "hunts" (fluctuates) at low degree of subcooling, especially between 0.5 ^{0}C and 2.5 ^{0}C. Rig "b" does not exhibit a good linear relationship because of imbalance between the major components.

It could be observed also that Q_e generally increases with degree of subcooling. This is as a result of increasing mass flow rate (Fig. 4.12) and therefore the compression work. On the other hand the liquid temperature reduction, which causes a slight gain in the refrigerating effect (Figs. 4.10 and 4.11), also leads to a slight increase in COP (Fig. 4.13) until the point when the degree of subcooling is about 7 ^{0}C; after which there is a sudden increase. This is caused by increase in mass flow rate. The COP predicted by the model approached that of Carnot closely when the condensing temperature approaches the ambient and the resulting COP is almost constant (Fig. 4.13)

Both Q_e and Q_c exhibit same relationship with degree of subcooling (Figs. 4.11 and 4.15) except for the fact that heat rejection Q_c is more than heat absorbed Q_e. This is due to the fact that water is circulated around the condenser to subcool the refrigerant so more heat is removed.

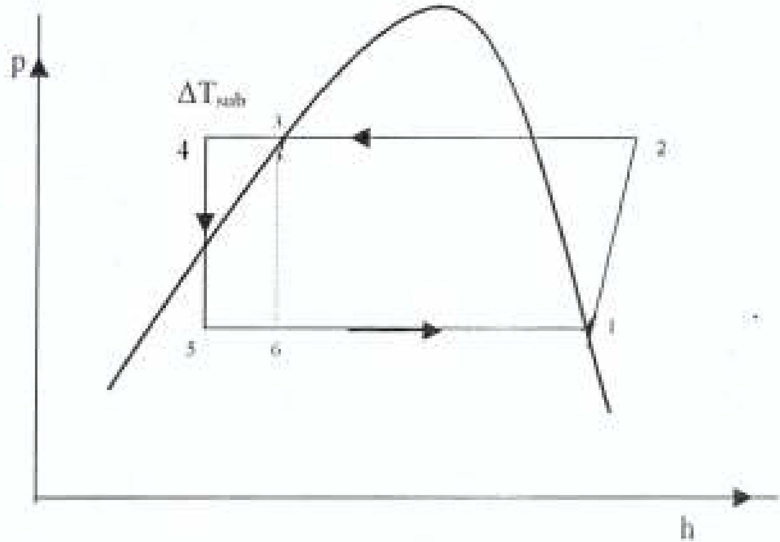

Fig. 4.10 p – h diagram for subcooling without superheating

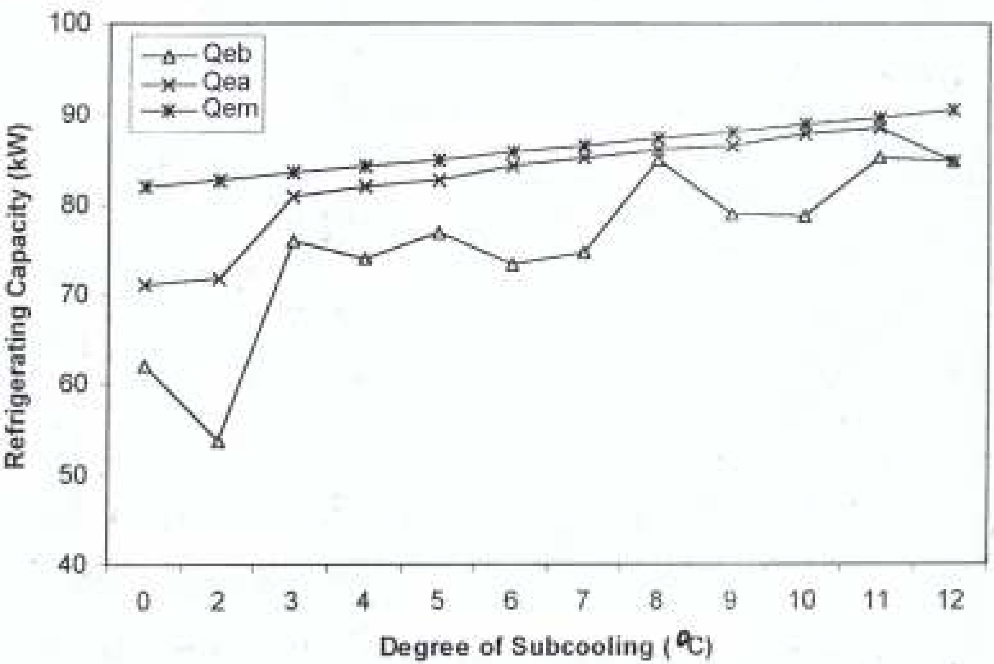

Fig. 4.11 Variation of Refrigerating Capacity with Degree of Subcooling

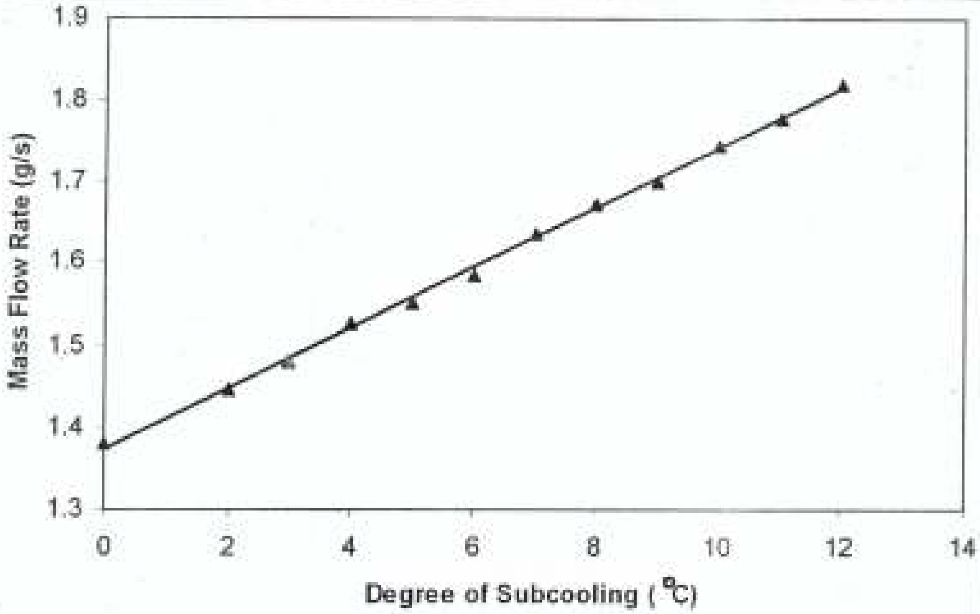

Fig. 4.12 Variation of Mass Flow Rate with Degree of Subcooling

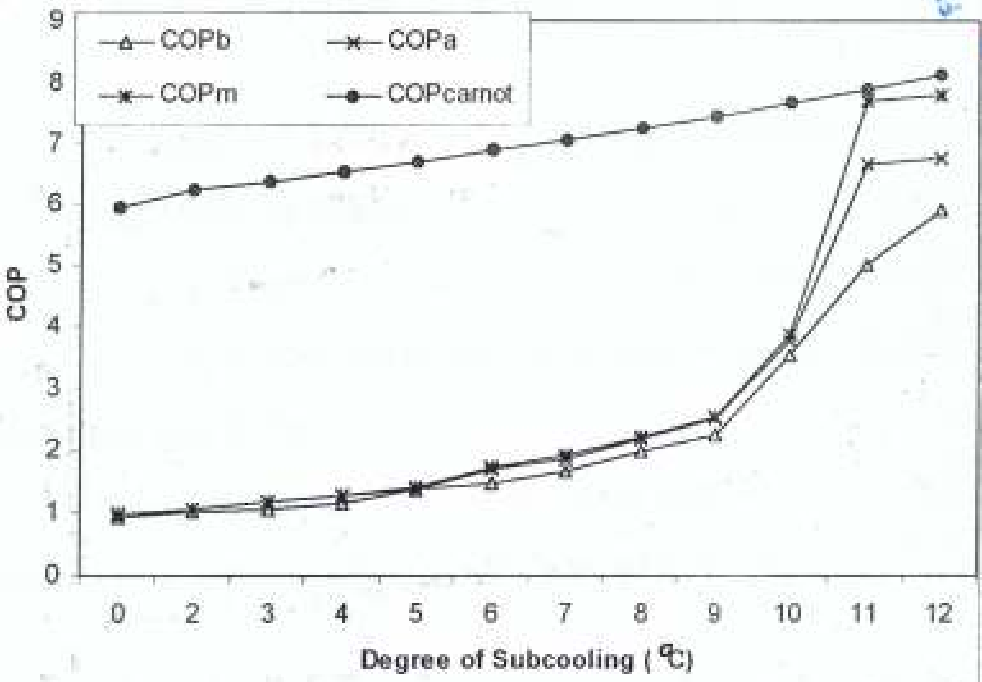

Fig. 4.13 Variation of COP with Degree of Subcooling

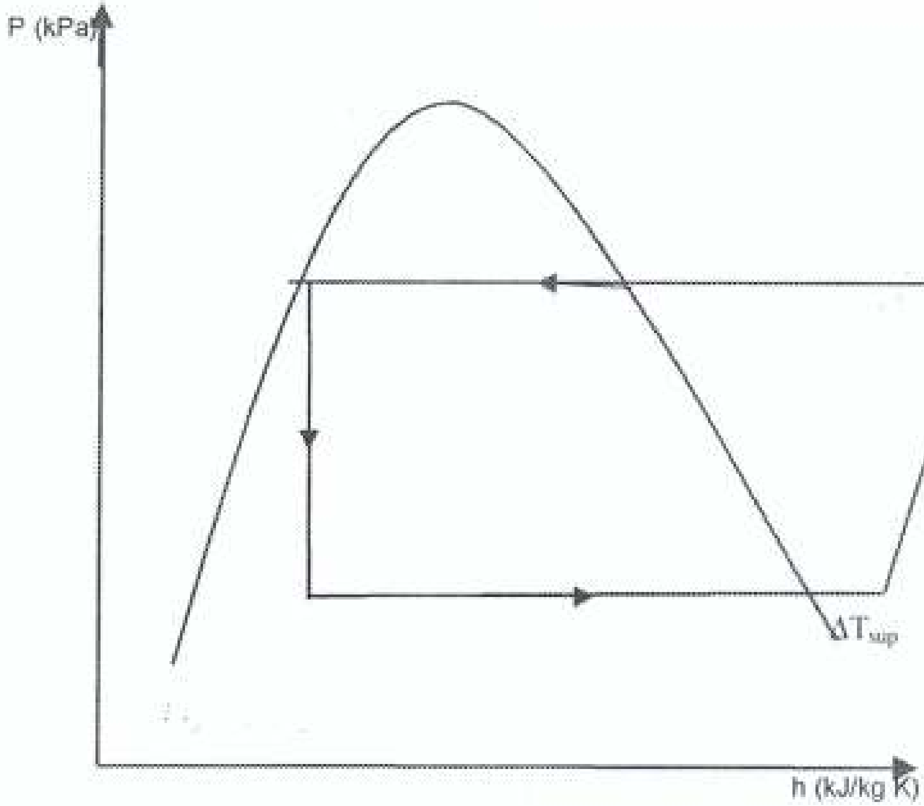

Fig. 4.14 P – h Curve for Degree of Superheating

As compared with Carnot cycle, efficiency decreased with increase in the degree of subcooling. (Figs. 4.15 and 4.16). This is due to the fact that COP_{Carnot} increases more rapidly with degree of subcooling than COP_a and COP_b (Fig. 4.13). This is possible because in the Carnot cycle there is no irreversible losses.

The variation of COP and efficiency with condensing temperature and degree of subcooling is as summarized in Fig. 4.17.

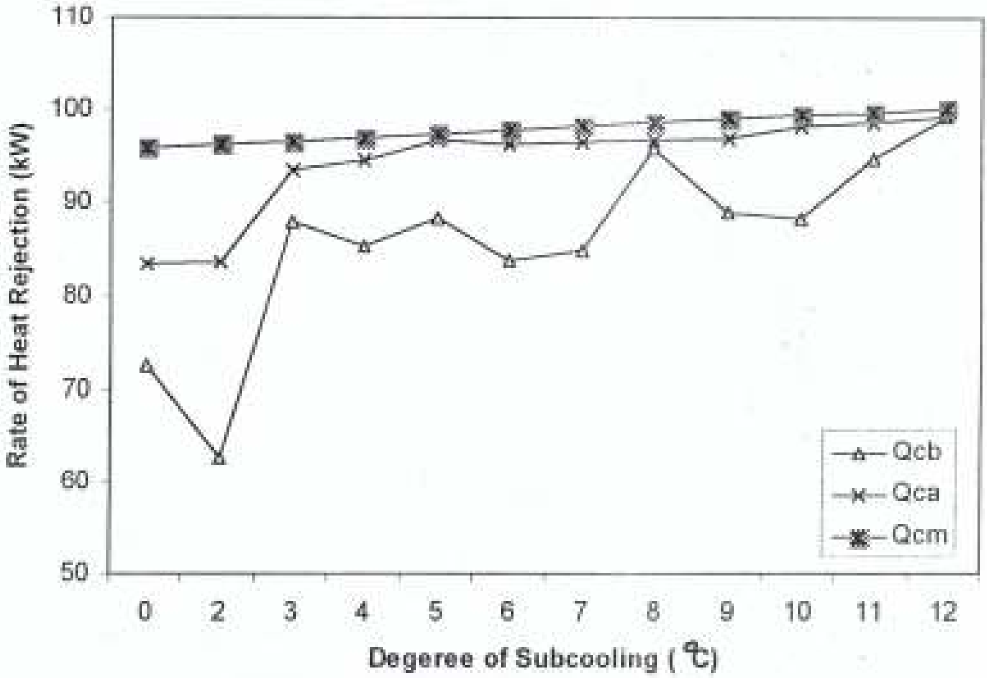

Fig. 4.15 Variation of Condsenser Capacity with Degree of Subcooling

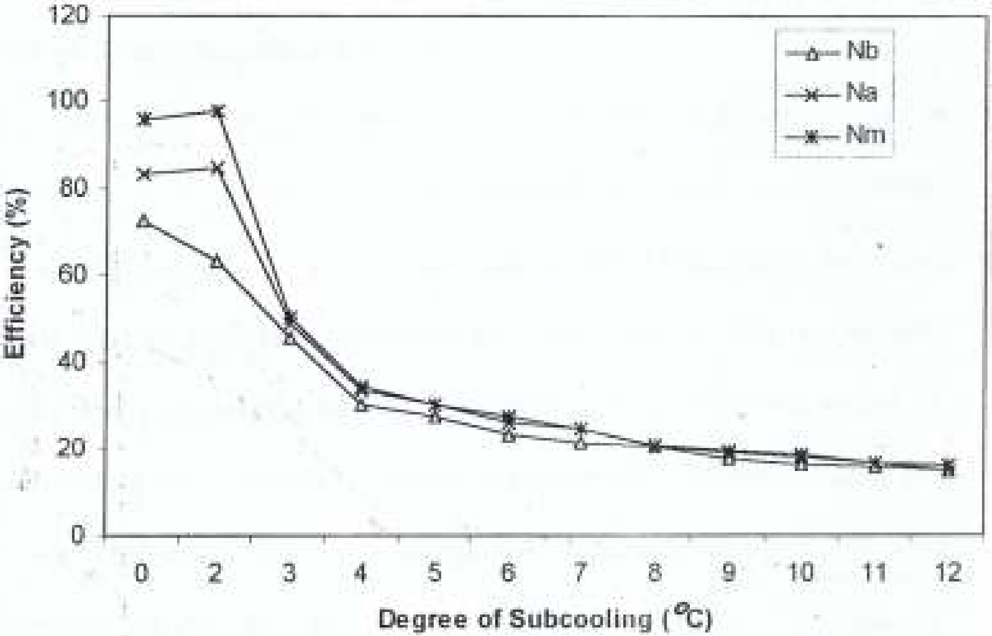

Fig. 4.16 Variation of Efficiency with Degree of Subcooling

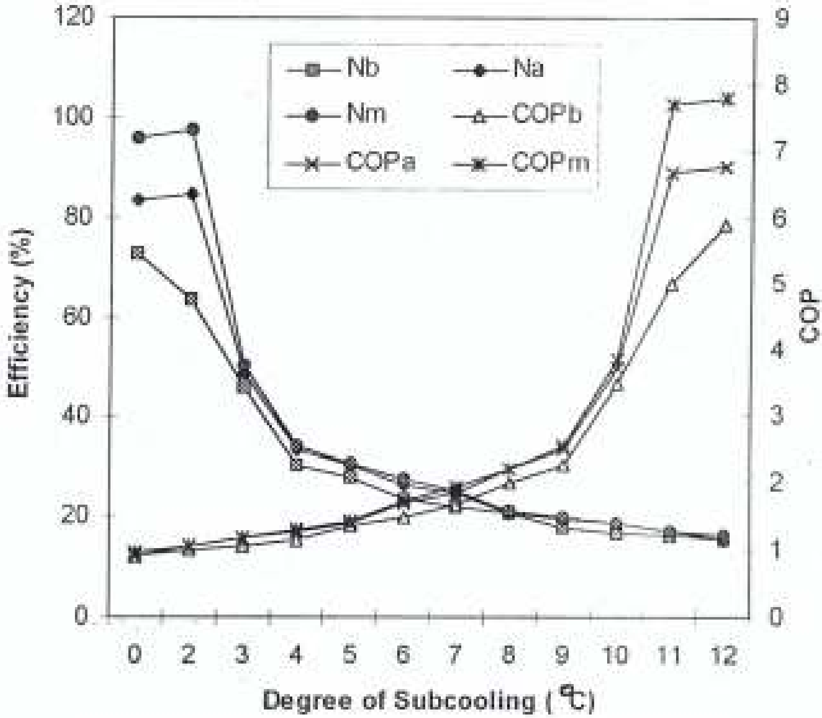

Fig. 4.17 Variation of Efficiency and COP with Degree of Subcooling

4.6.2 Effect of Superheating

Superheating of vapour usually occurs in the evaporator and is recommended as a prevention against droplets of liquid being carried over into the compressor. In this investigation, the refrigerant pressure at the exit of evaporator was adjusted to, and kept at, the saturation pressure (261 kPa) corresponding to the evaporating temperature of -5 °C. The flow rate of the circulating water was varied in order to vary the degree of superheating. The circulating water temperature used was varied between 20 °C to 35 °C to facilitate different degrees of superheating. The rigs were left to run for 30 minutes so that a steady evaporating temperature could be measured. The same process of section 4.6.1 was then followed in the measurement of the parameters and the estimations of Q_e, Q_c, COP, and the efficiency. The condenser temperature and pressure were kept constant at 40 °C and 961 kPa respectively.

As the degree of superheating increases, refrigerating effect decreases Fig. 4.18. This is easily explained from mass flow rate point of view. As the degree of superheat increases, the rate at which the refrigerant in the evaporator flashes into gas increases. This thereby increases the volume of gas in the evaporator, since the condensing temperature is kept constant, thus resulting into a decrease in the mass flow rate.

Normally, if saturated refrigerant leaves the evaporator it will be superheated at the end of the compression process (Fig. 4.10). Hence if the refrigerant leaving the evaporator is superheated, then the degree of superheat at the end of compression process is increased. This means that more heat transfer area will be required for the condenser for an effective rejection of the heat absorbed by the refrigerant. Since the heat transfer area is fixed in this case, the rate of heat rejection decreases with the increase in the degree of superheat. This is as shown in Fig. 4.19.

Generally, the rigs show almost the same pattern for both refrigerating effect and rate of heat rejection, (Figs 4.18 and 4.19). As could be expected, the rate of heat rejection is higher than the refrigeration effect.

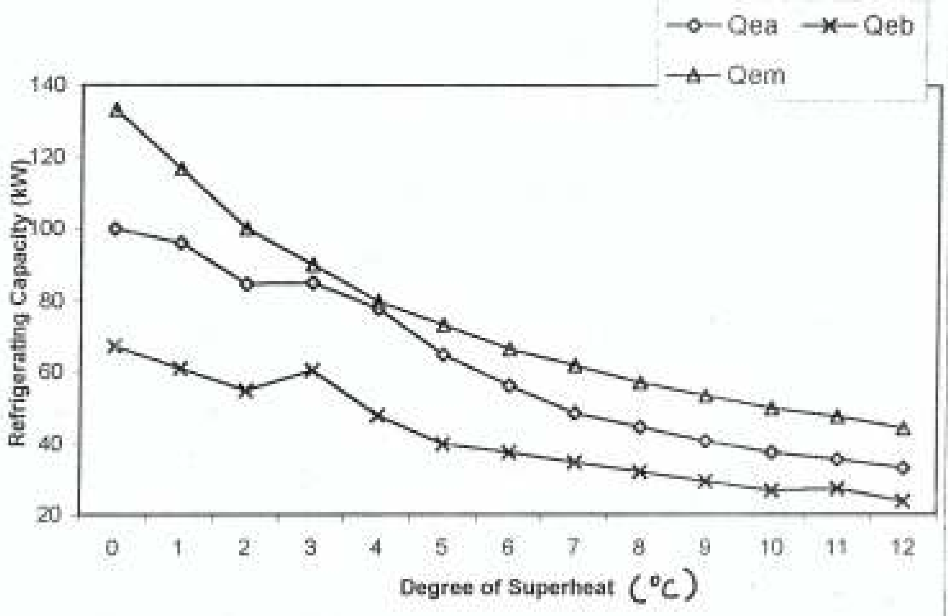

Fig. 4.18 Variation of Refrigerating Capacity with Degree of Superheat

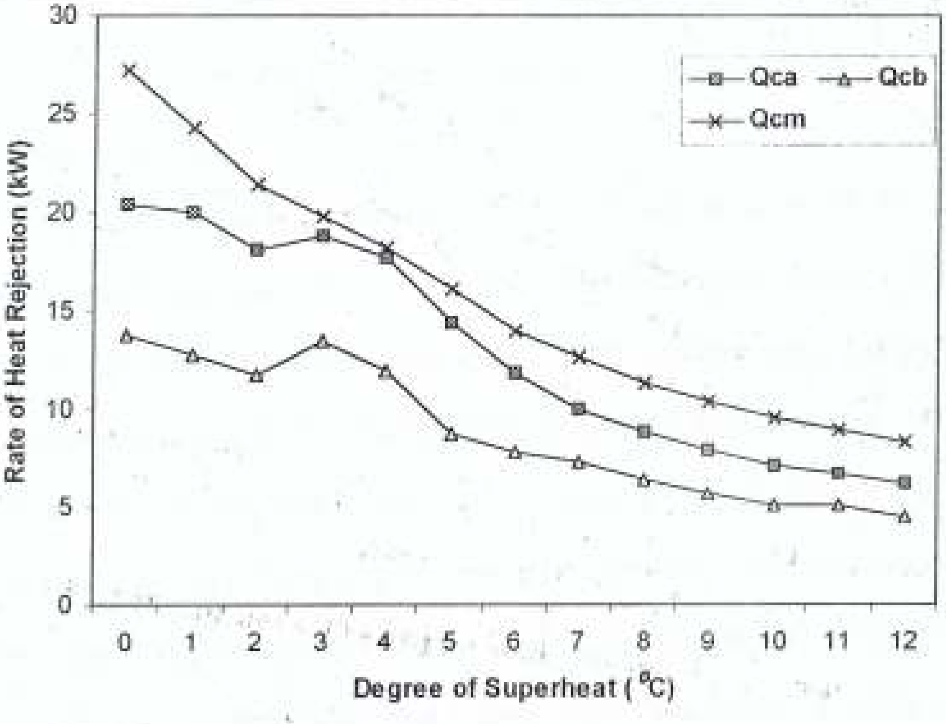

Fig. 4.19 Variation of Heat Rejection with Degree of Superheat

Also, from Figs 4.18 and 4.19, it can be seen that the characteristic curves of **rig a** is closer to that of the model than that of **rig. b** On the average, the parametric values of rigs a and b are 16.89 % and 35.13 % respectively below that of model.

The fluctuations observed in Figs. 4.18 and 4.19 between 1 ^{0}C and 3 ^{0}C of superheat can be justified by the works of many researchers, who have reported generally that evaporators show some degree of hunting (oscillations) with respect to refrigeration capacity in the early part of superheat between 1 ^{0}C and 4 ^{0}C (Mithraratne and Wijeysundera (2001); Wedekind, (1971); Ibrahim, (2001; Wijeysundera *et al*, (2000). The effect was much more pronounced in **rig b** than in **rig a**, this shows the effect of balancing the system components.

In Fig. 4.20, the efficiencies of the model and the rigs show similar trend, except for the fact that the values of **rig a** are closer to that of the model than that of rig b.

From Figs. 4.18 to 4.21, it was observed that as the degree of superheat increases the mass flow rate decreases and so also all the other parameters. It is worth noting that **rig a** always fell between the model and the **rig b**. This justifies the fact that balancing point is very important. Since the characteristic curves show the same trend or pattern, it means that the model is verified. The discrepancy noted between **"rig a"** and the model might be due to heat loss which could not be controlled and the defect or deficiency of the measuring instruments.

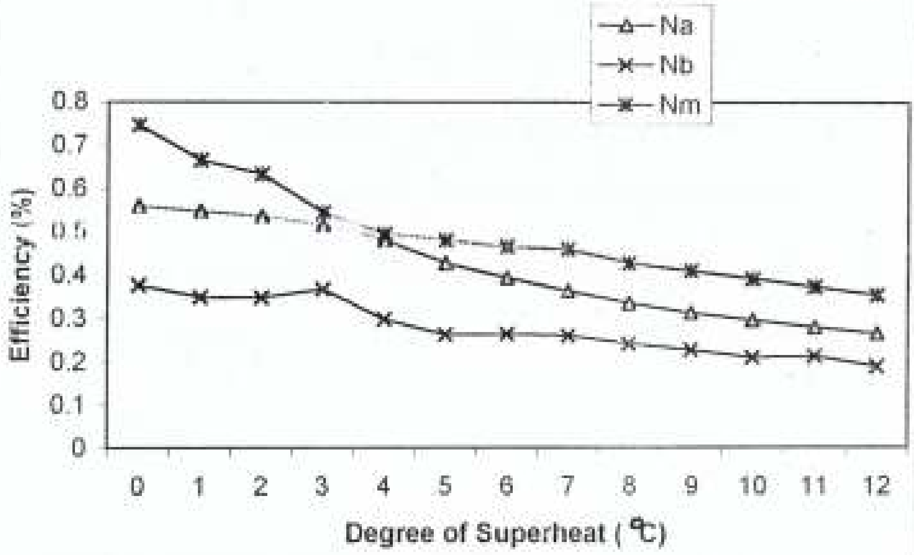

Fig. 4.20 Variation of Efficiency with Degree of Superheat

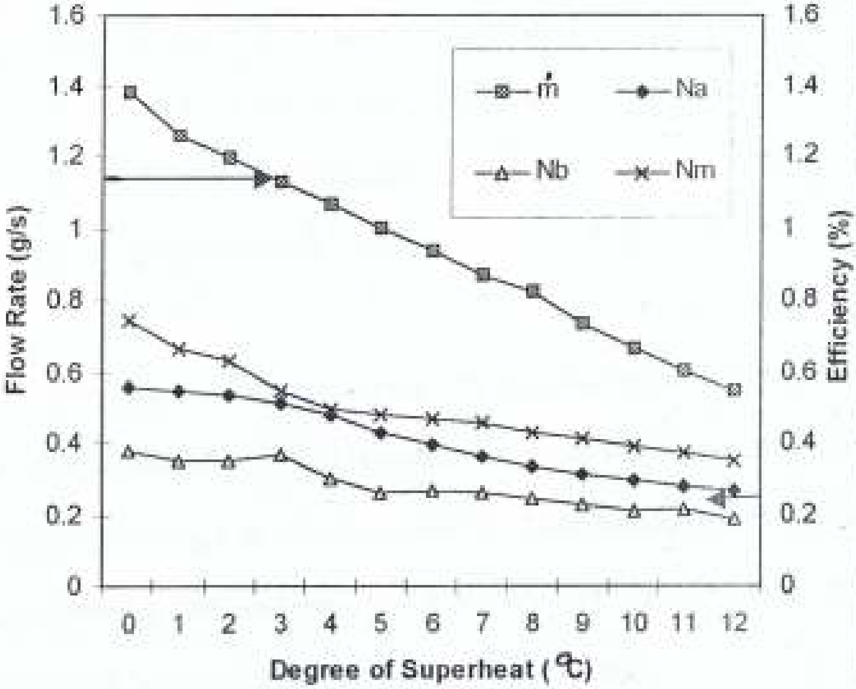

Fig.4.21 Variation of Efficiency and Flow Rate with Degree of Superheat

4.7 Comparison with other Empirical Equations

In Fig. 4.22 the present model was compared with several models and equations found in the literature. Generated values from the present work are compared with those of the ASHRAE design equation (1998), the empirical equation proposed by Kuehl and Goldschmidt (1990, 1991), Jung *et al's* equation (1999), Chen et al's equation (2000) and the Kim *et al's* equation (2002):

where:

m_1	ASHRAE design equation (1998)
m_2	Kuehl and Goldschmidt's empirical equation (1990)
m_3	Kuehl and Goldschmidt's model (1991)
m_4	Chen *et al's* equation (2000)
m_5	Jung *et al's* equation (1999)
m_6	Kim *et al's* equation (2002)
m_7	Present work (2003)

It could be observed that the present model compares favourably with the ASHRAE design equation, especially within, the condensing temperature range of 30 ^{0}C to 45 ^{0}C. This temperature range falls within the prevailing atmospheric condition in this country. Also it is within the condensing temperature found in the literature.

For clarity Fig. 4.23 was plotted for m_1, m_4 and m_7. This comparison was based on -5 ^{0}C evaporating temperature, the condensing temperature was varied while the mass flow rate was generated.

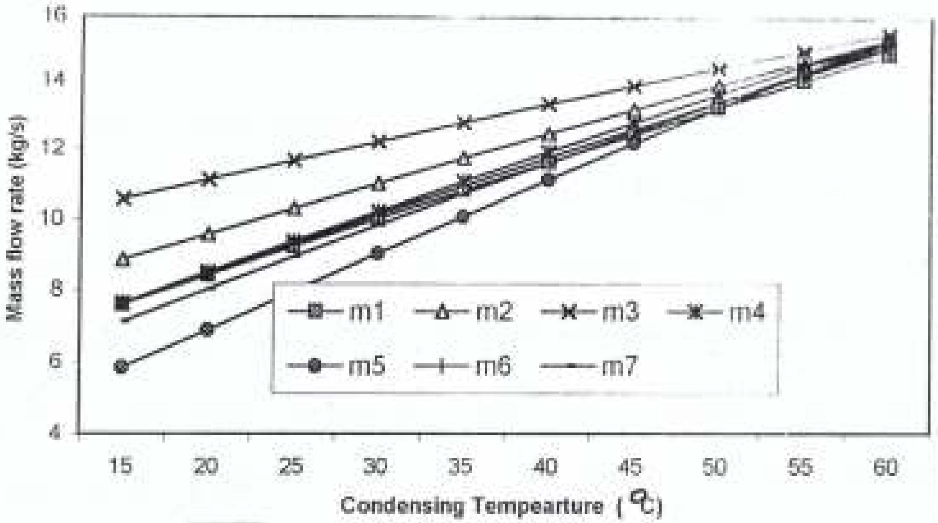

Fig. 4.22 Comparison with other equations

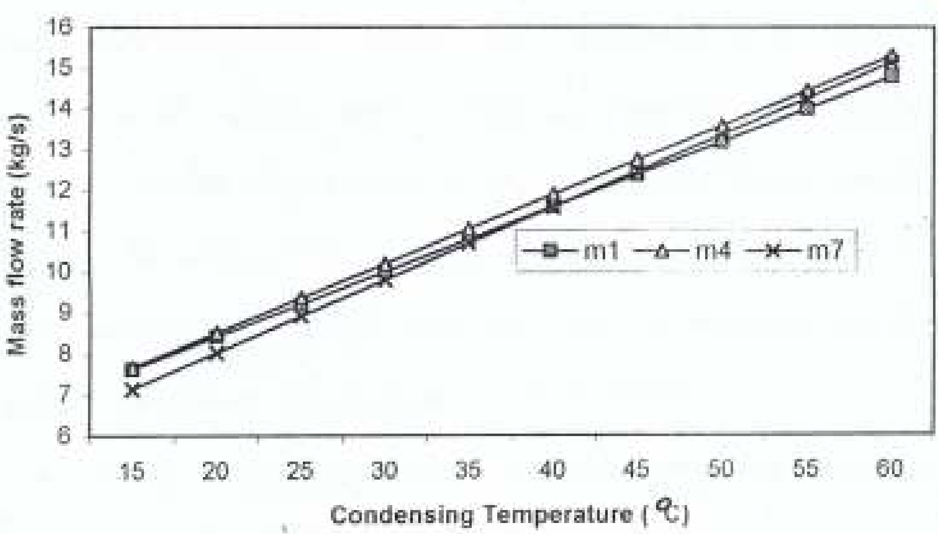

Fig. 4.23 Comparison with other equations

CHAPTER FIVE

5.0 CONCLUSIONS AND SUGGESTIONS FOR FURTHER WORK

5.1 CONCLUSIONS

The overall refrigeration system performance is strongly influence by the agreement between the major components and operationa parameters such as: ambient-, condensing-, evaporating- temperature and mass flow rate. A design model was developed in this work to strik a balanced point between these major components based on th operational parameters. Tests with the model, as the experimenta bench, in the present study has been planned in such a way to allow fo the evaluation of the effect of the operational parameters on syster performance of two separate systems, termed rig "a" and rig "b".

In addition, test data have been used to assess the quality of th computer simulation results. The simulated and the experimenta performance results were compared together with some additiona features related to the effect of the refrigerant charge, which is of majo concern to refrigeration system manufacturers, effects of overchargin and leakages. The results obtained from the experimental investigation justify adequately the developed design model.

From the experimental investigations the following genera remarks can be made:

i. COP is always affected negatively by increment of some particular parameters, such as, degree of superheating, compressor speed, ambient temperature and sudden change in the environmental conditions around the evaporator. In the case of the refrigerant charge, the effect is only significant under overcharged conditions.

ii. The COP is always affected positively by increase in flow rate and degree of subcooling.

iii. Refrigerating effect, mass flow rate and COP vary almost linearly with condensing and evaporating temperatures and compressor speed. There is a deviation from this linear behaviour at low refrigerating capacity (when the evaporator is starved, resulting into boiling of the refrigerant) and at overcharging conditions (causing flooding of the evaporator).

iv. Condensing temperature improves slightly the mass flow rate, refrigerating capacity and COP, an opposite effect to that observed with the evaporating temperature.

v. The effects of superheating and subcooling on the performance of the system indicated that the superheating has more negative influence on the COP of the system.

Present analysis and experimental investigations have shown that model results are comparable to the experimental ones. Table 6.1 shows the deviations of model results from those obtained in experiments under the same operational conditions. Maximum absolute deviations are within the range of 16 % to 19 % for rig "a" and 28 % to 34 % for rig "b" respectively as compared with the model results.

Table 6.1 Deviations of experimental results from those obtained from the model

Effects	Deviations (%)							
	Rig a				Rig b			
	Qe		COP		Qe		COP	
	max.	min	max	min	max	min	max	min
Compressor speed	-3.5	-2.5	1.4	0.5	-4.7	-3.0	3.8	1.6
Circulating water temperature	16	12	14	10	20	16	16	12
Superheating	16.89	12.72	16.75	15.6	35.1 3	30.55	33.5	29.5
Influence of charge loss	0.8	0.2	0.6	0.1	2.0	1.4	1.4	1.2
Subcooling	5.89	2.72	1.1	1.05	21.1 3	16.55	3.32	2.50
Subcooling and superheating			1.5	1.25			3.56	2.32

5.2 SUGGESTIONS FOR FURTHER WORK

A full performance evaluation of the system is required based on individual component. Each component should be fully equipped with modern measuring instruments.

More work is required on the capillary tube. Various sizes (length and diameter) should be used to verify the adequacy of capillary tube performance.

Evaporator exhibits lots of hunting at any slight change in both internal and external conditions. The cause(s) of this hunting requires investigation.

Performance of the system is required using alternative refrigerants.

Experimental investigation of Evaporator time constant is required.

REFERENCES

Adegoke, C. O. (2002) "Energy as Veritable Tool for Sustainable Environment". Inaugural Lecture Series 31. FUT., Akure 44 pp.

Ali, R. A. and Ramadhyani, M. H. (1992), Modelling of Condensers, Evaporators and Refrigeration Circuit in Automobile Air Conditioning System". International Journal of Refrigeration. Vol. 18 No. 5 pp 343 - 351.

Aluares, S. G. and Trepp, C. (1987) "Simulation of a Solar deriven Aqua-Ammonia Absorption Refrigeration System, Part I, Mathematical Description and System Optimisation". Journal of Refrigeration, Butterworth Science Ltd. England. Vol. 10, No. 1. pp 40 - 48.

ASHRAE HANDBOOK: Refrigeration, 1998, Chapter 45.1, "Insulation Systems for Refrigerant Piping".

ASHRAE HANDBOOK: Refrigeration, (2002), Chapters 49.7 and 45.26 "Adiabatic Capillary Tube Selection Procedure".

Beecher, D. T. (1968), "The Effects of Pattern Depth on the Performance of a Typical Air Conditioning Division Fin Tube Heat Exchanger". International Journal of Heat and Mass Transfer. Vol. 5 No 2, Pp 123 - 141.

Beecher, D. T. and Fagan, T. J. (1987), "Effects of Fin Pattern on the air-side Heat Transfer Coefficient in Plate finned-tube Heat Exchangers". ASHRAE Transaction, Vol. 93 No: 2, pp1961 - 1984

Calm, J. M. (2002) "Emission and Environmental Impacts from Air-Conditioning and Refrigeration". International Journal of Refrigeration. Vol. 25 No. 7. pp 293 – 305

Calm, J. M. and Didion, D. A. (1998) "Trade-offs in Refrigerant Selections: Past, Present and Future." Transaction of American Society of Heating Refrigerating and Air Conditioning Engineers. Vol. 21 No. 4. pp308-321

Calm, J. M.; Wuebbles, D. J.; and Jain, A. K. (1999) "Impacts on Global Ozone and Climate from use and Emission of 2,2-dichloro-1,1,1-trifluoroethane (HCFC-123). Journal of Climatic Change, Vol. 42 No. 3, pp 437 – 479.

Chang, S. D. and Ro, S. T., (1996), "Experimental and Numerical Studies on Adiabatic Flow of HF Mixtures in Capillary Tubes". International Journal of Refrigeration. Vol. 6, No: 1. pp 83 – 88.

Chen, S.L.; Cheng, Y. R.; Liu, C. H.; and Jwo, C. S. (2000) "Simulation of Refrigeration Flowing Through Adiabatic Capillary Tubes". HVAC&R Research. Vol. 6 No. 2, pp 101 – 115. Pergamon London.

Chen, W.; Zhijiu, C.; Ruiqi, Z. and Yezheng, W. (2002) "Experimental Investigation of a Minimum Stable Superheat Control System of an Evaporator. International Journal of Refrigeration. Vol. 25, No. 8 pp1137 – 1142.

Chen, Z. H; Li, R. Y; Lin, S; Chen, Z. Y. (1990) " A Correlation for Metastable Flow of Refrigerant 12 through Capillary Tubes. www.elsevier.com/locate/ijrefrig.

Chi, K. U; Wang, C. C; Chang, Y. J. and Chang, Y. P. (1999), "A Comparison Study of Compact Plate fin-and-tube Exchangers". Journal of Experimental Heat Transfer, Vol. 12, No: 1, pp 73 – 89.

Fukuta, M.; Yanagisawa, T.; Iwata, H. and Tada, K. (2002), "Performance of Compression/Absorption Hybrid Refrigeration Cycle with Propane/Mineral oil Combination". International Journal of Refrigeration, Vol. 25, No: 5 pp 907 – 915.

Foerg, W. (2002), "History of Cryogenics: the Epoch of the Pioneers from the Beginning to the year 1911". International Journal of Refrigeration. Vol. 25 No. 2 pp 283 – 292.

Glocker, G; Haussmann, G. H.; Heinritz, S.; Nowothy, S. and Thide, K. (1998) "Computer Assisted and Engineering of Plate Fin-type Heat Exchangers – Part I: Evaporator". Journal of Refrigeration Science and Technology. Commission B1. International Journal of Refrigeration, Paris. Pp 213 – 221.

Goldstein, L. and Sparrow, E. M. (1976), "Experiments on the Transfer Characteristics of a Corrugated Fin and Tube Heat Exchangers Having Plain Fins". International Journal of Heat Transfer, Vol. 12 No 7, pp 2745 – 2750.

Gordon, H.; Meyer, C.; Rautanberg, M. and McEwan, M. B. (1996) "Computer Modelling for the Performance of Centrifugal Water Chillers in Mine Refrigeration Installation". Journal of Refrigeration Science and Technology. Commission B1. International Journal of Refrigeration, Paris. Vol. 10 No. 1 pp 49 – 61.

Hopkin, N. E. (1996) "Rating the Restrictor Tube" Journal of Refrigeration Engineering. Vol. 58, No. 11, pp 1087 - 1094

Ibrahim, G. A. (2001), " Effect of Sudden Changes in Evaporator External Parameters on a Refrigeration System with an Evaporator Controlled by a Thermostatic Expansion Valve". International Journal of Refrigeration. Vol. 24, No. 4, pp 566 – 576.

Jabardo, J. M. S.; Mamani, W. G.and Ianalla, M. R. (2002) "Modelling and Experimental Evaluation of an Automotive Air-conditioning System with a variable Capacity Compressor". International Journal of Refrigeration. Vol. 25 No. 8, pp 1157 – 1172.

Jameel, V. M.; Xi, G. N.; Murata, T.; Hagiwara, Y.; and Suzuki, K. (1999) "Experimental Study on Heat Transfer Characteristics of Offset Fin Arrays – Effect of Fin Thickness in the Low and Middle Ranges of Reynolds Number". International Journal of Heat Transfer, Vol. 4, pp81 – 86.

Janssen, M. J. P; Kuijpers, L. J. M. and Dewit, J. A (1988) "Theoretical and Experimental Investigation of a Dynamic Model for Small Refrigeration Systems". Journal of Refrigeration Science and Technology. Commission B1. Paris. pp 245 – 262.

Jia, X.; Tso, C. P.; and Chia, P. K. (1999), "A Distributed Model for Prediction of the Transient Response of an Evaporator". International Journal of Refrigeration. Vol. 18 No. 5 pp 336 – 342.

Jung, D.; Park, C. and Park, B. (1999) "Capillary Tube Selection for HCFC-22 Alternatives". International Journal of Refrigeration, Vol. 22 No. 8. pp 604 – 614.

Khan, J. R.; and Zubair, S. M. (1999) "Design and Performance Evaluation of Reciprocating System". International Journal of Refrigeration. Vol. 22 No. 1, pp 235 - 241

Kim, N. H.; Yun, J. H. and Webb, R. L. (1997), "Heat Transfer and Friction Correlations for Wavy Plate Fin-and-Tube Heat Exchangers" ASME Journal of Heat Transfer, Vol. 119 No. 3 pp 560 – 567.

Kim, S. G.; Kim, M. S. and Ro, S. T. (2002) "Experimental Investigations of the Performance of R22, R407 and R410A in Several Capillary Tubes for Air-Conditioning". International Journal of Refrigeration, Vol. 25 No 3. pp 521 – 531.

Kim, S. G.; Lin, Y. T; Lee, C. J. and Chang, Y. J. (1999), "Investigation of Wavy Fin-and-tube Heat Exchangers: A Contribution to Databank". Journal of Experimental Heat Transfer. Vol. 12, No: 1, Pp 73 - 89

Klein, S. A. (1994) "Design Consideration for Refrigeration Cycle" ". International Journal of Refrigeration. Vol. 15 No. 3, pp 181 – 185

Klein, S. A. (1998) "Experimental Study of the Fundamental Properties of the Reciprocating Chillers and Their Relation to the Thermodynamic Modelling and Chiller Design". International Journal of Heat and Mass Transfer. Vol. 39 No. 11 pp 1233 – 1241

Ko, M. K. W.; Sze, N-D; Molnar, G.; Prather, M. J. (1993) "Global Warming From Chlorofluorocarbons and their Alternatives: Time Scales of Chemistry and Climate". Journal of Atmospheric Environment. Vol. 17, No. 4. pp 581 – 587.

Kuehl, S. J. and Goldschmidt, V. W. (1990) "Steady Flows of R22 through Capillary Tubes: Test Data. ASHRAE Transaction Vol. 96, pp 719 – 728

Kuehl, S. J. and Goldschmidt, V. W. (1991) "Modelling of Steady Flows of R22 through Capillary Tubes". ASHRAE Transaction. Vol. 97, pp 139 – 148

Kuehn, H. T.; and Liang, .H (1991) "Irreversibility Analysis of a Water to Water Mechanical-Compression Heat Pump. International Journal of Heat and Mass Transfer. Vol. 16 No. 6. pp 883 - 896.

Kutter, W. (1988), "Status and Future of Alternative Refrigerants to Chlorofluocarbons". Journal of Refrigeration Science and Technology. Commissions C2, D1, D2/3, E1. International Institute of Refrigeration, Paris. Pp 187 - 194.

Lee, J. H.; Bae, S. W.; Bang, K. H. and Kim, M. H. (2002), "Experimental and Numerical Research on Condenser Performance for R-22 and R-407c Refrigerants. International Journal of Refrigeration, Vol. 25 No: 8, pp 372 – 382.

Lee, J. H.; Yoo, K. H. and Moffat, R. J. (2000), "Performance and Simulation of Automobile Air-Condition System". International Journal of Refrigeration. Austria. Vol. 23 No. 2. pp 243 - 254.

Lorentzen, G. (1988a), "Ammonia: AN Excellent Alternative". Journal of Refrigeration Science and Technology. Commissions B1, B2, E1 & E2. Purdue university (USA). Pp 381 - 386.

Lorentzen, G. (1988b), "The CFC1 Problem; a Strategy to Reduce Atmospheric Release". Journal of Refrigeration Science and Technology. Commissions C2, D1, D2/3, E1. International Institute of Refrigeration, Pp177 – 186.

Mahayana, N. C. and Xu, L. P. (1983), "An Experimental Study of Flow and Heat Transfer in Parallel-Plate Arrays: Local, Row-by-Row and Surface Average Behaviour". International Journal of Heat and Mass Transfer. Vol. 40, No: 6. Pp 1366 – 1378.

McMullan, J. T. (2002), " Refrigeration and the Environment – Issues and Strategies for the Future". ". International Journal of Refrigeration, Vol. 25 No. 1. pp 89 - 99.

Melo, C.; DaSilva, R. T.; Ferreira, R. Pereira, H.; and Negrao, C. O. R. (1988)., "Dynamic Behaviour of a Vapour Compression Refrigerator: a Theoretical and Experimental Analysis". Journal of Refrigeration Science and Technology. Commission B1, pp 141, International Institute of Refrigeration.

Mithraratne, P.; and Wijeysundera, N. E. (2001), "An Experimental and Numerical Study of Hunting in thermostatic-Expansion-Valve-Controlled Evaporator". International Journal of Refrigeration. Vol. 25 No 3 PP 992 – 998.

Mirth, D. R. and Ramadhyani, S. (1994), "Prediction of Cooling-Coils Performance Under Condensing Conditions". International Journal of Heat and Fluid Flow Vol. 14, No. 4, pp 391 – 400.

McLinden. M. O. and Didion, D. A (1988) " The Search for Alternative Refrigerants – a Molecular Approach". Journal of Refrigeration Science and Technology. Commissions B1, B2, E1 & E2. Purdue university Pp 91 – 100.

Nakayama, W. and Xu, L.P. (1983), "Enhanced fins for air-cooled heat exchangers-heat transfer and friction correlations. International Journal of Heat Transfer. Vol. 1 N: 4, pp 495 – 502

Sahin, C. A. and Kodal, C. H. M. (2002), "Heat and Mass Transfer in Refrigeration Systems Capillary Tubes". International Journal of Refrigeration. Vol. 7 No: 6 Pp 348 – 357.

Sand, J. R.; Fischer, S. K.; Baxter, V. D. (1997) "Energy and Global Warming Impacts of HFC Refrigerants and Emerging Technologies: Alternative Fluorocarbons Environmental Acceptability Study (AFEAS). Journal of Climate Change. Vol. 10 No. 6. pp 1145 – 1152.

Schlager, L. M.; Pate, M. B. and Bergles, A. E. (1990), "Performance Predictions of Refrigerant-oil Mixtures in Smooth and Internally Finned Tubes-Part II. Design Equations". Journal of Refrigeration Science and Technology. Vol. 33 No 21. Pp 170 – 182.

Schultz, G. D. (1985), "Experimental Investigation of Refrigerant Flow Through Adiabatic Capillary Tube". International Journal Of Refrigeration. Vol. 4 No: 6, Pp 878 – 886.

Segelstard, T. V. (1998), "Carbon Cycle Modelling and the Residence Time of Natural and Anthropogenic Atmospheric CO_2 on the Construction of the Greenhouse Effect Global Warming Dogma". International Journal of Science and Environment. Vol. 2 No. 1. pp 185 – 218.

Shankland, I. R.; Basu, R. S. and Wilson, D. P. (1988). "Thermal Conductivity and Viscosity of a new Stratospherically Safe Refrigerant – 1-,1,1,2-Tetralfluoroethane (R-134a)". Journal of Refrigeration Science and Technology. Commissions B1, B2, E1 & E2. Purdue university, Pp 305 – 314.

Spauschas, H. O. (1991) "Development in Refrigeration: Technical Advances and Opportunities for the 1990s". International Journal of Refrigeration, Vol. 10. No. 5. pp 263 – 275.

Spauschas, H. O. (1987a) "HFC-134a as a Substitute Refrigerant for CFC 12". Refrigeration Science and Technology, Commissions B1, B2, E1 and E2. pp 397 – 400.

Spauschas, H. O. (1987b) "Development in Refrigeration: Technical Advances and Opportunities for the 1990's Int. of Refrigeration. Vol. 10, No. 5, pp 263.

Statt, T. G. (1988), "Use of Chlorofluorocarbons in Refrigeration, Insulation and Mobile Air Conditioning in USA". Journal of Refrigeration Science and Technology. Commissions B1, B2, E1 & E2. Pp 353 – 358.

Stoecker, W. F. and Jones, W. P.(1982) Refrigeration and Air-Conditioning". Second Edition. McGraw-Hill Book Company.

Wang, C. C., Fu, W. L. and Chang, C. T. (1995), " Heat Transfer and Friction Characteristics of Typical Wavy Fin-and Tube Heat Exchangers". Journal of Thermal Fluid Science. Vol. 8 No 4, pp 321 – 327.

Wang , C. C.; Hsieh, Y. C. and Lin, Y. T. (1997), "Performance of Plate Finned Tube Heat Exchangers Under Dehumidifying Conditions". ASME Journal of Heat Transfer, Vol. 119 No. 1pp 109 - 117.

Wang, C. C; Tao, W. H and Chang, C. J (1999), "An Investigation of the Airside Performance of the Slit Fin-and-tube Heat Exchangers". International Journal of Refrigeration. Vol. 22 No 2. Pp 595 – 603.

Webb, R. L. (1990), "Flow Structure in the Louvered Fin Heat Exchanger Geometry". Journal of Thermal and Fluid Science. Vol. 4 No: 2, Pp 205 – 217

Wedekind, G. L. (1971), "An Experimental Investigation into the Oscillatory Motion of Mixture-Vapour Transition Point in Horizontal Evaporator Flow". Journal of Heat Transfer. Vol. 93, No: 1, pp47 – 54.

Wijaya, H. (1992),"Adiabatic Capillary Tube Test Data for HF-134a". International Journal of Refrigeration. Vol. 11, No: 1. Pp 63 – 71.

Wijeysundera, N. E.; Mithraratne, P., and Bong, T. Y. (2000), "Simulation of Evaporator Stability and Control". International Journal of Refrigeration. Vol. 23, No: 3, pp 174 – 189.

Wolf, D. A.; Bittle, R. R. and Pate, M. B. (1995), "Adiabatic Capillary Tube Performance with Alternative Refrigerants". International Journal of Refrigeration. Vol. 23, No: 3, pp 190 – 200.

Wolf, D. A.; and Pate, M. B. (2001), "Capillary Tube-Suction Line Heat Exchanger Performance with Alternative Refrigerants". ASHRAE Transaction, Vol. 97, No: 1, pp 139 – 149.

Appendix I

Condensing and Complete Units

```
function akintundec(action)
%global T1 T2 tol Ta Tm Tw count Qe P Qc COP
   T1=eval(get(findobj('tag','T1'),'String')); % maximum evaporating temp
   T2=eval(get(findobj('tag','T2'),'String'));% condensing temp
   tol=findobj('tag','TOL');
   tol=eval(get(tol,'String'));%tolerance
   Ta=eval(get(findobj('tag','TA'),'String'));% ambient temp
   Tm=eval(get(findobj('tag','TM'),'String'));% minimum evaporating temp
   Tw=findobj('tag','Tw');
   Tw=eval(get(Tw(1),'String')); %Water Temperature
c=[137.402, 4.60437, 0.061652, -1.118157, -0.001525,...
      -0.0109119,-0.00040148, -0.00026682,0.000003873];
d=[1.00618, -0.893222, -0.01426, 0.870024, -0.0063397,...
      0.033889,-0.00023875, -0.00014746,0.0000067967];
count =1;

switch action
case  'calculate' % complete unit
for k=T1:-1:Tm;
   T21=0;
   while abs(T21-T2)>= tol
      Qe=c(1)+c(2)*k+c(3)*k^2+c(4)*T2+c(5)*T2^2+...
         c(6)*k*T2+c(7)*k^2*T2+c(8)*k*T2^2+c(9)*k^2*T2^2;
      P=d(1)+d(2)*k+d(3)*k^2+d(4)*T2+d(5)*T2^2+...
         d(6)*k*T2+d(7)*k^2*T2+d(8)*k*T2^2+d(9)*k^2*T2^2;
      Qc=Qe+P;
      T21=T2;
      T2=Qc/9.39+Ta;
      COP=Qe/P;
      end
   TT2(count)=T2;QE(count)=Qe;TT(count)=k;Cop(count)=COP;
   QC(count)=Qc;p(count)=P;
   count=count+1;
end
fid=fopen('condensingunit.txt','w');
out=[TT; TT2; p;  Cop; QE; QC];
obj=findobj('tag','StaticText2');
obj2=findobj('tag','StaticText3');
set(obj,'visible','on')
set(obj2,'visible','off')

case 'complete' % complete unit
for k=T1:-1:Tm;
   T21=0;
   while abs(T21-T2)>= tol
      Qe=c(1)+c(2)*k+c(3)*k^2+c(4)*T2+c(5)*T2^2+...
         c(6)*k*T2+c(7)*k^2*T2+c(8)*k*T2^2+c(9)*k^2*T2^2;
      P=d(1)+d(2)*k+d(3)*k^2+d(4)*T2+d(5)*T2^2+...
         d(6)*k*T2+d(7)*k^2*T2+d(8)*k*T2^2+d(9)*k^2*T2^2;
      Qc=Qe+P;
      a=0.046;
      b=-(2*0.046*Tw+1);
      C=a*Tw^2+Tw-Qe/6;
      Tb=(-b-sqrt(b^2-4*a*C))/(2*a);
      k=Tb;
      COP=Qe/P;
      T21=T2;
      T2=Qc/9.39+Ta;
            end
```

```
    TT2(count)=T2;QE(count)=Qe;TT(count)=Tb;Cop(count)=COP;
    QC(count)=Qc;p(count)=P;
    count=count+1;
 end
 fid=fopen('completeunit.txt','w');
 out=[TT; TT2; p;  Cop; QE; QC;T1:-1:Tm];
 obj=findobj('tag','StaticText2');
 obj2=findobj('tag','StaticText3');
 set(obj,'visible','off')
 set(obj2,'visible','on')

end
j=size(QE);j=j(2);



      for j=1:j-1
      fprintf(fid,'%6.4f %6.4f  %6.4f %6.4f %6.4f %6.4f\n',...
         TT2(j), p(j),TT(j), Cop(j),QE(j),QC(j));
      end
      fclose(fid);
      d=findobj('tag','Listbox1');
      %d=d(2);
      out=num2str(out');
      set(d,'string',num2str(out))
```

Appendix II

Condenser and Evaporator

```
function condenser(action)
T1=eval(get(findobj('tag','T1'),'String')); % maximum evaporating tem
T2=eval(get(findobj('tag','T2'),'String'));% condensing temp
QC=eval(get(findobj('tag','QC'),'String')); % maximum evaporating tem
Qe=eval(get(findobj('tag','QE'),'String'));% condensing temp
ID=eval(get(findobj('tag','ID'),'String')); % maximum evaporating tem
OD=eval(get(findobj('tag','OD'),'String'));% condensing temp
Ta=eval(get(findobj('tag','TA'),'String')); % maximum evaporating tem
x=(OD-ID)/2;E=Qc/Qe;

switch action
case 'condense'
rho=1109; k=0.674; mu=0.00216; g=9.806; c=390;ff=0.00176;
h1=200-1.172*T2+0.001854*T2^2;h2=405.5+0.3636-0.002273*T2^2;
hg=h2-h1;
DT=T2-Ta;
hc1=0.725*(g*rho^2*hg*k^3)^(1/4);
hc2=(3*mu*DT*OD)^(1/4);hc=hc1/hc2;
AO=pi*OD^2/4; AI=pi*ID^2/4;AM=(AO+AI)/2;
R=x/c*AO/AM;
fd=1/hc+R+(OD/ID)*(ff+1/5910);fd=1/fd;
kk=log((T2+3-Ta)/(T2-Ta));
lmtd=((T2+3-Ta)/(T2-Ta))/kk;
A=Qc*E*1000/(fd*lmtd);
lent=A/(pi*OD);
out=[A, lent];
num2str(out');

case 'evaporate'
rho=1209; k=0.0902; mu=0.30185; g=9.806; c=390;ff=0.00176;
h1=200-1.172*T1+0.001854*T1^2;h2=405.5+0.3636-0.002273*T1^2;
hg=h2-h1;
DT=8;
hc1=0.725*(g*rho^2*hg*k^3)^(1/4);
hc2=(3*mu*DT*OD)^(1/4);hc=hc1/hc2;
AO=pi*OD^2/4; AI=pi*ID^2/4;AM=(AO+AI)/2;
R=x/c*AO/AM;
fd=1/hc+R+(OD/ID)*(ff+1/5910);fd=1/fd;
kk=log((T1+20)/(T1+25));
lmtd=abs(((T1+20)-(T1+25))/kk);
A=Qe*1000/(fd*lmtd);
lent=A/(pi*OD);
out=[A, lent];
num2str(out');
end
set(findobj('tag','AREA'),'string',num2str(A));
d=findobj('tag','LEN');
set(d(2),'string',num2str(lent));
```

Appendix III

Capillary Tube

```
% function capillary
  T1=eval(get(findobj('tag','T1'),'String')); % maximum evaporating temp
  T2=eval(get(findobj('tag','T2'),'String'));% condensing
  D=eval(get(findobj('tag','D'),'String'));% condensing
% T1=input('enter T1')
% T2=input('enter T2')
% D=input('enter Diameter')

   T3=T2;T4=T1;W=0.01;
   L=0;A=pi*D^2/4;y=0;G=W/A;I=1;
   fid=fopen('capillary.txt','w');
%   fprintf(fid,
P=1000*exp(15.06-(2418.4/(T2+273.15)));% Pressure
VF=(0.777+0.002062*T2+0.00001608*T2^2)/1000;% Specific Volume Liquid
VG=(-4.26+94050*(T2+273.15)/P)/1000;% Specific Volume gas
HF=200+1.172*T2+0.001854*T2^2;%enthalpy Liquid
HG=405.5+0.3636*T2-0.002273*T2^2;%enthalpy gas
MF=0.0002367-1.715e-6*T2+8.869e-9*T2^2;% Friction, Liquid
MG=11.945e-6+50.06e-9*T2+0.256e-9*T2^2;% Friction Gas
V=G*VF;% Valocity
Re=V*D/(MF*VF);%Reynold's Number
mu=MF*(1-y)+y*MG;
H=HF*(1-y)+y*HG;% Enthalpy of Mixture
F=0.33/Re^0.25;% Friction Factor, Mixture
Vf=VF;Hf=HF;h=H;v=V;f=F;p=P;DL=0;Hg=HG; %swap values
t2(I)=T2;PP(I)=P/1000;VV(I)=V;dl(I)=DL;LI(I)=L;Y(I)=y;
for T2=T2-1:-1:T1
P=1000*exp(15.06-(2418.4/(T2+273.15)));
VF=(0.777+0.002062*T2+0.00001608*T2^2)/1000;
VG=(-4.26+94050*(T2+273.15)/P)/1000;
HF=200+1.172*T2+0.001854*T2^2;
HG=405.5+0.3636*T2-0.002273*T2^2;
MF=0.0002367-1.715e-6*T2+8.869e-9*T2^2;
MG=11.945e-6+50.06e-9*T2+0.256e-9*T2^2;

%V=G*VF;
a=0.5*(VG-VF)^2*G^2;
b=1000*(HG-HF)+VF*(VG-VF)*G^2;
c=1000*(HF-h)+0.5*G^2*VF^2-0.5*v^2;

y=(-b+sqrt(b^2-4*a*c))/(2*a);
miu=VF*(1-y)+y*VG;
%V=G*VF;% Valocity

V=G*miu;

M=MF*(1-y)+y*MG;
VM=(V+v)/2;
Re=VM*D/(M*miu);
H=HF*(1-y)+y*HG;
l=Vf*(1-y)+y*VG;
F=0.33/Re^.025;
FM=(F+f)/2;
J=p-P-G*(V-v);
%DL=2*J*D/(VM*FM*G^2);
DL=2*J*D/(VM*FM*G);

L=L+DL*10;
Vf=VF;Hf=HF;h=H;v=V;f=F;p=P;Hg=HG;
I=I+1;
t2(I)=T2;PP(I)=P/1000;VV(I)=V;dl(I)=DL;LI(I)=L;Y(I)=y;
end
out=[t2;PP;Y;VV;dl;LI]';
format long e;
gg=out(2:end,:);
d=findobj('tag','Listbox1');
set(d,'string',num2str(gg));
```

```
function fig = aakintunde1()
load aakintunde1

h0 = figure('Color',[0.8 0.8 0.8], ...
    'Colormap',mat0, ...
    'FileName','C:\MATLABR11\work\aakintunde1.m', ...
    'MenuBar','none', ...
    'Name','REF-2004', ...
    'NumberTitle','off', ...
    'PaperPosition',[18 180 576 432], ...
    'PaperUnits','points', ...
    'Position',[336 155 431 228], ...
    'Tag','Fig2', ...
    'ToolBar','none');
h1 = uicontrol('Parent',h0, ...
    'Units','points', ...
    'BackgroundColor',[0.752941176470588 0.752941176470588 0.752941176470588],
    'ListboxTop',0, ...
    'Position',[41.25 30.75 258.75 113.25], ...
    'Style','frame', ...
    'Tag','Frame1');
h1 = uicontrol('Parent',h0, ...
    'Units','points', ...
    'BackgroundColor',[0.752941176470588 0.752941176470588 0.752941176470588],
    'Callback','evaporator', ...
    'FontSize',14, ...
    'FontWeight','bold', ...
    'ListboxTop',0, ...
    'Position',[226.5 22.5 84.75 24.75], ...
    'String','Evaporator', ...
    'Tag','Pushbutton5');
h1 = uicontrol('Parent',h0, ...
    'Units','points', ...
    'BackgroundColor',[0.752941176470588 0.752941176470588 0.752941176470588],
    'Callback','akintundec11', ...
    'FontSize',14, ...
    'FontWeight','bold', ...
    'ListboxTop',0, ...
    'Position',[15 130.5 111 21.75], ...
    'String','Capillary Tube', ...
    'Tag','Pushbutton4');
h1 = uicontrol('Parent',h0, ...
    'Units','points', ...
    'BackgroundColor',[0.752941176470588 0.752941176470588 0.752941176470588],
    'Callback','akintunde', ...
    'FontSize',14, ...
    'FontWeight','bold', ...
    'ListboxTop',0, ...
    'Position',[192.75 126 122.25 26.25], ...
    'String','Condensing Unit', ...
    'Tag','Pushbutton2');
h1 = uicontrol('Parent',h0, ...
    'Units','points', ...
    'BackgroundColor',[0.752941176470588 0.752941176470588 0.752941176470588],
    'Callback','akintunde', ...
    'FontSize',14, ...
    'FontWeight','bold', ...
    'ListboxTop',0, ...
    'Position',[109.5 72.75 111 26.25], ...
    'String','Complete Unit', ...
    'Tag','Pushbutton1');
```

126

```
h1 = uicontrol('Parent',h0, ...
    'Units','points', ...
    'BackgroundColor',[0.752941176470588 0.752941176470588 0.752941176470588],
    'Callback','evaporator', ...
    'FontSize',14, ...
    'FontWeight','bold', ...
    'ListboxTop',0, ...
    'Position',[32.25 20.25 119.25 27.75], ...
    'String','Condenser', ...
    'Tag','Pushbutton3');
if nargout > 0, fig = h0; end
```

CONDENSING AND COMPLETE UNITS

Condensing Temperature (Celcius)	Ambient Temperature (Celcius)	Evaporating Temperature (Celcius)	Computaional Tolerance	Minimum Evaporating Temperature (Celcius)	Load Temperature (Celcius)
40	25	10	.0001	-10	23

T1	T2	P	COP	QE	QC
10	41.79494	27.71371	4.690484	129.9907	157.7045
9	41.34251	27.42791	4.594891	126.0283	153.4562
8	40.89662	27.14262	4.499444	122.1267	149.2693
7	40.45727	26.85663	4.404393	118.2871	145.1438
6	40.02445	26.56876	4.30998	114.5108	141.0796
5	39.59817	26.2779	4.21643	110.7989	137.0768
4	39.17844	25.98297	4.123955	107.1526	133.1356
3	38.76527	25.68294	4.032755	103.573	129.2559
2	38.35869	25.37683	3.943017	100.0613	125.4381
1	37.95871	25.0637	3.85492	96.61856	121.6823
0	37.56535	24.74264	3.768635	93.24599	117.9886
-1	37.17865	24.4128	3.684324	89.94468	114.3575

Condensing Unit

CONDENSING AND COMPLETE UNITS

Condensing Temperature (Celcius)	Ambient Temperature (Celcius)	Evaporating Temperature (Celcius)	Computaional Tolerance	Minimum Evaporating Temperature (Celcius)	Load Temperature (Celcius)
40	35	5	0.00012	-10	20

T1	T2	P	COP	QE	QC	Temp
8.215047	49.97575	31.58027	3.452852	109.042	140.6223	5
8.215039	49.97576	31.58027	3.452856	109.0421	140.6224	4
8.215044	49.97575	31.58027	3.452854	109.042	140.6223	3
8.215001	49.97581	31.58025	3.452873	109.0426	140.6228	2
8.214999	49.97581	31.58024	3.452874	109.0426	140.6229	1
8.214996	49.97581	31.58024	3.452875	109.0426	140.6229	0
8.214994	49.97582	31.58024	3.452877	109.0427	140.6229	-1
8.214991	49.97582	31.58024	3.452878	109.0427	140.6229	-2
8.214989	49.97582	31.58024	3.452879	109.0427	140.623	-3
8.214987	49.97583	31.58024	3.45288	109.0428	140.623	-4
8.215033	49.97577	31.58026	3.452859	109.0422	140.6224	-5
8.215034	49.97576	31.58026	3.452858	109.0422	140.6224	-6

Complete Unit

REF-2004 EVAPORATOR AND CONDENSER ESTIMATOR

Condensing Temperature (Celcius)	Ambient Temperature (Celcius)	Evaporating Temperature (Celcius)	Rate of Heat Absorbtion Qe (kW)
40	35	-5	81

Internal Diameter of Tube (meter)	External Diameter of Tube (meter)	Rate of Heat Rejection Qc (kW)
0.0016	0.0018	85

Evaporator

Heat Transfer Area (Square Meter)

67.1607

Required Tube Length (millimeter)

11876.6205

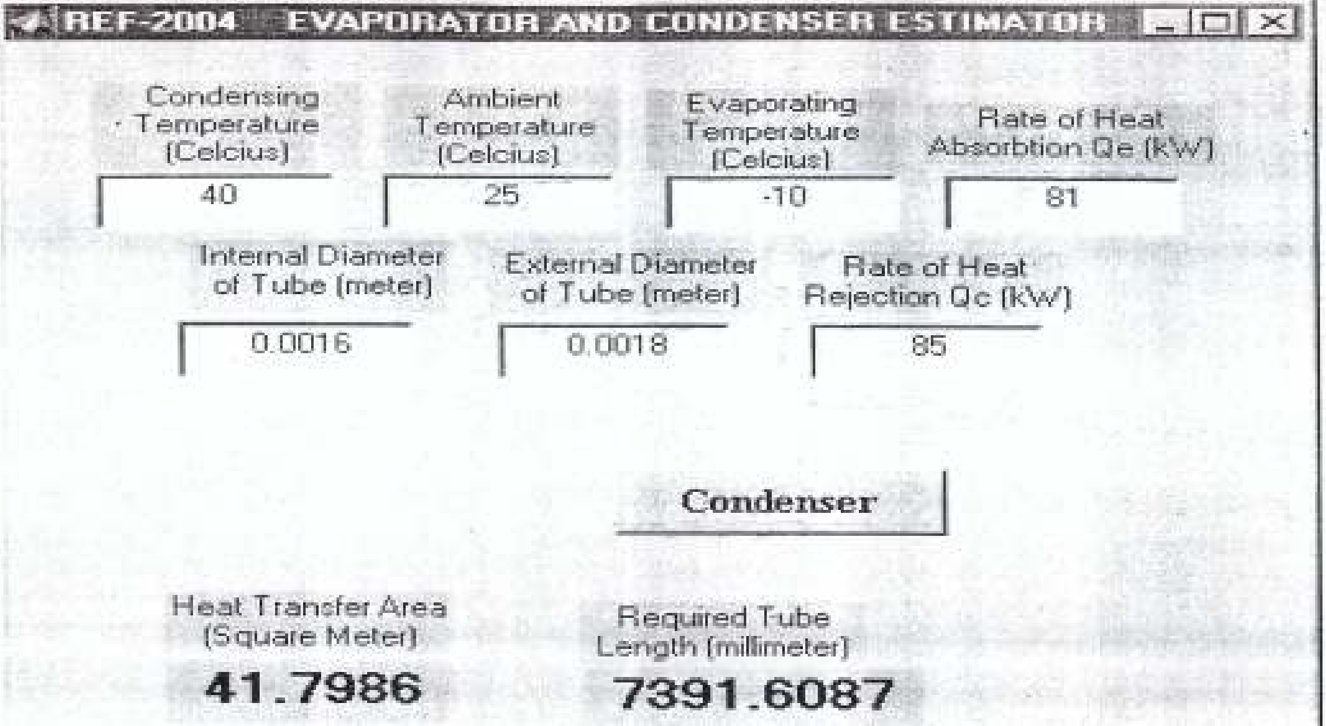
REF-2004 EVAPORATOR AND CONDENSER ESTIMATOR
Condensing Temperature (Celcius)
40
Ambient Temperature (Celcius)
25
Evaporating Temperature (Celcius)
-10
Rate of Heat Absorbtion Qe (kW)
81
Internal Diameter of Tube (meter)
0.0016
External Diameter of Tube (meter)
0.0018
Rate of Heat Rejection Qc (kW)
85
Condenser
Heat Transfer Area (Square Meter)
41.7986
Required Tube Length (millimeter)
7391.6087

Capillary Tube

Condensing Temperature (Celcius)	diameter of tube (meter)	Evaporating Temperature (Celcius)
40	0.00163	-10

Capillary Tube

T2	P	y	v	dl	L
12	719.71099	0.17943714	31.54076	0.0012269646	2.0350843
11	698.54688	0.18453105	33.196548	0.0010995005	2.0460793
10	677.8622	0.1895417	34.918663	0.00098197931	2.0558991
9	657.64988	0.19446867	36.709595	0.00087354704	2.0646346
8	637.90286	0.19931132	38.571906	0.00077343655	2.072369
7	618.61413	0.20406883	40.508233	0.00068095718	2.0791785
6	599.77669	0.2087402	42.521279	0.00059548588	2.0851334
5	581.38358	0.21332417	44.613816	0.00051645957	2.090298
4	563.42787	0.2178193	46.788678	0.0004433685	2.0947317
3	545.90267	0.22222391	49.048757	0.00037575049	2.0984892
2	528.80111	0.22653605	51.396998	0.00031318583	2.101621
1	512.11637	0.23075357	53.836391	0.00025529288	2.104174
0	495.84166	0.23487402	56.369964	0.00020172419	2.1061912
-1	479.97021	0.2388947	59.000773	0.00015216308	2.1077128
-2	464.49533	0.24281264	61.731891	0.00010632057	2.108776
-3	449.41032	0.24662457	64.566397	6.3932735e-005	2.1094154